The Role of Plectin in Pancreatic Cancer

A Dissertation

Presented to

the faculty of the School of Engineering and Applied Science

University of Virginia

---

in partial fulfillment

of the requirements for the degree

Doctor of Philosophy

by

Soo Jung Shin

December

2013

APPROVAL SHEET

The dissertation

is submitted in partial fulfillment of the requirements

for the degree of

Doctor of Philosophy

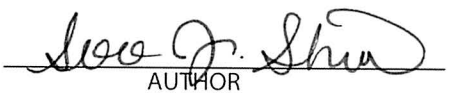

AUTHOR

The dissertation has been read and approved by the examining committee:

Kimberly Kelly

Advisor

Kevin Janes

Brent French

Todd Bauer

Amy Bouton

Accepted for the School of Engineering and Applied Science:

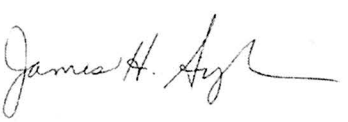

Dean, School of Engineering and Applied Science

December

2013

ABSTRACT

Pancreatic ductal adenocarcinoma (PDAC) is an intractable clinical problem. It is the fourth leading cause of cancer deaths in the United States and the five-year survival rate of PDAC is only 6%. The prognosis remains poor due to its highly aggressive nature and resistance to extant therapies. Unlike other cancer types such as prostate, colon, and breast cancer, there have been no significant improvements in PDAC survival over the past 40 years despite a large number of clinical trials. This is because most patients are diagnosed with metastatic disease due to the lack of specific symptoms and the absence of suitable biomarkers for early detection. Because early detection and complete surgical resection offer the best hope for long term survival, there has been significant focus in recent years on the development of improved diagnostic methods.

Using phage display and functional proteomics, we previously demonstrated that the cytoskeletal linker protein plectin is a robust biomarker for PDAC. We showed that 100% of human PDAC specimens overexpressed plectin, whereas plectin was absent in normal pancreata. Because the phage display technique identifies cell surface antigens, we hypothesized that plectin, normally cytoplasmic, is aberrantly localized to the cell surface in PDAC cells. Aberrant protein localization has been associated with the pathogenesis of many human diseases. Given its abnormal localization and expression in PDAC, mislocalized plectin could have direct functional roles in the transition from pre-invasive to invasive disease and/or be of importance for the established primary and metastatic tumors. Although plectin has been studied extensively in normal physiology and other diseases such as epidermolysis bullosa, the biological role of plectin in pancreatic cancer has not been studied. Understanding the biology of aberrant

localization of plectin to the cell surface is important because it provides insights into a functional role for this important biomarker of PDAC.

In this dissertation, we confirmed the abnormal cell surface localization of plectin and identified a mechanism for plectin deregulation in cancer. We demonstrated that plectin is secreted through exosomes (nanometer-sized membrane particles) in PDAC cell lines but not in non-transformed human pancreatic ductal epithelial cells. We also showed that integrin β4, a known binding partner of plectin, is found in the PDAC exosomes and necessary for plectin inclusion in the exosomes. Remarkably, plectin-positive exosomes could also be isolated from serum of tumor-bearing mice. Plectin-positive exosomes derived from PDAC were taken up by cells that were devoid of cell surface plectin and induced migration and invasion. Moreover, plectin-positive exosomes were able to enhance the growth tumors that were unable to produce exosomes. *In vitro* shRNA and overexpression studies as well as *in vivo* models collectively demonstrated a positive role of plectin for tumor growth, migration, and invasion. Taken together, this series of studies establishes a novel and critical role for plectin expression and mislocalization in PDAC progression.

ACKNOWLEDGEMENT

First, I would like to thank my advisor, Dr. Kimberly Kelly, for her excellent mentorship and training. Throughout my graduate school career, Kim encouraged me keep an open mind, think critically, be confident, and remain positive. I am grateful for her time, patience, and endless support. Without her guidance, I wouldn't have been able to complete this work and grow as a scientist. I would also like to thank my dissertation committee members Dr. Kevin Janes, Dr. Brent French, Dr. Amy Bouton and Dr. Todd Bauer for their valuable scientific perspective and input in our discussions.

I thank all the members of the Kelly Lab I've worked with. I thank Stephanie, for teaching me various experimental techniques and assays necessary for this research; Jeff, for his invaluable advice on both science and life; and Marc, for giving me various advice as a senior grad student in this lab and helping me with animal studies. I thank Siva, Jaymes, Lindsey, and Dustin, who have provided useful feedback on my research and presentations. I also thank all the great friends I've made during this process, especially Judith and Cynthia, for helping me celebrate the good days and forget about the bad ones.

I owe many thanks to Dr. Lauren Sefcik Anderson, who was my graduate student mentor during my undergraduate years, for being a great mentor and inspiring me to go to graduate school. She continued to provide support even after leaving UVA and I'm grateful for her advice on the NSF fellowship application. It has been through her help that I was able to win the NSF fellowship.

Finally, I’d like to thank my husband, Kevin, for his encouragement, trust, patience, sacrifice, and love. Thank you for being there for me and for your support in this venture. I couldn’t have done this without you.

This work was supported by the National Institutes of Health (R01 CA137071 to Kimberly A. Kelly) and the National Science Foundation Graduate Research Fellowship (DGE-0809128 to Soo J. Shin).

TABLE OF CONTENTS

NOMENCLATURE

5-FU	5-fluorouracil
ABD	Actin binding domain
AKT/PKB	Protein kinase B
ANOVA	Analysis of variance
ATP	Adenosine triphosphate
AVPR2	Arginine vasopressin receptor 2
BCA	Bicinchoninic acid
BRCA2	Breast cancer type 2 susceptibility protein
BrdU	5-bromo-2'-deoxyuridine
BrdUTP	5-Bromo-2´-Deoxyuridine 5´-Triphosphate
BSA	Bovine serum albumin
CA-19-9	Carbohydrate antigen 19-9, serum marker for pancreatic cancer
CD	Cluster of differentiation
Cdk1	Cyclin-dependent kinase 1
cDNA	Complementary DNA
CID	Collision-induced dissociation
DAPI	4',6-diamidino-2-phenylindole
DLS	Dynamic light scattering
DNA	Deoxyribonucleic acid
DTT	Dithiothreitol
EDTA	Ethylenediaminetetraacetic acid
EGFP	Enhanced green fluorescence protein
EGFR	Epidermal growth factor receptor

EMB-MD	Epidermolysis bullosa simplex associated with muscular dystrophy
ER	Endoplasmic reticulum
ERCP	Dndoscopic retrograde cholangiopancreatography
F-actin	Filamentous-actin
FAC	Focal adhesion contact
FBS	Fetal bovine serum
FDR	False discovery rate
FnIII	Fibronectin type III
FOXO	Forkhead box class O
g	Acceleration
GAPDH	Glyceraldehyde 3-phosphate dehydrogenase
GFAP	Glial fibrillary acidic protein
GSK	Glycogen synthase kinase
HD	Hemidesmosome
HEPES	4-(2-hydroxyethyl)-1-piperazineethanesulfonic acid
HPDE	Human pancreatic ductal epithelium
HPLC	High-performance liquid chromatography
HSP	Heat shock protein
HUVEC	Human umbilical vein endothelial cell
IF	Intermediate filament
IFBD	Intermediate filament binding domain
IgG	Immunoglobulin G
ILV	Intraluminal vesicles
IPMN	Intraductal papillary mucinous neoplasia
kDa	Kilodalton (atomic mass unit, molecular weight)

K-Ras	V-Ki-ras2 Kirsten rat sarcoma viral oncogene homolog
MAPK	Mitogen-activated protein kinase
MCN	Mucinous cystic neoplasias
MHC-II	Major histocompatibility complex class II
miRNA	Micro RNA
MMP	Matrix metalloproteinase
µM	Micromolar (molar concentration unit, mol/m^3)
mRNA	Messenger RNA
MVB	Multivesicular body
NTA	Nanoparticle tracking analysis
$p16^{Ink4A}$	Cyclin-dependent kinase inhibitor 2A
p21	Cyclin-dependent kinase inhibitor 1, CDK-interacting protein 1
p27	Cyclin-dependent kinase inhibitor 1B
p53	Tumor protein 53
PanIN	Pancreatic intraepithelial neoplasia
PBS	Phosphate buffered saline
PCP	Planar cell polarity
PCR	Polymerase chain reaction
PDAC	Pancreatic ductal adenocarcinoma
PDEC	Pancreatic ductal epithelial cell
PET	Polyethylene terephthalate
PFA	Paraformaldehyde
PI3K	Phosphoinositide 3-kinase
PKA	Protein kinase A
PKC	Protein kinase C

PLEC-TRUNC	Truncated plectin
PTEN	Phosphatase and tensin homolog
PTP	Plectin-targeting peptide
PVDF	Polyvinylidene fluoride
RACK1	Receptor for Activated C Kinase 1
RNA	Ribonucleic acid
s.c.	Subcutaneous (i.e., injection)
SD	Standard deviation
SDS	Sodium dodecyl sulfate
PAGE	Polyacrylamide gel electrophoresis
SEM	Standard error of the mean
shRNA	Short Hairpin RNA
SPECT	Single photon emission computed tomography
TBST	Tris-buffered saline with 0.1% Tween-20
TEM	Transmission electron microscopy
TGFβ	Transforming growth factor β
TMB	3,3',5,5'-tetramethylbenzidine
TRC	The RNAi Consortium
tPTP	Tetrameric plectin-targeting peptide
TUNEL	Terminal deoxynucleotidyl transferase dUTP nick end labeling
UV	Ultraviolet
WGA	Wheat germ agglutinin

LIST OF FIGURES

LIST OF TABLES

CHAPTER 1

INTRODUCTION

1.1. Pancreatic Ductal Adenocarcinoma (PDAC)

1.1.1. Clinical problem of pancreatic cancer

Pancreatic adenocarcinoma (PDAC) is the most common type of pancreatic cancer, representing more than 85% of all pancreatic neoplasms. It is a highly malignant tumor of the exocrine pancreas (1). Although pancreatic cancer is only the tenth most commonly occurring cancer, the diagnosis of PDAC carries the worst prognosis of all malignancies. It is estimated that 45,220 new cases of pancreatic cancer will be diagnosed with an estimated 38,460 deaths in 2013. The five-year survival rate of PDAC is only 6% and the prognosis remains poor due to its highly aggressive nature and resistance to existing therapies (2-4). The poor prognosis of PDAC is attributed to the lack of specific symptoms and the late diagnosis of the disease. Unfortunately, most patients are diagnosed with metastatic disease and surgical resection is no longer an option by the time symptoms become apparent (5). As shown in colon and breast cancer (6, 7), early detection that allows surgical resection would likely result in a significant increase in PDAC patient survival.

1.1.2. Current PDAC diagnostic methods

While many pancreatic cancer serum biomarkers have been studied, the only clinically useful biomarker is CA-19-9. Although CA-19-9 has been used to monitor treatment and recurrence of pancreatic cancer (8-10), it is limited because it lacks the sensitivity for detection of early stage pancreatic cancer (5). This serum marker has only demonstrated its use in already diagnosed pancreatic cancers and cannot be used as a diagnostic tool for early detection of previously undiagnosed pancreatic cancer due to its poor sensitivity. Additionally, multidetector helical computed tomography (CT) with intravenous contrast injection has been shown to have a potential in predicting surgical

resectability (11). However, this method of cross-sectional abdominal imaging showed unreliable detection of early stage PDAC in high-risk patients (12, 13). Other diagnostic methods, such as endoscopic retrograde cholangiopancreatography (ERCP), are used to obtain tissue samples for diagnosis. Although ERCP is relatively accurate, these endoscopic procedures are invasive and cause potential injury to the pancreas (14). Therefore, there has been significant focus on the development of improved diagnostic methods using approaches like serum proteomics (15) and genetic profiling (16) for early detection of PDAC in recent years.

1.1.3. PDAC treatment

Once PDAC is diagnosed, treatment options depend on the tumor burden, local tissue invasion, and distant metastases. In order to determine if patients are eligible for surgery, CT is used to determine if the tumor is surgically resectable. According to the National Comprehensive Cancer Network Pancreatic Adenocarcinoma Panel, tumor is resectable if distant metastases and tumor thrombus are absent and without invasion into mesenteric and portal veins, which are surrounding blood vessels that supply blood to the intestines (17). In addition, a clear fat plane must be present around the mesenteric artery, hepatic artery, and celiac axis indicating lack of their involvement. Only 15-20% of PDAC patients present with surgically resectable tumor at the time of diagnosis, and even for the patients who received pancreatectomy (Whipple procedure), PDAC commonly recurs (18).

In the majority of cases, patients are not eligible to undergo surgical resection because the disease has already metastasized. For locally advanced PDAC, the gold standard for first-line of therapy is gemcitabine or gemcitabine combinatorial therapy (19). The study by Burris *et al.* in 1997 demonstrated that 23.8% of patients treated with gemcitabine

treatment alone experienced clinical benefit response compared to only 4.8% in 5-fluorouracil (5-FU)-treated patients. The results showed that gemcitabine treatment also resulted in an increase in overall patient survival compared to 5-FU chemotherapy (20) as the survival rate at 12 months was 18% for gemcitabine-treated patients but only 2% for 5-FU patients. A recent study confirmed that gemcitabine remains the first-line of therapy for advanced PDAC as gemcitabine was better tolerated than an alternative treatment with 5-FU, folinic acid and cisplatin combination (LV5FU2-CDDP), which did not show any strategic advantage (21). Other treatments using gemcitabine in combination with other targets, such as matrix metalloproteinases (MMPs), have been shown to have no benefit over gemcitabine treatment alone in phase III clinical trials (22-24). The only combinatorial therapy that has been shown to have benefit over gemcitabine alone is erlotinib (epidermal growth factor receptor [EGFR] inhibitor) plus gemcitabine (25). A recent study showed that erlotinib prolongs PDAC patient survival by inhibiting gemcitabine-induced mitogen-activated protein kinase (MAPK) signaling (26). However, the overall survival was increased by only 0.33 months (25). Therefore, the clinical advantage of using both gemcitabine and erlotinib is still being debated.

1.1.4. Molecular biology and progression of PDAC

PDAC arises from progression of increasing grades of precursor lesions known as pancreatic intraepithelial neoplasia (PanIN-I, -II, and -III). The cystic tumors, intraductal papillary mucinous neoplasias (IPMN) and mucinous cystic neoplasias (MCN) are less common and alternate precursors to PDAC (**Fig. 1.1**) (1). Low grade PanIN-I have low malignant potential and are very common in aged populations and in patients with pancreatitis, whereas PanIN-III are advanced carcinoma in situ lesions that readily progress to PDAC (27). Although clinical trials have aimed at testing screening tools for detecting precursor lesions PanIN and IPMN, the results have not been successful

because they are microscopic lesions that do not cause any symptoms and often missed because they cannot be observed by available non-invasive imaging methods (28). In terms of developing methods of early PDAC diagnosis, PanIN-III would be ideal targets because they have a high chance of progressing into invasive PDAC.

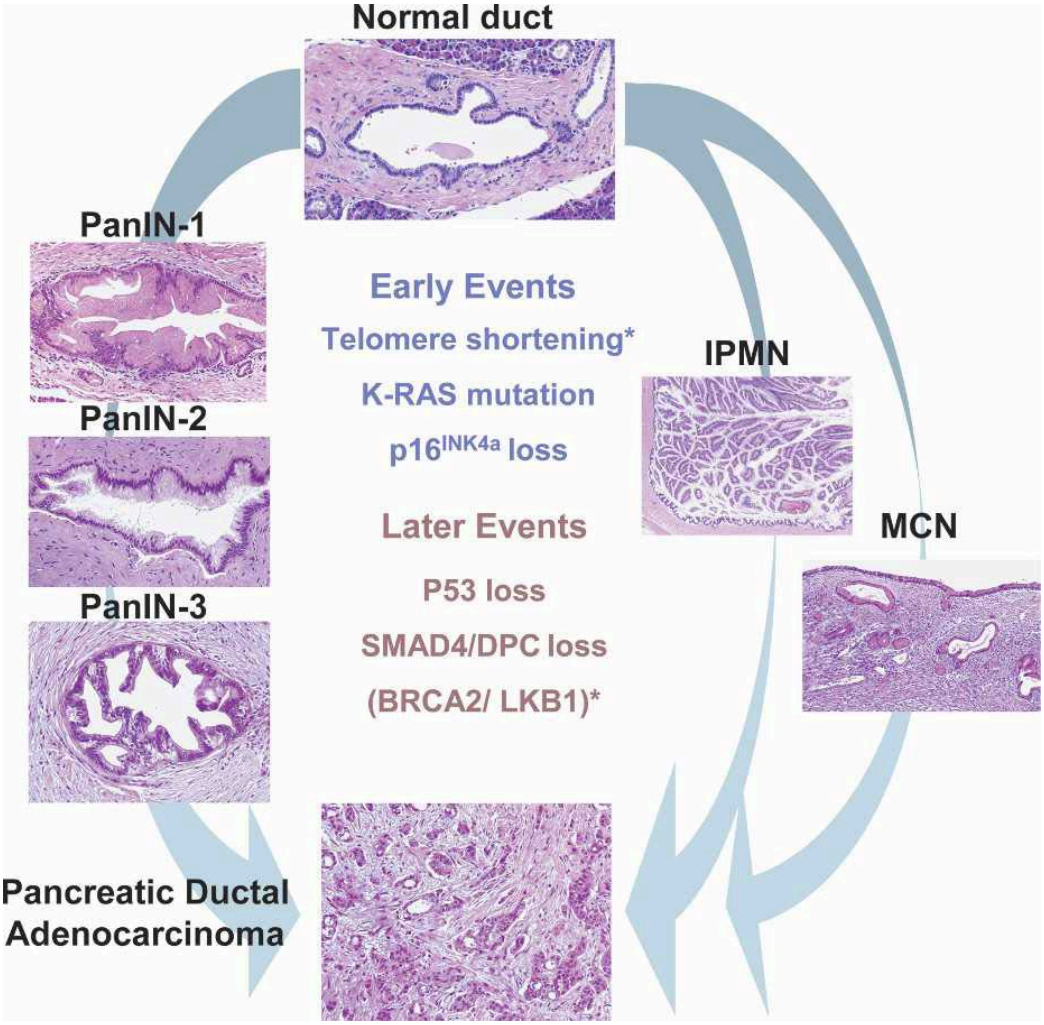

Figure 1.1. Molecular Genetics of PDAC. PDAC progression model showing histological evolution of lesions in the pancreatic ducts (PanINs) to invasive PDAC. Progression is associated with a temporally ordered series of mutations. IPMN and MCN also progress to PDAC. Reprinted with permission from Cold Spring Harbor Laboratory Press, *Genes & Dev*., Hezel *et al.* 2006 (1).

The *K-Ras* oncogene is mutationally activated in PanIN-I, while the *p16*^{Ink4a} and *p53* tumor suppressors are inactivated in PanIN-II and III, respectively. Importantly, the mutational profile of PDAC is highly recurrent, as activating mutations in the *K-Ras* oncogene has been found in nearly 100% of PDAC. In addition, mutations in *p16*^{Ink4a} and in the *Arf-p53* pathway were identified in more than 95% of cases. Mutation in *p16*, a key regulator G1-S cell cycle transition, results in increased proliferation and *p53* mutation results in altered senescence, apoptosis, and DNA damage response. Finally, *SMAD4/DPC* mutation, which occurs in about 50% of PDAC cases, disrupts the transforming growth factor β receptor (TGF-β) signaling cascade (1). Although *K-Ras* mutation occurs in nearly 100% of PDAC patients, it serves as a poor therapeutic target because *K-Ras* mutations also occur in the inflamed ductal epithelium and non-inflamed, non-neoplastic pancreas (29, 30).

1.2. Plectin

1.2.1. Plectin as a biomarker of PDAC

Because low grade PanIN lesions (PanIN-I and II) are commonly present in normal pancreas and patients with pancreatitis, they are not suitable candidates for early detection of PDAC. PanIN-III serves as the best candidate for early detection because patients with PanIN-III lesions have high risk for developing PDAC. However, these lesions are hard to detect using current non-invasive imaging methods due to lack of symptoms and serum markers are not efficient for detecting PanIN-III as well as previously undiagnosed PDAC. Therefore, we employed phage display screening and functional proteomics to identify novel biomarkers of PDAC progression (31). We were able to screen peptides that specifically bound to cell surface antigens on PDAC cells. The results yielded several peptides that were specific to PDAC cells compared to normal pancreatic cells. Upon proteomics analysis of the most specific peptide, plectin was identified as a novel biomarker of PDAC. In addition, plectin was further validated through immunohistochemistry and immunoblot analyses using specimens of human PDAC, chronic pancreatitis, PanIN lesions, and normal pancreata. Notably, plectin specifically marks the transition between early and advanced pancreatic lesions, as it is absent in PanIN-I and –II, but readily detectable in 60% of PanIN-III and 100% of PDAC specimens tested (41 of 41) (32). To further validate plectin as an imaging target for early detection, tetrameric plectin-targeting peptides (tPTP) were used as a contrast agent for single photon emission computed tomography (SPECT) in a mouse model of orthotopic PDAC and liver metastasis. *In vivo* imaging was able to detect both the primary and metastatic tumors, demonstrating its clinical usability for detecting PDAC and potential for early diagnosis by detecting preinvasive PanIN-III lesions.

1.2.2. The scaffolding protein plectin

Plectin is a large (≥500kDa) cytoskeletal linker protein that is normally expressed in the cytoplasm and present in various tissues including skin, muscle, and brain (33). Plectin expression was shown to be especially prominent in stratified epithelia (34), cells forming the blood brain barrier (35), and fluid-filled cavities such as glomerular visceral epithelial cells, bile canaculi, urothelium, intestinal villi, epidermal layers lining the cavities of brain, and endothelial cells of blood vessels (35-37). It was originally discovered as a major component of intermediate filament (IF)-enriched extracts from rat glioma C6 cells (38). Plectin is composed of a central rod domain that is composed of approximately 200 nm long α-helical coiled flanked by globular domains (**Fig. 1.2**) (39). In normal cells, it plays a crucial role in cytoskeleton network organization by binding to all three major cytoskeletal filaments: filamentous (F)-actin, microtubules, and IFs, anchoring them to the plasma membrane skeleton and to plasma membrane-cytoskeleton junctional complexes (33). Plectin was shown to be concentrated at the basal surface and recruited into hemidesmosomes, which are structures that mediate adhesion to the basement membrane by anchoring the IFs (33, 40), linking the IFs to the cytoplasmic domain of transmembrane glycoproteins such as integrin α6β4 (40-42). In addition, plectin is also concentrated at desmosomes (43), focal adhesion contacts (FACs), Z-disks and dense plaques of striated and smooth muscle, and intercalated discs of cardiac muscle (44, 45), further indicating its role in linking the cytoskeleton to plasma membrane junctions. Due to plectin's importance in cytoskeletal network organization, plectin deficiency lead to epidermolysis bullosa simplex associated with muscular dystrophy, (EBD)-MD, a severe hereditary skin blistering disease combined with muscular dystrophy (46-49).

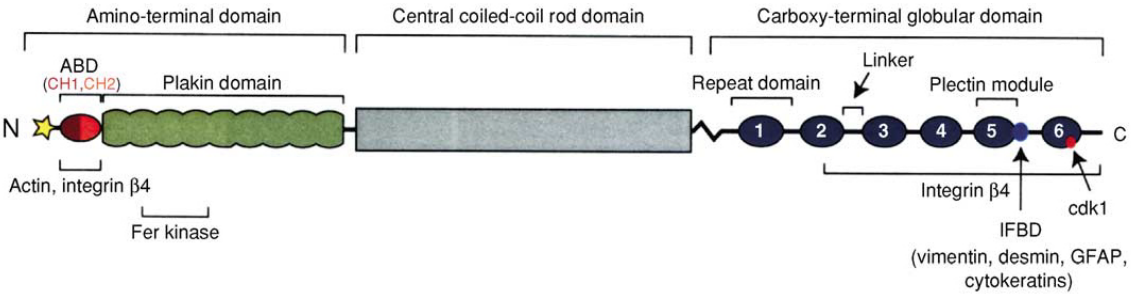

Figure 1.2. Schematic map of the plectin protein. Plectin is made up of a central rod flanked by N-terminal and C-terminal (globular) domains. The N-terminal domain contains an actin-binding domain (ABD, shown in red), and a region called plakin domain (light green). The C-terminal globular domain contains six highly homologous plectin repeat domains (blue), each consisting of a plectin module and a linker region, one of which harbors an intermediate filament binding domain (IFBD, shown in light blue). The C-terminal domain also contains a cell cycle kinase cdk1 phosphorylation site (50) shown in red. Alternative splicing of plectin transcripts leads to expression of various isoforms with different N-termini (shown in yellow star). Reprinted with permission from Elsevier Inc., *Methods Cell Biol*., Rezniczek *et al.* 2004 (51).

Plectin interaction with IF requires a specific binding domain in the C-terminal end of the protein (52), whereas a functional actin-binding domain (ABD) is located in the N-terminal domain (53, 54). Binding sites for integrin β4 are located at both C-terminal and N-terminal domains of plectin (40). However, the ABD located in the N-terminal domain was shown to have the highest affinity to actin and integrin β4 (55). In addition, plectin has been shown to directly interact with vimentin (38, 39, 56), cytoplasmic IF proteins such as glial fibrillary acidic protein (GFAP), epidermal cytokeratins, neurofilament triplet proteins, and desmin (57), and also bind to the nuclear IF protein, lamin B (58). Interestingly, plectin was shown to harbor a phosphorylation site for cyclin-dependent kinase 1 (Cdk1) in C-terminal repeat 6 domain (50) and the non-receptor tyrosine kinase Fer binding site in the N-terminal globular domain, in which the absence of plectin results in an increased Fer kinase activity (59).

1.2.3. Isoforms and functions

Plectin has multiple isoforms produced through complex, tissue-specific regulatory processes including alternative promoter usage and alternative splicing (55). The

molecular weight prediction of plectin isoforms varies from 507 to 527 kDa depending on alternative first coding exons (53). Analysis of the organization of the mouse plectin gene revealed a total of 16 alternatively spliced exons in which 11 of them (exons 1-1j) directly splicing into a common exon 2, three (exons −1, 0a, 0) into exon 1c. Exons 2α and 3α are optionally spliced within the exons encoding the ABD (**Fig. 1.3**). Of the 11 first exon variants, 8 of them were shown to be coding, resulting in 8 different isoforms of plectin (55). In analysis of the human plectin gene, a total of 8 alternative first exons have been identified so far (60). It is possible that various plectin isoforms with distinct N-terminal ends encoded by alternative first coding exons may lead to plectin's functional diversity. For example, plectin isoform 1 was shown to be involved in leukocyte infiltration during wound healing (61). Plectin-1a, the isoform most predominantly present in keratinocytes, was shown to control keratin cytoarchitecture potentially through the MAPK signaling cascade (62). Plectin isoform 1b was shown to form a mitochondrial signaling platform and regulate organelle shape by tethering mitochondria to IFs (63). **Table 1.1.** summarizes various functions of plectin isoforms.

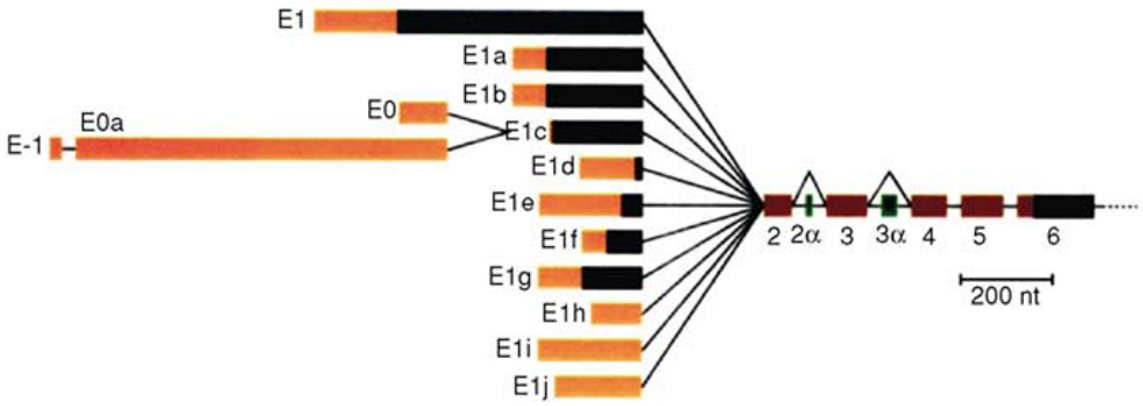

Figure 1.3. Schematic representation of alternative plectin transcripts. Alternative splicing of the N-terminus of the plectin gene gives rise to 16 different transcripts. Exons are shown as boxes and splice events as lines connecting individual boxes, noncoding regions are orange, regions coding in all cases are black, regions coding only in conjunction with a first coding exon are brown, and the optionally spliced exons 2α and 3α are green. Reprinted with permission from Elsevier Inc., *Methods Cell Biol*., Rezniczek *et al.* 2004 (51).

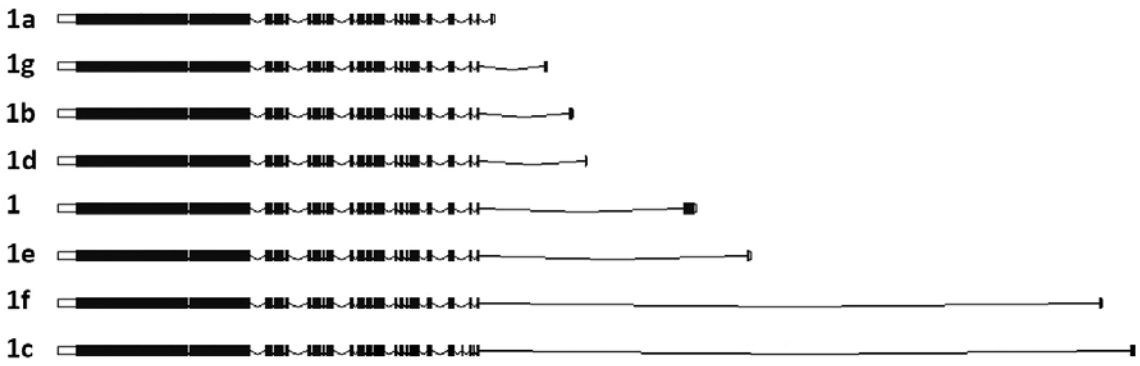

Figure 1.4. Schematic representation of 8 different coding plectin transcripts. Modified from Ensembl.

Table 1.1. List of plectin isoforms and their functions

Isoform	Function	Reference
Plectin-1	Plays an important role in inflammatory phase of wound healing by recruiting leukocytes	(61)
Plectin-1a	Key element for assembly and homeostasis of hemidesmosomes Binds to integrin β4 Controls keratin cytoarchitecture through MAPK signaling Regulates keratin-integrin α6β4 anchorage via Ca2+/calmodulin	(64, 65) (41) (62) (66)
Plectin-1b	Mediates mitochondrion–intermediate filament network linkage and controls organelle shape	(63)
Plectin-1c	Regulator of microtubule dynamics in keratinocytes	(67)
Plectin-1d	Integrate muscle fibers by targeting and linking desmin IFs to Z-disks and costameres	(68)
Plectin-1e	Not studied	N/A
Plectin-1f	Stabilizes FA-evolved fibrillar adhesions and turns them into recruitment sites for motile vimentin filament intermediates Integrate muscle fibers by targeting and linking desmin IFs to Z-disks and costameres Links the contractile apparatus as a whole via desmin IFs to the sarcolemmal costameric protein skeleton	(69) (68) (70)
Plectin-1g	Not studied	N/A

Although we have a good understanding of the role of plectin in other cell types through genetic studies (45, 71), the role of plectin in PDAC has not been studied. Based on preliminary data (31, 32), we believe that plectin has an important role in PDAC and as such, understanding plectin's contribution to PDAC could enable better methods for detection and better therapies.

1.3. Protein mislocalization

As discussed earlier, plectin was discovered as a PDAC biomarker through phage display screening. Phage cannot penetrate the plasma membrane, and therefore only binds to cell surface antigens. This indicates that plectin was localized to the surface of PDAC cells. However, to date, plectin has not been identified on cell surfaces. In order for proteins to exert their biological functions, they require proper spatiotemporal milieu of an intact cell. The proteins need correct spatial and temporal arrangements in order to gain access to their molecular interaction partners and trigger the appropriate signaling cascades based on information from the environment. For this reason, aberrant localization of proteins has been associated with the pathogenesis of many human diseases (72). Deleterious gain-of-function or dominant negative effects caused by aberrant subcellular localization of misfolded proteins have been implicated in the pathophysiology of several neurodegenerative diseases (72-74). For example, mislocalization of microtubule-associated protein tau to dendritic spines has recently been reported to mediate a synaptic dysfunction that is associated with impaired brain function at the preclinical disease stages that immediately precede neurodegeneration (75). Additionally, aberrant localization of several essential enzymes results in different metabolic diseases (76) such as nephrogenic diabetes insipidus that results from endoplasmic reticulum (ER) retention of the protein arginine vasopressin receptor 2 (APVR2) (77). Importantly, deregulation of the spatiotemporal dynamics of cancer signaling proteins, such as p53 (78), forkhead box class O (FOXO) (79, 80), and p21 (81-83), has been shown to promote tumorigenesis and metastasis. For example, cell cycle inhibitors p21 and p27, which normally are functional in the nucleus, were shown to become oncogenic when mislocalized to the cytoplasm (81, 84, 85). In addition, the binding of p21 to MAPK kinase kinase 5 (MAP3K5 or ASK1) in the cytoplasm was

shown to inhibit the MAPK cascade (82, 83). However, no studies have reported mislocalization of cytoplasmic proteins to the cell surface. The works in this dissertation is the first to study the function of a protein that is mislocalized from cytosol to the cell surface and to elucidate the potential consequences of such an aberrant process.

1.4. Exosomes

To communicate with their surrounding environment, cells are known to release signaling proteins and other cytokines that bind to receptors on neighboring cells. Cells also secrete more complex structures like membrane vesicles, which are composed of plasma membrane lipid bilayers with transmembrane proteins and enclosed cytoplasm. Of these membrane-enclosed vesicles, exosomes are smaller in size and are formed in endosomal compartments (multivesicular body, MVB) and released into the extracellular environment by fusion of MVB to the plasma membrane (86). The importance of exosomes in the tumor microenvironment has been demonstrated in recent years. Studies in gliomas have suggested that trafficking of the exogenic receptor EGFRvIII via membrane vesicles can promote neoplastic transformation of non-transformed neighboring cells (87). Because many cancer cells produce exosomes, secreted exosomes from PDAC may play an important role in PDAC progression and aggressiveness.

1.4.1. Biogenesis

The process of exosome formation begins when cell surface proteins and parts of the plasma membrane become endocytosed. This membrane-enclosed endocytic vesicles are either recycled back to the plasma membrane or delivered to the late endosomes. Inward budding of the late endosome membranes result in multivesicular bodies (MVBs), which consists of multiple smaller vesicles known as intraluminal vesicles (ILVs) within them. MVBs can either fuse with lysosomes to degrade proteins or fuse with the plasma membrane to release ILVs through exocytosis. These ILVs exocytosed from MVBs are exosomes (88-90). The size of exosomes vary between 40 and 100 nm in diameter, and has been shown to be produced from various cell types including reticulocytes (91-93),

dendritic cells (94, 95), B- and T-lymphocytes (96-98), mast cells (99), platelets (100), and various cancer cells (87, 101-103).

Although the exact mechanism behind exosome secretion is still unclear, progress has been made in identifying the molecular mechanism of exosome biogenesis. Extensive studies have been done by Théry and colleagues on the role of Rab GTPases in exosome secretory pathways. They showed that Rab27a and Rab27b control different steps of exosome production. Specifically, Rab27a silencing was shown to inhibit MVB from docking to the plasma membrane and increased the size of MVBs. Rab27b silencing was shown to redistribute MVBs to the perinuclear region. The overall exosome production was decreased upon Rab27a and Rab27b knockdown without changing exosomal protein content or morphology (104). In another study, they showed that Rab27a inhibition resulted in not only decreased exosome production, but also decreased matrix metalloproteinase 9 (MMP9) secretion in mammary carcinoma cells. Rab27a inhibition subsequently resulted in decreased primary tumor growth and lung metastasis, indicating a potential role for exosomes in modulating tumor microenvironment for metastasis (105). Another Rab protein, Rab11, was shown to regulate exosome production by promoting MVB docking and fusion to the plasma membrane (106). Transfection with mutant Rab11 resulted in decreased exosome secretion.

1.4.2. Characteristics and composition

Exosomes range from 40 - 100 nm in diameter and have a cup-shaped morphology (88). Due to their endocytic origin, exosomes have a rigid lipid bilayer that is enriched in cholesterol, sphingolipids, and ceramide (107). Proteomic studies by various groups have shown that exosomes are mainly composed of membrane transport and fusion

proteins (such as Rab GTPases, annexins, and flotillins), proteins associated with lipid microdomains (integrins and tetraspanins), cytoskeletal proteins (ezrin and actin), and heat shock proteins (Hsp60, Hsp70, and Hsp90) (96, 97, 108-110). In addition to proteins, exosomes were also shown to carry mRNAs and miRNAs. Importantly, exosomes were able to exchange genetic information between cells by transferring mRNAs and miRNAs and that transferred exosomal mRNAs can potentially be translated after being delivered to the neighboring cell (111). Recently, many studies have demonstrated that exosomes can influence distant cell signaling (112), suggesting that exosomes may also carry various signaling ligands. ExoCarta, a database for exosomal proteins, lipids, and RNAs, currently lists 4,563 proteins, 1,639 mRNAs, and 764 miRNAs that have been identified in exosomes (http://exocarta.org/). Exosomes may be involved in modulating numerous amounts of targets, further highlighting the importance of studying exosomes in the context of cancer.

1.4.3. Functions

The function of exosomes has been shown to vary depending on the cell of origin and their composition. Due to various proteins, RNAs, and lipids present in exosomes, they were shown to have functional diversity. The discovery of exosomes contributed to novel mechanisms for intercellular communication (113). For example, Raposo *et al.* showed that exosomes from transformed B-cells have major histocompatibility complex class II (MHC-II) and are able to stimulate CD4+ T-cells in an antigen-specific manner (97). In addition to antigen presentation, exosomes were also shown to have immunosuppressive functions. Peche *et al.* showed that injection of donor-type (but not syngeneic) exosomes derived from bone marrow dendritic cells prior to cardiac allograft transplantation resulted in a significantly prolonged heart allograft survival in a rat model (114). Another study demonstrated immunospressive role of exosomes, in which

exosomes released by mesenchymal stem cells were shown to reduce the infarct size during myocardial ischemia/reperfusion injury in a mouse model, possibly by mediating cardioprotection (115). Although it is clear that exosomes have a diverse range of functions, it is still unclear whether exosomes interact with host cells by fusing with the plasma membrane, internalization, or through a receptor-ligand process.

1.4.4. Exosomes in cancer

Studies in cancer have shown various functions of exosomes produced by cancer cells. They can either promote tumor growth and metastasis or elicit an anti-tumor response by turning on the immune system. This bimodal effect of cancer exosomes is likely due to the heterogeneous nature of tumors, resulting in a complex network of interactions.

Luga *et al.* investigated the role of exosomes secreted from fibroblasts in tumor microenvironments (116). They showed that fibroblast-derived exosomes were able to promote protrusion and migration of breast cancer cells through Wnt-planar cell polarity (PCP) signaling. They also showed that coinjecting breast cancer cells and fibroblasts in a mouse model resulted in a dramatic increase in PCP signaling-dependent metastasis. Trafficking of breast cancer cell exosomes were shown to promote tethering of autocrine Wnt11 to exosomes derived from fibroblasts, suggesting a pro-tumor role of exosomes during intercellular communication between fibroblasts and tumors cells.

More evidence illustrates that exosomes can mediate tumorigeneis. A study by Peinado *et al.* demonstrated that exosomes derived from melanoma cells were able to promote the formation of primary tumors as well as metastases in mice (117). Melanoma-derived exosomes were shown to induce leaky vasculature at pre-metastatic sites and promote bone marrow progenitors to become pro-vasculogenic that were positive for receptor

tyrosine kinases c-Kit, Tie2, and Met. They further demonstrated that reducing Met expression decreased pro-metatstatic behavior of bone marrow cells. Inhibiting exosome production through Rab27a interference resulted in decreased tumor growth and metastasis. This study indicates that production and transfer of exosomes promote melanoma tumorigenesis and metastasis.

However, there are also a number of studies that demonstrate the anti-tumor effect of exosomes. One example is demonstrated in a lung cancer model by Li *et al.* where they tested the hypothesis that exosomes can be used as an immunotherapeutic agent (118). In this study, they showed that exosomes derived from non-small-cell lung cancer cells overexpressing Rab27 upregulated MHC-II as well as CD80 and CD86 (co-stimulatory molecules) in dendritic cells. In addition, when dendritic cells were treated with exosomes derived from Rab27-rich cells, CD4+ T-cell proliferation significantly increased. They also tested exosomes from Rab27-rich cells in a mouse model and showed that tumor growth decreased upon exosome injection. This study showed that exosomes can induce antitumor immune effects.

In another study, Ristorcelli *et al.* showed that pancreatic cancer cells produce exosomes, and that purified pancreatic cancer exosomes induced decreased tumor cell proliferation (101). In addition, pancreatic cancer derived exosomes increased Bax (pro-apoptotic regulator), but decreased Bcl-2 (anti-apoptotic regulator) expression. They also showed that pancreatic cancer exosomes induced activation of phosphatase and tensin homolog (PTEN) and glycogen synthase kinase (GSK)-3β, which are involved in the feedback regulation of the phosphoinositide 3-kinase (PI3K)/Akt pathway (119). They showed that PTEN formed complexes with actin, β-catenin, and GSK-3β in exosome-treated cells, and therefore β-catenin may no longer be available to activate the survival

pathway. This study suggests that exosomes produced by pancreatic tumor cells may have autocrine control of tumor growth by restoring PTEN and GSK-3β activities, thus driving cells toward apoptosis.

1.5. Motivation and objectives

In our previous studies using phage display, we showed that plectin is upregulated. In addition, because phage can only detect cell surface antigens, plectin may be present on the surface of pancreatic cancer cells (31). However, plectin is normally absent in the pancreas and is exclusively cytoplasmic in other tissue types (55). Therefore, the first objective of this dissertation is to conclusively validate that plectin is mislocalized to the cell surface in pancreatic cancer cells and determine the potential mechanism behind this mislocalization. We examined the interaction between plectin and integrin β4, a cytosolic binding partner of plectin (40, 120), that was also shown to play a role in pancreatic cancer cells (121). The objective was to determine if integrin β4 is responsible for plectin mislocalization to the cell surface in PDAC.

Many studies have demonstrated that membrane vesicles known as exosomes are able to transfer proteins and RNAs to cells of other types. Exosomes are nanometer-sized particles containing cytoplasm and plasma membrane that are secreted by both normal and cancerous cells. Recently the importance of exosomes in cross-talk in the tumor microenvironment has been demonstrated. Fusion of exosomes to the cellular membrane in either a paracrine or autocrine manner may result in aberrant protein localization. Ristorcelli *et al.* revealed the presence of plectin binding partners in pancreatic cancer exosomes (101), therefore, we hypothesized that plectin may be present on the cell surface through an exosome-mediated mechanism and its presence is important to tumor function. The objective was to explore the role of plectin in exosome formation, the effect of plectin-containing exosomes on cancer cell proliferation, migration and invasion, and finally the effect that plectin has on PDAC exosome

proteome. We hypothesized that the aberrant localization of plectin to the surface of PDAC cells arises from trafficking of plectin through exosomes.

Although plectin was validated as a PDAC biomarker; the role of plectin in tumorigeneisis, progression and other important cancer phenomena has not been studied. Therefore, the last part of the dissertation focuses on determining the functional role of plectin in pancreatic tumor growth and invasion. Based on the prominent upregulation of plectin in advanced precursor lesions (PanIN-III), PDAC, and metastasis but absent in normal pancreata (32), plectin could play direct functional roles in the transition from pre-invasive to invasive disease. The role of plectin in organizing the cytoskeletal network in tissues such as brain, skin, and muscle has been studied extensively and plectin dysfunction is connected to epidermolysis bullosa as well as muscular dystrophy (49, 71). However, the mechanism of the biological function that plectin may have in PDAC has not been examined. Due to the direct interaction between plectin and integrin β4, we also investigated the contribution of plectin-integrin β4 interactions on migration and invasion of PDAC cells as well as cells of the microenvironment (stroma and endothelium). We hypothesized that there is a cross-talk between plectin and integrin β4 and that plectin interaction with integrin β4 has a significant effect on PDAC growth and migration. The key innovation of this research is the elucidation of the functional role of plectin, a protein previously not found to play a role in pancreatic cancer. In addition, although most of the plectin isoforms have been studied in normal physiology or other diseases, the isoforms that are present in pancreatic cancer and their functional role have not been explored before. Understanding the role of specific plectin isoforms in PDAC will provide important insights into current therapeutic approaches.

CHAPTER 2

PLECTIN MISLOCALIZATION TO THE CELL SURFACE IN PDAC

Works from chapters 2-4 are published in Unexpected gain of function for the scaffolding protein plectin due to mislocalization in pancreatic cancer. Shin SJ, Smith JA, Rezniczek GA, Pan S, Chen R, Brentnall TA, Wiche G, and Kelly KA. *Proc Natl Acad Sci U S A.* 2013 Nov;110(48): 19414–19419. (122)

2.1. Introduction

We have shown previously that plectin is a robust biomarker for pancreatic cancer and that it is overexpressed in human pancreatic ductal adenocarcinoma (PDAC) specimens (32). Plectin as a PDAC biomarker was discovered through phage display and functional proteomics techniques. From our previous data, we deduced that plectin is localized to the surface of PDAC cells as phage can only bind to cell-surface proteins. In normal physiology, however, plectin is linked to the β4 subunit of a transmembrane protein integrin α6β4 in the cytoplasm (40, 120). The N-terminal actin-binding domain (ABD) of plectin directly binds to the region containing fibronectin type III (FnIII) domains of β4 integrin (123). The interaction between the integrin α6β4 and plectin is essential for the assembly and stability of hemidesmosomes, which are junctional adhesion complexes that anchor epithelial cells to the basement membrane (66).

Protein subcellular localization plays an important role in cellular signal transduction (72). Therefore, proper spatiotemporal localization of proteins within a cell is crucial. Abnormal protein localization has been linked to many human diseases that result from gain-of-function or dominant negative effects (72). For example, mislocalization of tau, microtubule-associated protein, from the axonal compartment to dendritic spines has been shown to facilitate a synaptic dysfunction that immediately precedes neurodegeneration (75). Aberrant spatiotemporal dynamics of signaling proteins were shown to enhance tumorigenesis and metastasis (78, 80). In one of many examples, cytoplasmic mislocalization of p53 tumor suppressor was shown to inhibit its ability to regulate the cell cycle (78).

The overall aim of this study was to understand the means by which plectin localizes to the surface in PDAC. Ristorecelli *et al.* recently showed that exosomes, nanometer-sized membrane particles, secreted from pancreatic cancer cells, have spectrin and filamin (101), which are known binding partners of plectin (41, 124). We hypothesize that the aberrant localization of plectin to the surface of PDAC cells is mediated by an exosome secretion pathway and this aberrant localization plays a role in PDAC. Lastly, we investigated the interaction between plectin and integrin β4 in PDAC through shRNA knockdown of integrin β4 to determine if integrin β4 is involved in the exosome-mediated mislocalization of plectin. Additionally, previous studies have shown that the ABD of plectin is mainly responsible for plectin interaction with integrin β4. This region is encoded by exons 2-8 have the highest affinity to actin (55). Therefore, we created a truncated form of plectin, PLEC-Trunc (covering plectin exons 1a-9), the overexpression of which should interfere with endogenous plectin binding to integrin β4. Understanding the plectin-integrin β4 interaction will provide insights into the pathophysiological processes involved in this cancer and help delineate the mechanism behind plectin mislocalization in PDAC.

2.2. Materials and methods

2.2.1. Cell Culture

Three different PDAC cell lines were chosen due to their mutation profiles. Bx.Pc3 has wildtype *K-Ras*, whereas both L3.6pl and Panc-1 have mutant *K-Ras*. However, L3.6pl represents highly metatstatic PDAC and Panc-1 represents a dedifferentiated phenotype. Bx.Pc3, C6, and Panc-1 cell lines were obtained from the American Type Culture Collection (ATCC) and were grown in Roswell Park Memorial Institute (RPMI) medium, Kaign's Modification of Ham's F-12 (F-12K) medium, and Dulbecco's Modified Eagle's Medium (DMEM) respectively. L3.6pl and HPDE were obtained from Dr. Craig Logsdon (University of Texas, MD Anderson Cancer Center). L3.6pl was grown in DMEM; HPDE was grown in keratinocyte medium. All media were supplemented with 10% (vol/vol) fetal bovine serum (FBS), 1% penicillin-streptomycin (pen-strep), and 1% L-glutamine except keratinocyte medium (supplemented with human recombinant epidermal growth factor 1-53 and bovine pituitary extract) and F-12K medium (supplemented with 2.5% FBS, 15% horse serum, 1% pen-strep, and 1% L-glutamine).

2.2.2. shRNA lentiviral transduction

Lentivirus vector encoding shRNA against human plectin was obtained from Dr. Nabeel Bardeesy (Massachusetts General Hospital and Harvard Medical School). Cells were seeded on 12-well plates and grown to 50% confluence. Old media were replaced by media containing polybrene (4 µg/ml). Plectin shRNA lentiviral particles were thawed at room temperature and gently mixed before adding to the cells. Three different ratios of virions to cells were used (1:1, 2:1, and 3:2). The infected cells were incubated overnight and media were replaced (without polybrene). Stably transfected cells were selected by

puromycin treatment (2 µg/ml for Bx.Pc3, 3 µg/ml for L3.6pl, and 4 µg/ml for Panc-1). To further select stable clones, a single colony was isolated using the trypsin method (125). Downregulation of each protein was verified via immunoblot.

2.2.3. Flow Cytometry

Trypsinized control and plectin knockdown cells were incubated with biotin conjugated anti-plectin antibody (eBioscience) for 30 minutes on ice, washed 3 times with phosphate buffered saline (PBS), then incubated with Alexa Fluor® 488 conjugated streptavidin (Invitrogen) for 30 minutes on ice. After antibody incubation and washing, the cells were fixed with 4% paraformaldehyde (PFA) for 15 minutes at room temperature. Cell nuclei were then stained with DAPI (Invitrogen). Flow cytometry using fluorescein conjugated plectin-targeted peptide (PTP) was performed in a similar manner, except 10 µM PTP was used instead of antibodies. Cell fluorescence data and images were acquired using ImageStream^X Mark II (Amnis) and the data was analyzed using the ImageStream Data Analysis and Exploration Software (IDEAS).

2.2.4. PTP binding on the cell surface

$1x10^4$ cells were seeded into wells of a 96-well plate and incubated at 37°C and 5% CO_2 for 24 h. The cells were washed once with PBS and fixed with 4% PFA for 10 min. The cells were blocked with 1% BSA in PBS for 1 h and incubated with 1 µM fluorescein-coupled plectin-targeting-peptide (PTP) in PBS-1% BSA for 2 h. Then the cells were incubated with horseradish peroxidase (HRP)-conjugated anti-fluorescein antibodies (Invitrogen) for 30 min. After washing, the cells were incubated with 3,3',5,5'-tetramethylbenzidine (TMB) (Sigma) for 10 min and absorbance was measured at 650 nm.

2.2.5. Immunogold staining for transmission electron microscopy (TEM)

The cells were washed with PBS, blocked with Aurion blocking solution (Aurion) for 1 hour at room temperature, and incubated with 5 µg/ml mouse anti-plectin antibody (Abcam [7A8]) or CD63 antibody (Abcam [MEM-259]) for 1 hour at room temperature. The cells were washed with 0.1 % BSA-c PBS (Aurion) for 6x10 min then incubated with 10nm gold conjugated anti-mouse IgG secondary antibody for 1 hour at room temperature. The cells were washed with 0.1% BSA-c PBS for 6x10 min and PBS for 2x10 min, and fixed with 2.5% glutaraldehyde for 15 min. Cells were embedded and imaged via TEM.

2.2.6. Purification of exosomes

Exosomes were collected from conditioned media by standard procedures via ultracentrifugation as previously described (101) and also ExoQuick-TC (System Biosciences). For ultracentrifugation, the conditioned media was centrifuged at 300 *g* for 5 min to remove dead cells and at 12,000 *g* for 10 min to eliminate other cellular debris. Exosomes were pelleted by ultracentrifugation at 200,000 *g* for 16 h using a 45 Ti rotor (Coulter-Beckman). The exosome pellet was resuspended in 300 µl of 4-(2-hydroxyethyl)-1-piperazineethanesulfonic acid (HEPES) buffer for TEM negative staining and PBS or lysis buffer for other analyses. For ExoQuick-TC purification of exosomes, 10 ml of conditioned media were centrifuged at 300 *g* for 5 min to remove dead cells and at 12,000 *g* for 10 min to eliminate other cellular debris. The supernatant was then mixed with 2 ml of ExoQuick-TC and incubated at 4°C overnight. The mixture was centrifuged at 1,500 *g* for 30 min; supernatants were removed, and centrifuged for additional 5 min to remove all fluid. The exosome pellet was resuspended in 100 µl of buffer.

2.2.7. TEM negative stain for exosomes and dynamic light scattering (DLS)

10 µl of exosomes resuspended in HEPES buffer were placed on non glow-discharged carbon-coated grids for 10 min and then stained with 10 µl of 2% uranyl acetate. After 1 min of incubation, the liquid was removed using filter paper and the grids were allowed to air dry. Digital dark-field images were recorded using a JEOL 1230 transmission electron microscope. For DLS, exosomes resuspended in PBS were diluted in deionized water and the size distribution data was collected using Malvern Zetasizer Nano ZS90 (Malvern) and analyzed with Zetasizer Software.

2.2.8. Antibodies for immunoblotting

Primary antibodies were purchased from Abcam (plectin [E398P] and CD63 [MEM-259]); Cell Signaling Technology (Hsp90 [C45G5] and Alix [3A9]); and System Biosciences (Exosome antibody kit containing CD9, CD63, CD81, and Hsp70). HRP-conjugated secondary antibodies were purchased from R&D Systems. Primary antibodies were diluted 1:1000 in 1% Tris-buffered saline with 0.1% Tween-20 (TBST) containing 1% milk and secondary antibodies were diluted 1:5000 in 1% milk-TBST for immunoblotting.

2.2.9. SDS-PAGE and Immunoblotting

Cells were grown in 10-cm petri dishes (BD Falcon) to approximately 70% confluence and were lysed in 500 µl of lysis buffer (1% Triton X-100, 1mM EDTA, and 1mM protease inhibitor cocktail in PBS). Protein concentrations were determined using a bicinchoninic acid (BCA) protein assay kit (Thermo Scientific). Equal amounts (20 µg) of proteins in SDS sample buffer (containing β-mercaptoethanol) were resolved on 5% or 4-15% polyacrylamide gels (BioRad) and transferred onto polyvinylidene fluoride (PVDF) membranes. The membranes were blocked with 1% milk-TBST, incubated with primary antibody solution for 3 h at room temperature, washed 3x5 min with TBST, incubated

with secondary antibody solution for 30 min at room temperature, and washed 4x5 min with TBST. The membranes were then subjected to chemiluminescence and autoradiography.

2.2.10. Subcutaneous tumor injection and serum collection

1×10^6 of Panc-1 cells were subcutaneously (s.c.) injected into the dorsal flanks of male immune-deficient nude mice. The animals were euthanized 60 days post injection and blood was collected via cardiac puncture. Serum was separated from plasma via centrifugation. All in vivo experiments were performed according to a protocol approved by the University of Virginia Animal Care and Use Committee.

2.2.11. Treatment of plectin-positive and plectin-negative exosomes

Purified exosomes were subjected to BCA protein assay kit (Thermo Scientific). NIH-3T3 and HUVEC were treated with 1 µg of each exosome sample, incubated overnight at 37°C and 5% CO_2, and subjected to PTP binding assay for cell surface plectin quantification.

2.2.12. Plasmids and transfections.

pGR244 and pGR258, encoding C-terminal fusions of EGFP to full-length plectin-1a and plectin-1f inserts, respectively, were derived from pEGFP-N2 (Clontech) and have previously been described (126). pDS89 and pDS94 (derived from pBS with full-length plectin-1 and plectin-1c inserts [exons 1 to 32] flanked by in-frame EcoRI sites, respectively) were provided by Dr. Gerhard Wiche. PLEC-Trunc, corresponding to exons 1a-9 (containing the actin-binding domain of plectin which also serves as the N-terminal integrin β4 binding region of plectin), was generated by PCR using pGR244 as a template (forward primer: 5'-GCGAATTCACCATGTCTCAGCACCGGCTCCGTGTG-3',

reverse primer: 5'-GCGGATCCGGAACTTGCGCTCCTCAAAAGCAGCGG-3'). The PCR product was inserted into pEGFP-N2 using EcoRI and BamHI restriction sites. Plasmids were transfected into cells with Lipofectamine LTX (Invitrogen) according to the manufacturer's protocol. Transfection of the EGFP-tagged plasmids (pGR244 and pGR258) was verified via fluorescence microscopy.

2.2.13. Confocal microscopy

$1x10^5$ cells were seeded on 4-chamber slides (Lab-Tek), transfected with pGR244 and pGR258, and incubated at 37°C and 5% CO_2 for 24 h. Chamber dividers were removed and the cells were washed, fixed, and stained with 10 µg/ml wheat germ agglutinin. The slides were then mounted with ProLong Gold anti-fade reagent with DAPI (Invitrogen). The cells were imaged with Nikon a C1 confocal microscope equipped with a 60X oil immersion objective.

2.2.14. Immunoprecipitation (IP)

To detect plectin bound to integrin β4 on the cell surface, cells were incubated with antibodies to plectin for 4 h at 4°C, washed three times with PBS, lysed, and incubated with Protein G magnetic beads (Invitrogen) for 4 h at 4°C. Protein G beads were incubated with PBS containing 1% BSA overnight at 4°C prior to incubating with lysate to prevent nonspecific binding. The antibody-antigen complex was captured with a magnet and the complex was washed four times with PBS. The complex was resuspended in Laemmelli sample buffer and boiled to disrupt the complex. The supernatant was then analyzed by immunoblotting following SDS-PAGE for integrin β4 binding to plectin. The whole cell lysates were also evaluated for total plectin expression as a loading control.

2.2.15. Statistical analysis

All statistical analyses were performed using Prism (GraphPad Software, Inc., La Jolla, CA). Results are presented as mean ± standard error of the mean (SEM), unless otherwise noted. All statistical analyses were performed using a one-way general linear ANOVA, followed by Tukey's test for pairwise comparisons, except for PTP binding on integrin β4-knockdown cells (**Fig. 2.15**). For integrin β4-knockdown PTP binding assay, two-tailed unpaired t-test was performed. Significance was asserted at $p < 0.05$.

2.3. Results

2.3.1. Quantification of plectin presence on PDAC cell surface

Previous data indicated that plectin is a robust biomarker for pancreatic cancer and that it is overexpressed in PDAC specimens (31, 32). Plectin as a PDAC biomarker was discovered using phage display, and because phage is unable to penetrate the plasma membrane, we hypothesized that plectin is abnormally localized to the cell surface. However, in normal physiology, plectin is exclusively cytoplasmic (33). Therefore, we sought to conclusively demonstrate cell surface localization and identify the path by which this protein localizes to the surface in PDAC. First, to confirm the cell surface localization of plectin, we performed flow cytometric analysis on PDAC cells and human pancreatic ductal epithelial (HPDE) cells using plectin antibodies (**Fig. 2.1**). In order to avoid membrane permeabilization, the cells were fixed with 4% PFA after antibody incubation. Compared to non-transformed HPDE, PDAC cells had increased cell surface plectin (**Fig. 2.1A**). In addition, knockdown of plectin via shRNA diminished cell surface binding to levels equivalent to those observed with HPDE cells in Bx.Pc3 and L3.6pl (**Fig. 2.1B** and **C**).

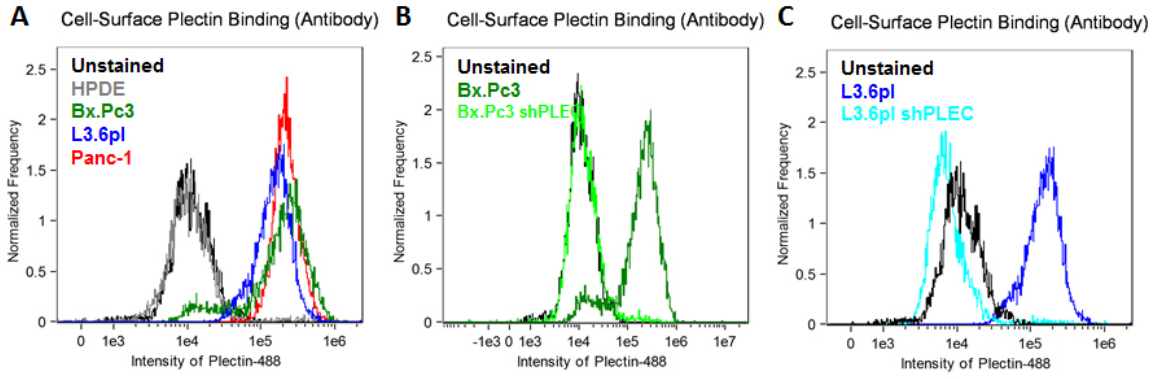

Figure 2.1. Flow cytometry of PDAC cells using plectin antibody. **A)** HPDE vs. PDAC cells, **B)** Bx.Pc3 vs. Bx.Pc3 shPLEC, and **C)** L3.6pl and L3.6pl shPLEC cells using plectin antibody.

We also confirmed cell surface plectin localization through flow cytometry using fluorescein-conjugated plectin-targeting-peptide (PTP, sequence: KTLLPTP) (**Fig. 2.2**), which has been shown to have high affinity and specificity to PDAC cells (31). Because PTP exhibited higher affinity to plectin compared to plectin antibodies, we used PTP in subsequent assays to quantify cell surface plectin.

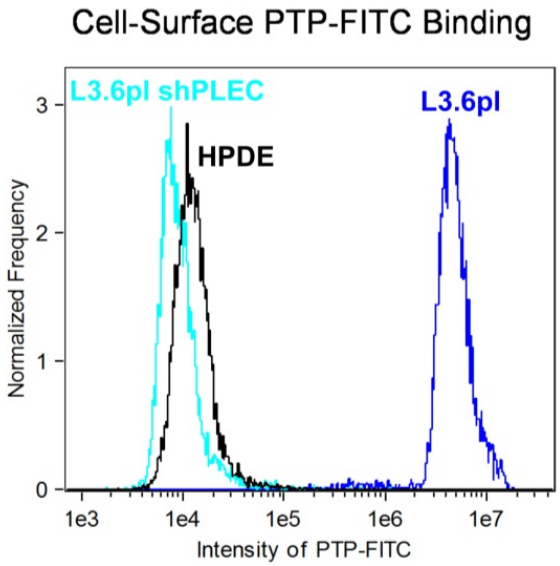

Figure 2.2. Flow cytometry of cells using plectin-targeted peptide (PTP). L3.6pl vs. L3.6pl shPLEC cells using PTP (10 µM).

To further validate cell surface localization of plectin, PTP binding assay was used instead of subcellular fractionation because it enables quantification of protein levels on the outer leaflet of the plasma membrane, whereas subcellular fractionation is indiscriminate between proteins that are extracellularly or intracellularly bound to transmembrane proteins. Scrambled peptide (Scr) was used as a control for the binding assay. Consistent with our previous findings (31), we demonstrated strongly increased binding of PTP to the surface of PDAC cell lines, as compared to binding to C6 glioma and HPDE controls (**Fig. 2.3**). C6 was used as a negative control, since it is a cancer cell line that is known to express cytosolic plectin (38). HPDE was used as a control to

compare with PDAC cell lines. Overall, our data indicates that the cytosolic protein plectin is mislocalized to the cell surface in PDAC.

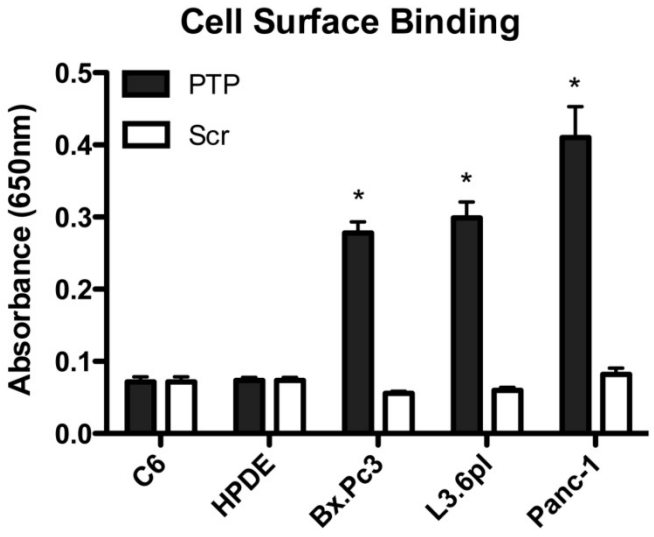

Figure 2.3. PTP binding assay. PTP (1µM) was used to quantify cell surface plectin. C6 and HPDE were used as a negative control. PDAC cell lines exhibited approximately 3-fold increase in cell surface plectin expression. *Significant to HPDE ($p<0.0001$).

2.3.2. Visualization of PDAC cell membrane through electron microscopy

Our findings that plectin is mislocalized led us to examine the cell surface and plasma membrane of PDAC cells more closely by using transmission electron microscopy (TEM). Intriguingly, in PDAC cell lines, there were nanometer-sized particles emanating from the plasma membrane (**Fig. 2.4**). However, in plectin-knockdown L3.6pl, the nanoparticle structures were absent and the membrane morphology was more similar to that of HPDE rather than that of cancerous cells. Further analysis using immunogold TEM revealed the presence of plectin on surface PDAC cells as well as the nanometer-sized particles (**Fig. 2.5**). Plectin knockdown cells and HPDE cells showed no plectin cell surface localization.

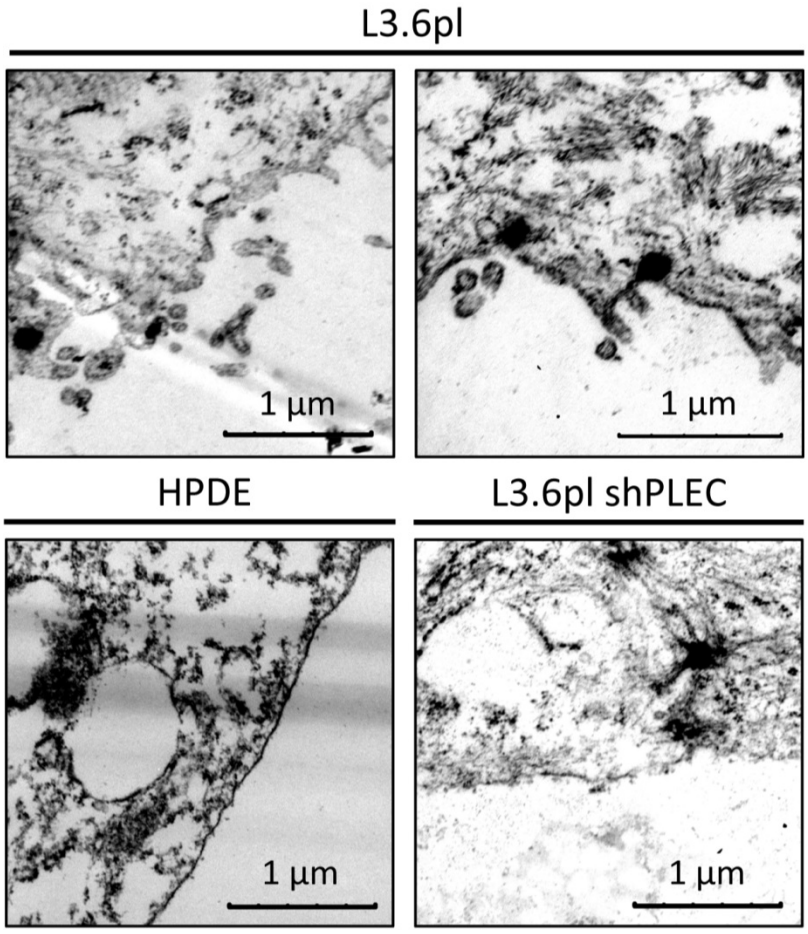

Figure 2.4. Transmission electron micrograph (TEM) showing the membrane morphology of L3.6pl, L3.6pl shPLEC, and HPDE. Scale bar = 1 µm.

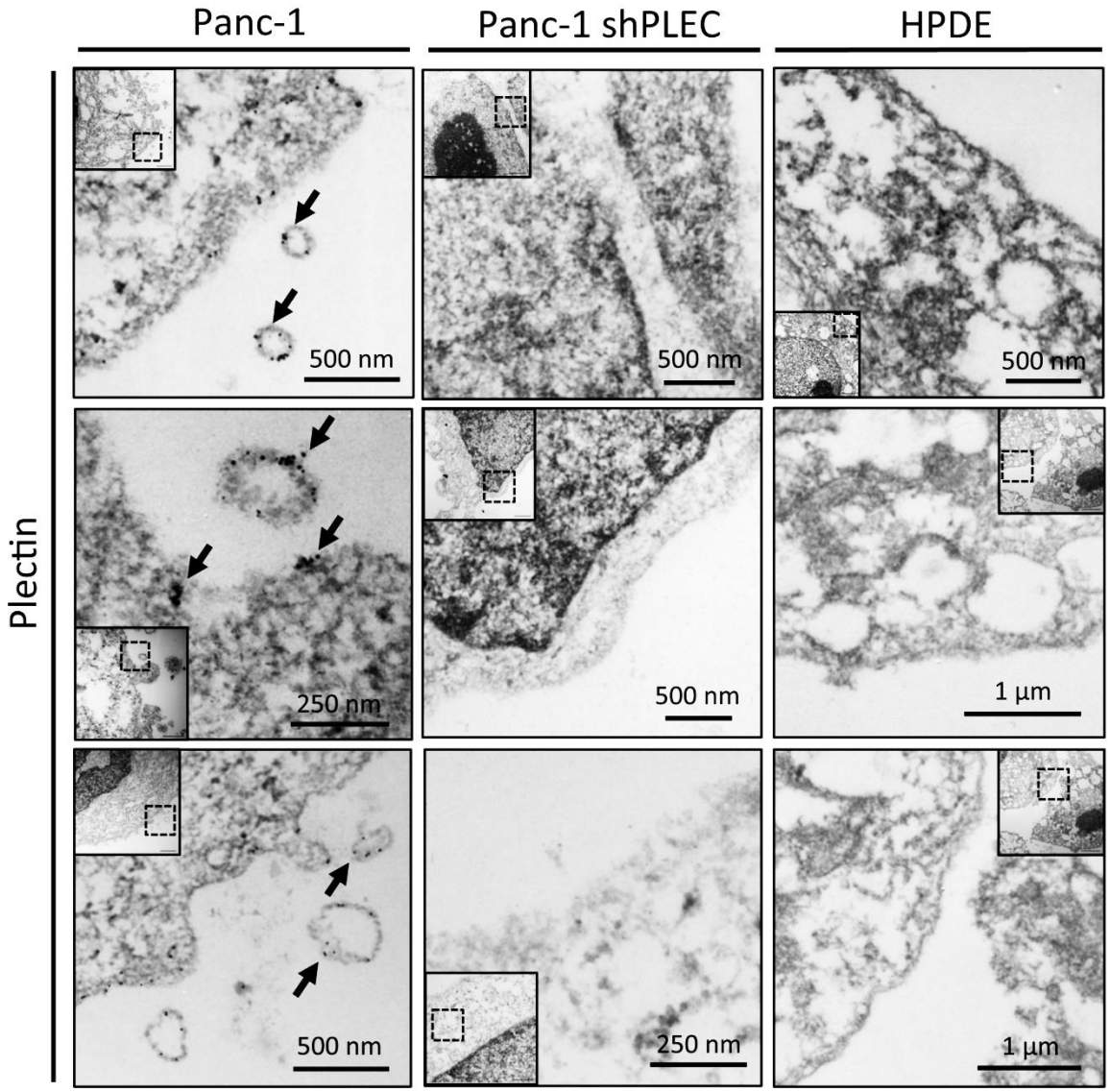

Figure 2.5. Immunogold TEM showing plectin on the cell membrane and in the exosomes of Panc-1 but not in Panc-1 shPLEC. Arrows indicate bound gold-IgG.

Various types of cells are known to produce membrane-enclosed particles known as exosomes. These structures have been implicated in cellular movement, cell-cell signaling, tissue development and cancer. Notably, tumor cells communicate with the tumor microenvironment through exosomes during the progression into a tumor mass and metastases (105, 117, 127). To assess whether plectin-positive nanometer-sized particles from PDAC cells were exosomes, we first purified the particles from conditioned medium of PDAC cells and subjected them to TEM and particle size analysis using dynamic light scattering (DLS) (**Fig. 2.6**). Particles were collected via serial centrifugation and ultracentrifugation purification procedures according to established protocols (101). DLS analysis revealed that the mean size of PDAC particles was 63.53 ± 4.46 nm in diameter and the mode size 50.75 nm. This size distribution was consistent with exosomes and not microvesicles (128). Immunoblot analysis of the purified PDAC exosomes confirmed that plectin is indeed present (**Fig. 2.7**).

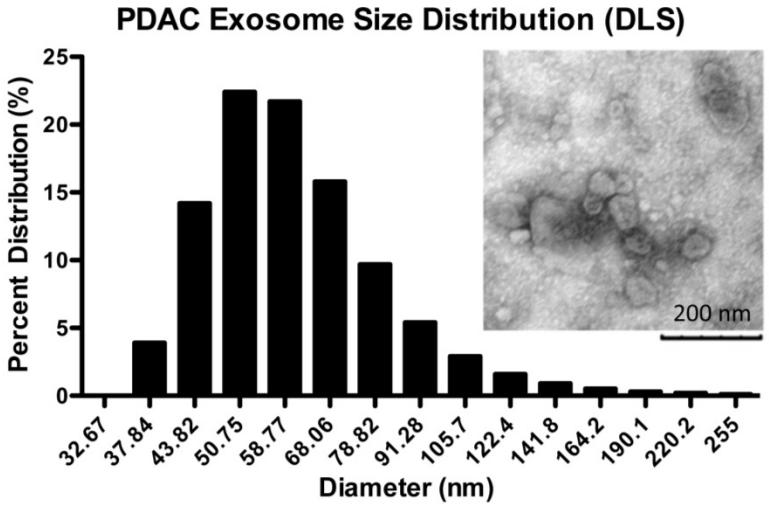

Figure 2.6. Size distribution of exosomes analyzed by dynamic light scattering (DLS). Inset shows TEM visualization of secreted PDAC exosomes. PDAC exosomes have an average diameter of 63.53 nm. Inset scale bar = 200 nm.

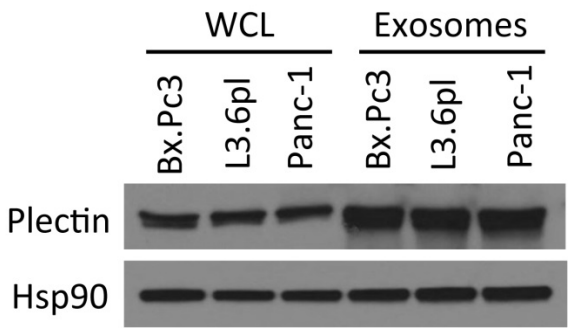

Figure 2.7. Immunoblot analysis showing plectin presence in both whole cell lysates and purified exosomes of PDAC cell lines.

Intriguingly, plectin-positive exosomes could also be purified from the serum of mice with PDAC xenografts (**Fig. 2.8A**). Exosomes from the serum of healthy, non-tumored mice were devoid of plectin (**Fig. 2.8B**). The presence of plectin in exosomes from the serum of animals with PDAC represents the potential for plectin as a serum marker, further indicating the importance of studying plectin in PDAC.

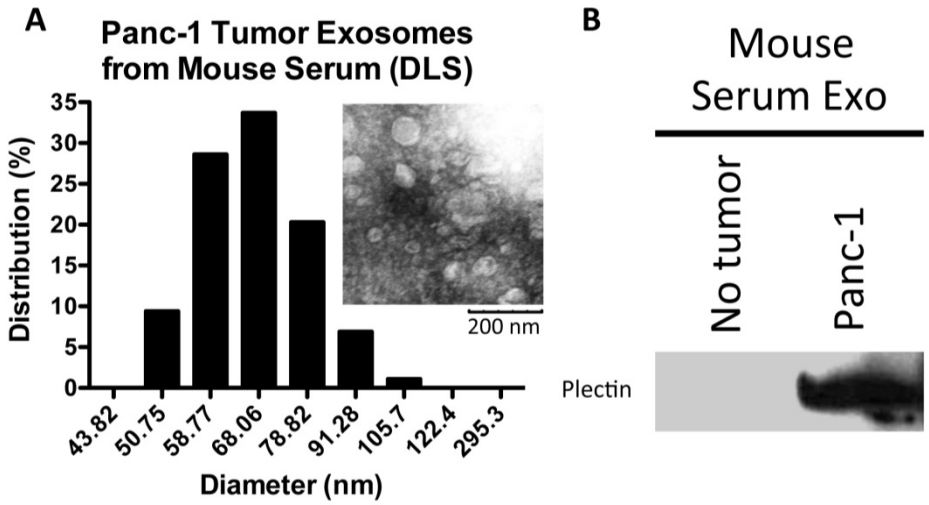

Figure 2.8. A) Exosomes collected from the serum of a Panc-1 tumor-bearing animal were examined by DLS for size distribution and TEM (negative staining) for visualization. Inset scale bar = 200 nm. **B)** Immunoblot analysis of exosomes purified from serum of immune-deficient mice with and without Panc-1 xenografts.

2.3.3. Verification of exosome markers

For further validation, purified particles were analyzed by western blotting using well-characterized exosome protein markers (Alix, CD9, CD63, CD81, and Hsp70) (**Fig. 2.9**). In addition to the positive presence of these markers, immunogold staining showed that the plectin-positive particles initially observed by TEM were positive for the exosome marker CD63 (**Fig. 2.10**). Together these data identified that nanometer-sized particles secreted by PDAC cells are plectin-positive exosomes.

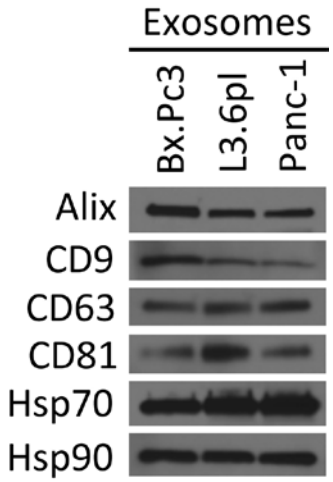

Figure 2.9. Immunoblot analysis of purified PDAC exosomes for the presence of various exosome markers.

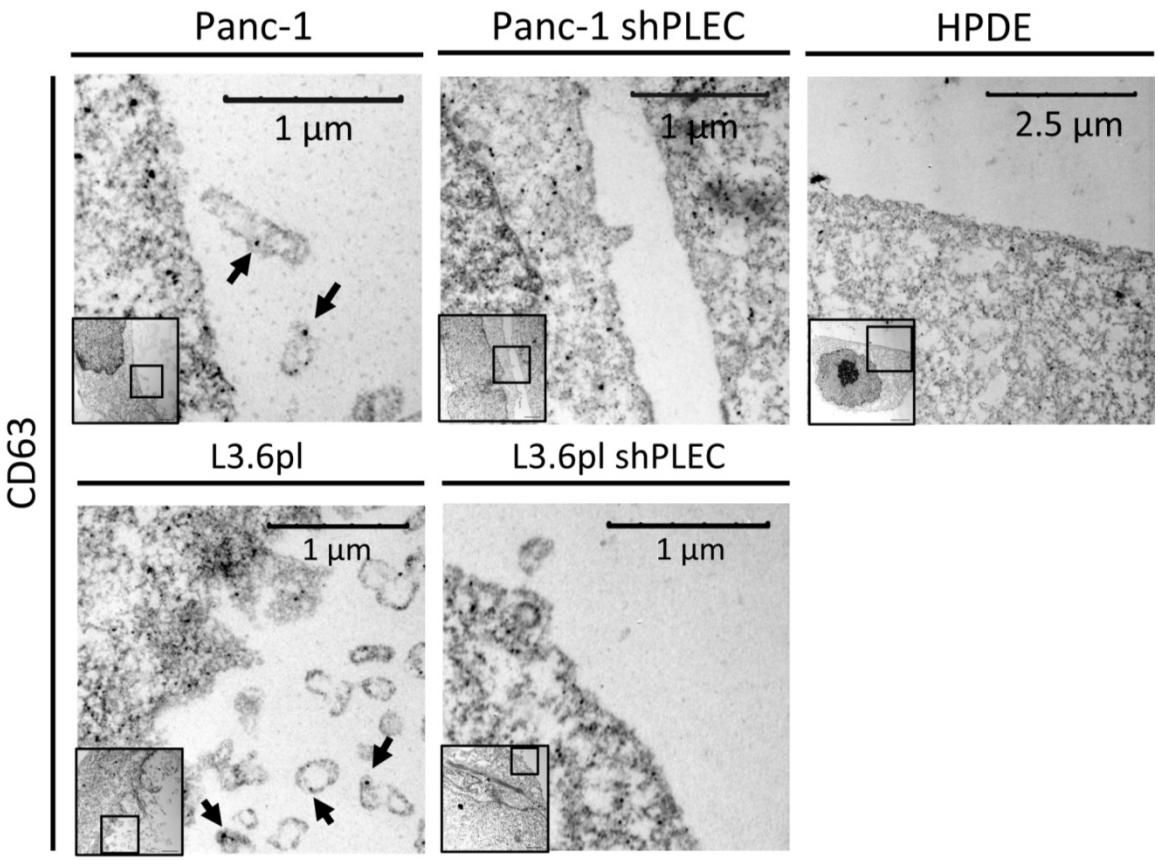

Figure 2.10. Immunogold TEM showing CD63 on the cell membrane and in the exosomes of Panc-1 but not in Panc-1 shPLEC or HPDE. Arrows indicate bound gold-IgG.

2.3.4. Plectin transfer via exosomes induces cell surface plectin localization in other cell types

Plectin exhibited dramatic effects on the membrane morphology (**Fig. 2.4**). To further validate exosomes as a potential route for cell surface plectin localization, we sought to determine whether exosome treatment would transfer plectin to the surface of other cell types that are normally devoid of cell surface plectin (**Fig. 2.11**). NIH-3T3 fibroblasts and human umbilical vein endothelial cells (HUVEC) were incubated with 10 µg/ml exosomes from the various PDAC cell lines, their plectin-knockdown counterparts, or from C6 glioma cells, which do not have cell surface plectin or plectin in their exosomes (**Fig. 2.3** and see **Fig. 2.12E**). Notably, treatment with PDAC exosomes resulted in a four-fold increase in PTP binding suggesting that the surface of the fibroblasts and endothelial cells recruited the plectin from the exosomes to their cell surfaces. In contrast, there was no increase in PTP binding to cells treated with the same number of exosomes from C6 or from the plectin-knockdown PDAC cells.

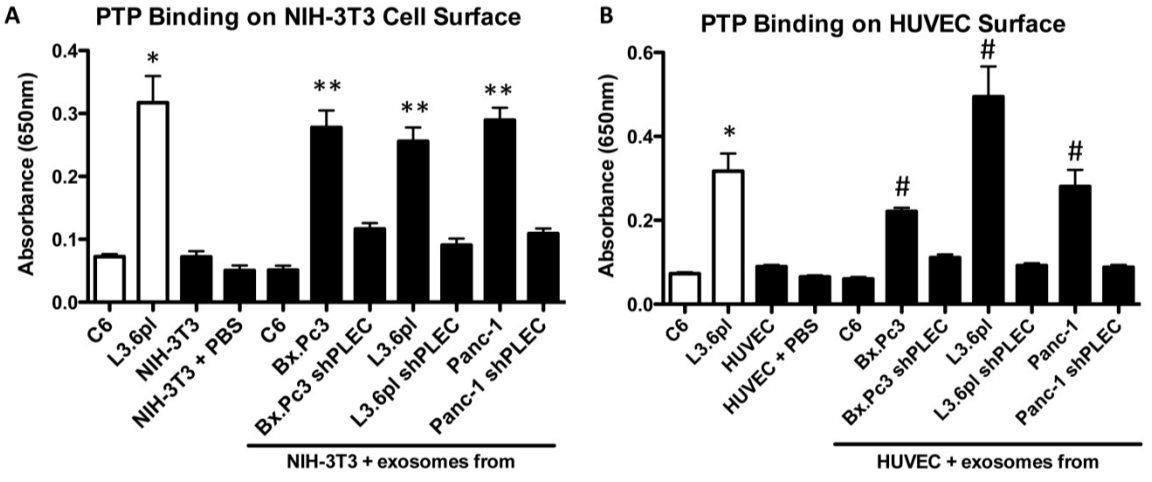

Figure 2.11. A) Cell-surface PTP binding on NIH-3T3 cells with or without exosome treatment. *Significant to C6 ($p<0.0001$), **significant to C6, NIH-3T3, and NIH-3T3 + PBS ($p<0.0001$). **B)** Cell-surface PTP binding on HUVECs with or without exosome treatment. White bars are the controls (C6 = negative, L3.6pl = positive). Black bars indicate respective cells treated with plectin-negative or positive exosomes. *Significant to C6 ($p<0.0001$), #significant to C6, HUVEC, and HUVEC + PBS ($p<0.0001$).

2.3.5. Exogenous plectin colocalizes with cell membrane and traffics through exosomes

Results shown in **Figure 2.11** demonstrate that cells lacking cell surface plectin expression can be induced to localize plectin on the cell surface by treatment with plectin-containing exosomes. In light of these results, we determined whether exogenous expression of plectin-1a or -1f in C6 and HPDE, cells that lack cell surface plectin, could induce cell surface plectin localization. The cells were transfected with pGR244 (EGFP-tagged mouse plectin-1a), pGR258 (EGFP-tagged mouse plectin-1f), or pEGFP-N2 (backbone vector). The cells were then stained with fluorescent wheat germ agglutinin (WGA) to visualize cell membranes (pseudocolored red) and were analyzed via confocal microscopy (**Fig. 2.12A-B**). Exogenously expressed plectin-1a and 1f colocalized with the cell membrane, whereas the EGFP (pEGFP-N2 backbone vector) was cytosolic. The cells were subjected to the PTP binding assay to determine if the plasma membrane localized plectin was on the cell surface. The cells expressing plectin-1a and 1f showed increased binding of PTP on the cell surface (**Fig. 2.12C-D**) as compared to the cells transfected with pEGFP-N2 controls. Thus, the expressed plectin was localized to the cell surface.

These results led us to investigate whether plectin can traffic through exosomes in cells lacking plectin. For this, we transfected C6 cells (expressing cytosolic plectin) and plectin-knockdown PDAC cell lines with pGR244 and pGR258, purified exosomes from these transfected cells, and performed immunoblot analysis to evaluate plectin expression in the exosomes (**Fig. 2.12E**). In support of our hypothesis, expression of plectin-1a and -1f both resulted in accumulation of the protein in the C6 exosomes, suggesting plectin trafficking through the exosomes. Such accumulation of exogenously expressed plectin was also observed in PDAC exosomes in which endogenous

expression was silenced. Thus, C6 and plectin-knockdown PDAC cells secreted plectin through exosomes upon 1a and 1f transfection. This indicates that plectin-1a and -1f show trafficking through exosomes leading to cell surface localization of plectin as assessed through PTP binding.

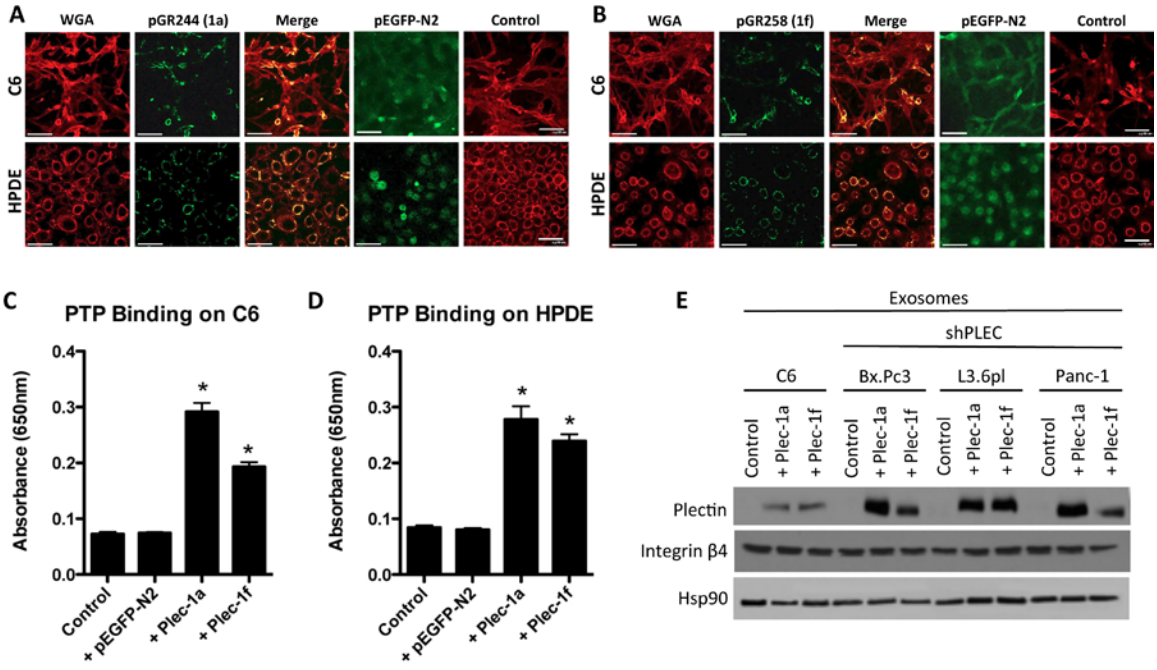

Figure 2.12. Exogenous isoforms **A)** 1a and **B)** 1f colocalize with the plasma membrane in C6 and HPDE. Exogenous plectin-1a and 1f increased PTP binding on the surface of **C)** C6 glioma and **D)** HPDE cells. *Significant to both control and control + pEGFP-N2 ($p<0.0001$). **E)** Exosomes collected from C6 and plectin-knockdown PDAC cells transfected with plectin-1a or 1f contain plectin.

2.3.6. Integrin β4 is required for plectin mislocalization in PDAC

To understand the mechanism of how plectin is trafficking in exosomes, we focused on the role of integrin β4, a transmembrane protein that is a direct binding partner of plectin in keratinocytes (40, 120) and pancreatic cancer cells (121), and a known constituent of exosomes (129). Western blot analysis of PDAC cell lysates and purified exosomes revealed the presence of plectin as well as integrin β4 in exosome samples from all PDAC cell lines (**Fig. 2.13**). Hsp90, a known component of secreted PDAC exosomes

(101) (also see **Tables 3.1-2**), was used as a loading control in these studies. Notably, shRNA-mediated knockdown of integrin β4 resulted in an almost complete loss of plectin in PDAC-secreted exosomes whereas plectin expression was still detectable in whole cell lystates, indicating that the presence of plectin in exosomes requires integrin β4 anchorage.

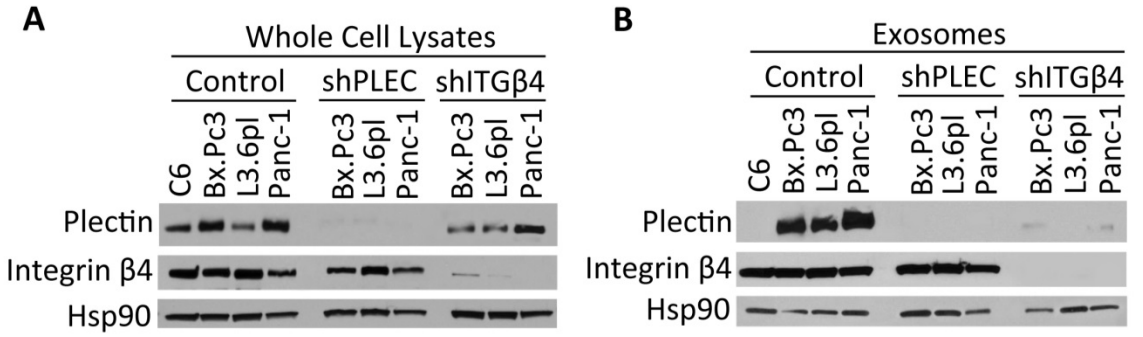

Figure 2.13. Plectin expression is absent in exosomes produced from the plectin- and integrin β4-knockdown cells, but not from whole cell lysates of integrin β4-knockdown cells.

We also confirmed via IP that plectin and integrin β4 directly interact with each other (**Fig. 2.14**). To further examine the role of integrin β4 in cell surface localization of plectin, we performed the PTP binding assay on control and integrin β4-knockdown PDAC cells (**Fig. 2.15**). There was a 5 to 10-fold decrease (depending on the cell line) in PTP binding of the integrin β4-knockdown cells, equivalent to background levels, illustrating the importance of the β4-plectin interaction for plectin cell surface localization.

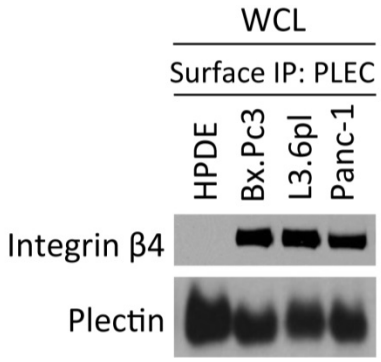

Figure 2.14. Co-immunoprecipitation of integrin β4 and plectin.

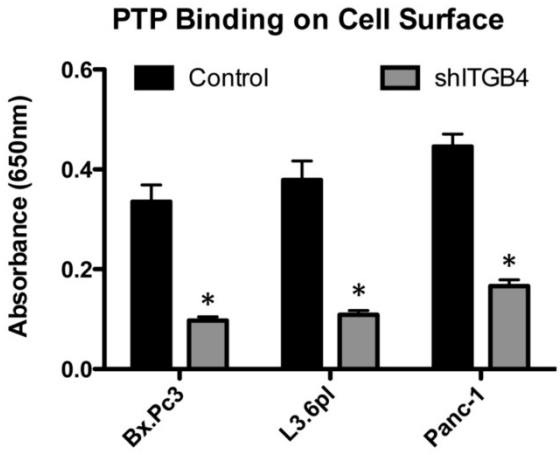

Figure 2.15. PTP binding was assessed on integrin β4-knockdown PDAC cells. *Significant to control ($p<0.0001$ for Bx.Pc3 and Panc-1, $p=0.0003$ for L3.6pl). Integrin β4-knockdown cells exhibited a 5 to 10-fold decrease in plectin expression on the cell surface.

2.3.7. Interference of plectin-integrin β4 interaction abrogates cell surface plectin localization in PDAC

Previous studies have shown that the complete N-terminal end of plectin is mainly responsible for plectin-integrin β4 interaction and that the actin binding domain (ABD), encoded by exons 2-8 have the highest affinity to actin (55). Therefore, we created a truncated form of plectin, PLEC-Trunc (including first exon 1a and the ensuing exons 2-8-encoded sequences), the overexpression of which should interfere with the localization of endogenous plectin on the PDAC cell surface by hindering plectin-integrin β4 interaction (**Fig. 2.16**). PDAC cell lines transfected with PLEC-Trunc showed a pronounced decrease in PTP binding, indicating reduced plectin on the cell surface (**Fig. 2.17**). Our results further indicate that integrin β4 is important for plectin mislocalization to the cell surface and exosomes.

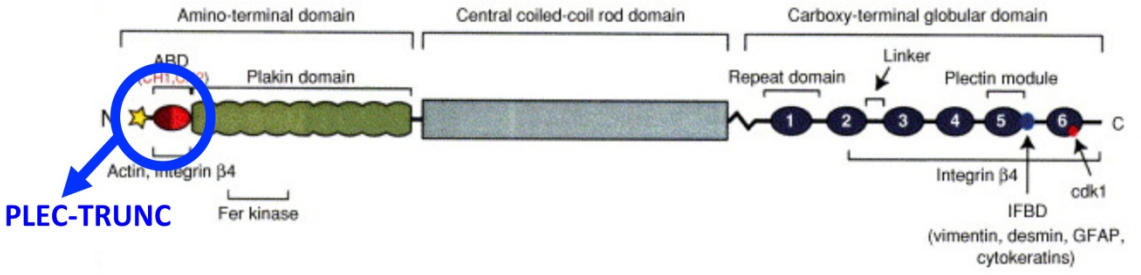

Figure 2.16. A schematic map of plectin. The plectin gene is made up of a central rod flanked by amino-terminal and carboxy-terminal domains. The N-terminal domain contains an actin-binding domain shown in red, where plectin binds integrin β4. Circled region indicates the engineered plectin (PLEC-Trunc). Reprinted and modified with permission from Elsevier Inc., *Methods Cell Biol*., Rezniczek *et al.* 2004 (51).

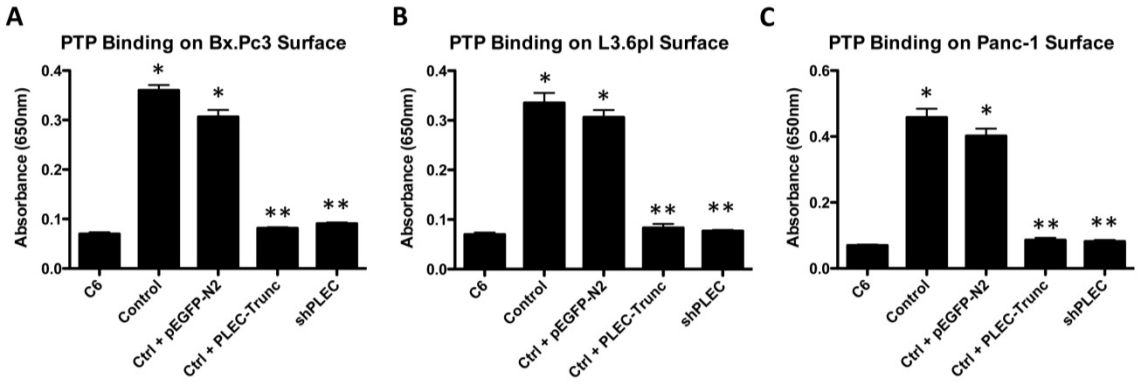

Figure 2.17. When transfected with PLEC-Trunc, plectin expression on the cell surface decreased. Cell surface expression of plectin remained reduced in both plectin-knockdown and integrin β4-knockdown cells that were transfected with PLEC-Trunc. * Significant to C6 ($p < 0.0001$), ** Significant to both control and control + pEGFP-N2 ($p < 0.0001$).

2.4. Summary and discussion

In this chapter, we validated the cell surface localization of plectin and investigated the mechanism behind plectin mislocalization in PDAC. We observed nanoparticle structures arising from the plasma membrane of PDAC cells. Based on this data and studies by Ristorecelli *et al.*, which showed that exosomes secreted from pancreatic cancer cells have spectrin and filamin (101) (known binding partners of plectin (130)), we examined whether plectin is localized on the surface of PDAC cell lines via an exosome-mediated process. We showed conclusively that plectin is localized to the cell surface and exosomes. PTP binding assay was selected because it facilitates quantification of plectin presence on the outer leaflet of plasma membrane. We showed that PDAC cell lines exhibited a significantly increased binding of PTP on the cell surface compared to that of non-transformed HPDE or C6 glioma controls. C6 serves as an excellent control because it is a transformed cancer cell line that is known to produce copious amounts of exosomes (131) and also express cytosolic plectin (38).

We also demonstrated that PDAC cell lines produce exosomes, as analyzed by dynamic light scattering (DLS), transmission electron microscopy (TEM), and immunoblotting. Exosomes produced by PDAC cells not only expressed well-characterized exosome markers, but also were plectin-positive, indicating a possibility of plectin transfer to cell surface as exosomes are known to exchange RNAs and proteins between various cell types (111). Notably, plectin was found in exosomes isolated from serum of mice bearing subcutaneous PDAC tumor. This indicates a potential for plectin as a serum marker for screening and diagnosing pancreatic cancer patients.

We showed that plectin-rich exosomes are able to transfer plectin to the surface of cells that do not normally express cell surface plectin. Additionally, overexpression of plectin isoforms 1a and 1f in C6 and HPDE cells results in plectin colocalization with the cell membrane, suggesting that plectin, normally cytoplasmic, is translocated to the cell surface when abnormally upregulated. Importantly, analysis of exosomes isolated from these transfected cells showed that exogenous plectin isoforms 1a and 1f traffic through exosomes.

Our results that plectin mislocalizes to the cell surface through exosomes in PDAC led us to investigate the determinants for plectin localization to the exosomes. Because integrin β4 an established binding partner of plectin in normal keratinocytes (40, 120), we investigated the interaction between plectin and integrin β4 through shRNA knockdown of β4. Through our analysis, we found knockdown of integrin β4 abrogated the presence of plectin in secreted PDAC exosomes, demonstrating that plectin is unable to translocate to exosomes without integrin β4. Further, we observed significantly less plectin on the cell surface after integrin β4 knockdown, as analyzed by PTP binding assay.

Further investigation on the role of plectin and its relationship with integrin β4 by using a truncated plectin construct (PLEC-Trunc) revealed that overexpressing PLEC-Trunc resulted in a significant decrease in cell surface plectin. Because PLEC-Trunc has a higher affinity to integrin β4 than full-length plectin, reduction in plectin mislocalization to the cell surface is most likely due to disruption of interaction between endogenous plectin and integrin β4.

Taken together, the results from this chapter support the hypothesis that plectin is mislocalized to the cell surface and produced through exosomes. Previously, studies have only shown mislocalization of nuclear proteins or genes to the cytoplasm or membrane proteins being abnormally internalized. This is the first study to demonstrate a novel mechanism in which a cytoplasmic protein is mislocalized to the cell surface. Due to the profound effect that plectin exhibited on PDAC cell membrane, the role that plectin may have on exosome secretion and the effect of plectin localization in the exosomes have on PDAC is explored in the next chapter.

CHAPTER 3

THE ROLE OF PLECTIN ON PDAC EXOSOME SECRETION AND TUMOR GROWTH

Works from chapters 2-4 are published in Unexpected gain of function for the scaffolding protein plectin due to mislocalization in pancreatic cancer. Shin SJ, Smith JA, Rezniczek GA, Pan S, Chen R, Brentnall TA, Wiche G, and Kelly KA. *Proc Natl Acad Sci U S A.* 2013 Nov;110(48): 19414–19419. (122)

3.1. Introduction

Various types of cells are known to produce membrane-enclosed particles, which are either secreted through exocytosis (exosomes) or directly shed from the plasma membrane (microvesicles) (132). Exosomes have been implicated in cellular movement, cell-cell signaling, tissue development and cancer. These structures communicate between cells by transferring exosomal molecules (111). Notably, tumor cells communicate with the tumor microenvironment through exosomes during the progression into a tumor mass and metastases (105, 127).

Transmission electron microscopy (TEM) analysis from chapter 2 showed that PDAC cells exhibited changes to the membrane morphology upon plectin knockdown (**Fig. 2.4**). Therefore, we hypothesized that plectin may play a role in the formation and/or secretion of exosomes in PDAC. In addition, Ostrowski *et al.* have recently shown that Rab27a and Rab27b are involved in the exosome secretory pathway (104). Specifically, they showed that silencing *RAB27A* and *RAB27B* inhibits exosome secretion without changing the protein composition of exosomes. Therefore, we used Rab27a and Rab27b knockdown PDAC cell lines to further examine their effect on exosome production and presence of plectin on the cell surface.

Lastly, exosomes differ in RNA and protein composition compared to their donor cells, and the molecular contents of exosomes have shown potential for disease prognosis and diagnosis (117). Due to exosome involvement in communication between various cancers and their microenvironment (105, 117, 127), and plectin presence in the exosomes, we investigated the proteomic difference between exosomes derived from

plectin-positive and -negative PDAC cells. As a scaffolding protein, plectin is likely to carry a complex of signaling molecules in the exosomes. Knockdown of intracellular plectin may influence protein levels in the cell, resulting in altered proteome in the exosomes, and subsequently on PDAC tumor growth.

3.2. Materials and methods

3.2.1. Cell culture

Bx.Pc3, C6, HUVEC, NIH-3T3, and Panc-1 cell lines were obtained from ATCC. Bx.Pc3 was grown in RPMI medium; C6 was grown F-12K medium; HUVEC was grown in Endothelial Basal Medium (EBM); and NIH-3T3 and Panc-1 were grown in DMEM. L3.6pl and HPDE were obtained from Dr. Craig Logsdon (University of Texas, MD Anderson Cancer Center). L3.6pl was grown in DMEM; HPDE was grown in keratinocyte medium. All media were supplemented with 10% (vol/vol) FBS, 1% pen-strep, and 1% L-glutamine except EBM (supplemented with bovine brain extract with heparin, hEGF, hydrocortisone, GA-1000, and 5% FBS), keratinocyte medium (supplemented with human recombinant EGF 1-53 and bovine pituitary extract), and F-12K medium (supplemented with 2.5% FBS, 15% horse serum, 1% pen-strep, and 1% L-glutamine).

3.2.2. Purification of exosomes

Exosomes were collected from conditioned media by standard procedures either via ultracentrifugation as previously described (101) and also ExoQuick-TC (System Biosciences). For ultracentrifugation, the conditioned media was centrifuged at 300 *g* for 5 min to remove dead cells and at 12,000 *g* for 10 min to eliminate other cellular debris. Exosomes were pelleted by ultracentrifugation at 200,000 *g* for 16 h using a 45 Ti rotor (Coulter-Beckman). The exosome pellet was resuspended in 300 μl PBS or lysis buffer. For ExoQuick-TC purification of exosomes, 10 ml of conditioned media were centrifuged at 300 *g* for 5 min to remove dead cells and at 12,000 *g* for 10 min to eliminate other cellular debris. The supernatant was then mixed with 2 ml of ExoQuick-TC and incubated at 4°C overnight. The mixture was centrifuged at 1,500 *g* for 30 min,

supernatants were removed, and centrifuged for additional 5 min to remove all fluid. The exosome pellet was resuspended in 100 µl of buffer.

3.2.3. NanoSight Exosome Characterization

Exosome characterization was performed with NS300 (NanoSight). The samples were injected in the sample chamber with sterile syringes (BD) until the liquid reached the tip of the nozzle. All measurements were performed at room temperature. The software used for capturing and analyzing the data was the Nanoparticle Tracking Analysis (NTA) Version 2.3. The samples were measured for 90 s. Three measurements of the same sample were performed for all exosome samples. Released exosomes and exosome protein content data represent mean ± SEM. Exosome size data represents mode ± SD to show the most commonly observed size of the exosome samples.

3.2.4. PTP binding on the cell surface

$1x10^4$ cells were seeded into wells of a 96-well plate and incubated at 37°C and 5% CO_2 for 24 h. The cells were washed once with PBS and fixed with 4% PFA for 10 min. The cells were blocked with 1% BSA in PBS for 1 h and incubated with 1 µM PTP in PBS-1% BSA for 2 h. Then the cells were incubated with HRP-conjugated anti-fluorescein antibodies (Invitrogen) for 30 min. After washing, the cells were incubated with TMB (Sigma) for 10 min and absorbance was measured at 650 nm.

3.2.5. Antibodies for immunoblotting

Primary antibodies were purchased from Abcam (plectin [E398P], EEF1A2 [EPR1265(B)], CD55 [EPR6689], and RPL28); R&D Systems (integrin β4 [422325]); Cell Signaling Technology (Hsp90 [C45G5]); and Proteintech (Rab27A and Rab27B). Horseradish peroxidase-conjugated secondary antibodies were purchased from R&D

Systems. Primary antibodies were diluted 1:1000 in 1% milk-TBST and secondary antibodies were diluted 1:5000 in 1% milk-TBST for immunoblotting.

3.2.6. SDS-PAGE and Immunoblotting

Cells were grown in 10-cm petri dishes (BD Falcon) to approximately 70% confluence. Cells and exosomes samples were lysed in 300 - 500 µl of lysis buffer (1% Triton X-100, 1mM EDTA, and 1mM protease inhibitor cocktail in PBS). Protein concentrations were determined using a bicinchoninic acid (BCA) protein assay kit (Thermo Scientific). Equal amounts (20 µg) of proteins in SDS sample buffer (containing β-mercaptoethanol) were resolved on 5% or 4-15% polyacrylamide gels (BioRad) and transferred onto PVDF membranes. The membranes were blocked with 1% milk-TBST, incubated with primary antibody solution for 3 h at room temperature, washed 3x5 min with TBST, incubated with secondary antibody solution for 30 min at room temperature, and washed 4x5 min with TBST. The membranes were then subjected to chemiluminescence and autoradiography.

3.2.7. Cell proliferation assay

The number of viable cells was determined by quantifying ATP presence using the CellTiter-Glo Cell Viability Luminescent Assay according to the manufacturer's protocol (Promega). Briefly, 10,000 cells were seeded into wells of an opaque-walled 96-well plate and incubated at 37°C and 5% CO_2 for 24 h. The CellTiter-Glo® Buffer and CellTiter-Glo® Substrate were thawed, equilibrated to room temperature, and mixed 1 min prior to the experiment. 100 µl of the substrate mixture was then added to each well and gently mixed and incubated for 10 min at room temperature in dark. The luminescence was recorded using FLUOstar OPTIMA microplate reader.

3.2.8. APO-BrdU TUNEL Assay

The TUNEL assay was performed according to the manufacturer's protocol (A23210, Invitrogen). Briefly, cells were washed with PBS, then fixed with 1% PFA for 15 minutes on ice, then incubated with ice-cold 70% ethanol overnight at -20°C. The cells were washed with wash buffer twice, incubated with DNA-labeling solution containing reaction buffer, TdT enzyme, and BrdUTP for 1 hour at 36°C, washed with rinse buffer twice, then incubated with antibody solution containing AlexaFluor® 488 dye–labeled anti-BrdU antibody. The cells were washed three times with rinse buffer and fluorescence was recorded using FLUOStar Omega microplate reader.

3.2.9. shRNA lentiviral transduction

Lentivirus vector encoding shRNA against human plectin was obtained from Dr. Nabeel Bardeesy (Massachusetts General Hospital and Harvard Medical School). shRNA against Rab27a and Rab27b were designed as described in Ostrowski *et al.* (104). Cells were seeded on 12-well plates and grown to 50% confluence. Old media were replaced by media containing polybrene (4 µg/ml). Plectin shRNA lentiviral particles were thawed at room temperature and gently mixed before adding to the cells. Three different ratios of virions to cells were used (1:1, 2:1, and 3:2). The infected cells were incubated overnight and media were replaced (without polybrene). Stably transfected cells were selected by puromycin (2 µg/ml for Bx.Pc3, 3 µg/ml for L3.6pl, 4 µg/ml for Panc-1) treatment. To further select stable clones, a single colony was isolated using the trypsin method (125). Downregulation of each protein was verified via immunoblot.

3.2.10. Subcutaneous tumor growth and intratumoral injection of exosomes

500,000 of the control cells were s.c. injected into the left dorsal flank of male immune-deficient nude mice. 500,000 of the Rab27a-knockdown cells were s.c. injected into the

right dorsal flanks. Tumor sizes were measured with a caliper and the volumes were calculated as $V = ab^2/2$ (a = longest diameter, b = shortest diameter). The same number of exosomes from indicated cell lines was injected into the tumors as described by Bobrie *et al.* (105). Briefly, exosomes were injected into tumors in 50 µl of PBS at 5 µg/tumor on days 3, 6, 9, 12, 15, and 18. Control tumor was injected with 50 µl of PBS on the same days. All in vivo experiments were performed according to a protocol approved by the University of Virginia Animal Care and Use Committee.

3.2.11. Migration and invasion assay

A transwell migration assay (BD Biosciences) was used to determine cell migration and invasion. Briefly, the chambers were rehydrated with serum free media at 37°C and 5% CO_2 for two hours. After rehydration, $5x10^4$ cells were plated in each chamber with serum free media. The chambers were placed into the wells containing media with 10% FBS and incubated overnight at 37°C and 5% CO_2. 8.0 µm polyethylene terephthalate (PET) membrane chambers were used for migration and matrigel-coated 8.0 µm PET membrane chambers were used for invasion. After overnight incubation, non-migrating and non-invading cells were removed from the upper membrane surface with a cotton swab. The membranes were washed with PBS, fixed with 4% PFA, and stained with 1% crystal violet in 20% ethanol. To quantify migrating and invading cells, the membranes were imaged at 40X magnification and the cell numbers were counted in 5 different fields of view in triplicate (15 measurements total for each group). Percent invasion was determined as number of invading cells / number of migrating cells x 100.

3.2.12. Human phospho-kinase array

The phospho-kinase array analysis was performed using the Proteome Profiler (R&D Systems) according to the manufacturer's instructions. Briefly, cells and purified

exosomes were lysed with Lysis Buffer 6 (R&D Systems) and agitated for 30 min at 4°C. The array membranes were blocked with Array Buffer 1 (R&D Systems) for 1 h and incubated with 350 µg of cell and exosome lysates overnight at 4°C on a rocking platform. The membranes were then washed 3x10 min with 1X Wash Buffer (R&D Systems), incubated with biotinylated detection antibodies for 2 h at room temperature, washed 3x10 min with 1X Wash Buffer (R&D Systems), and incubated with streptavidin-HRP secondary antibodies for 30 min at room temperature. Chemiluminescence and autoradiography were used to detect spot densities. Array images were analyzed using ImageJ densitometry tool.

3.2.13. Sample preparation for proteomics analysis

150 µg of each exosome sample was diluted with 50 mM ammonium bicarbonate buffer. Samples were then reduced with 10 mM DTT for 1 hour at 50°C, alkylated with 25mM iodoacetamide for 30 min at room temperature in dark, and reduced again with 10 mM DTT for 15 min at room temperature. Samples were loaded onto 3 kDa filter (Millipore) to concentrate and to wash twice with 50 mM sodium bicarbonate buffer. After washes, sample volumes were adjusted to 80 µl and digested with trypsin at 1:50 ratio for 18 hours at 37°C. After digestion, samples were collected by reverse spin and the filters were washed twice with 80 µl 100mM sodium acetate buffer, pH5.5. For each cell line, the sample was combined with the washes and the pH was adjusted to pH5.5 with 10% acetic acid. The parental L3.6pl exosome sample was labeled with formaldehyde-H2 (light-label) and L3.6pl shPLEC exosome sample was labeled with formaldehyde-D2 (heavy-label), respectively. To label each sample, 5 µl of 20% labeling agent was added to the samples, immediately followed by addition of 5 µl of freshly prepared 3 M sodium cyanoborohydride solution. The samples were incubated for 15 minutes at the room temperature, with vigorous vortex every few minutes. The light- and heavy-labeled

samples were combined and purified through C18 purification columns (the Nest Group, Inc., Southborough, MA) following the manufacturer's instructions.

3.2.14. Mass spectrometry analysis

An LTQ-Orbitrap Elite mass spectrometer (Thermo Fisher Scientific, Waltham, MA) coupled with a nano-flow HPLC (Eksigent Technologies, Dublin, CA) was used in this study. 1.5 µg of sample was injected for the mass spectrometric analysis. The samples were first loaded onto a 1.5 cm trap column (IntegraFrit 100 µm, New Objective, Woburn, MA) packed with Magic C18AQ resin (5 µm, 200Å particles; Michrom Bioresources, Auburn, CA) with Buffer A (D.I. water with 0.1% formic acid) at a flow rate of 3 µL/minute. The peptide samples were then separated by a 27cm analytical column (PicoFrit 75µm, New Objective) packed with Magic C18AQ resin (5 µm, 100Å particles; Michrom Bioresources) followed by mass spectrometric analysis. A 60-minute non-linear LC gradient was used as follows: 5% to 7% Buffer B (acetonitrile with 0.1% formic acid) versus Buffer A over 2 minutes, then to 35% over 60 minutes. The flow rate for the peptide separation was 300 nL /minute. The mass spectrometry method consisted of 1 MS scan followed by 10 data dependent MS/MS scans. The MS1 scan was collected in the Orbitrap at a resolution of 120,000 in the profile mode (m/z range of 400-1800). The dynamic exclusion settings were as follows: repeat count of 1, repeat duration of 15 seconds, exclusion list size of 500, exclusion duration of 30 seconds, with an exclusion mass width of 10 ppm. The preview mode for the Fourier Transform Mass Spectrometry (FTMS) master scans function was enabled, and charge state screening was enabled to reject charge states +1 and +4. Monoisotopic precursor selection was also enabled. The collision-induced dissociation (CID) fragmentation parameters were as follows: default charge state was 2+, Isolation width of 2.0m/z, normalized collision energy set at 35.0, activation Q was 0.25 and the activation time was 10 msec.

3.2.15. Mass Spectrometry Data analysis

Raw machine output files of MS/MS spectra were converted to mzXML files and searched with X!Tandem (133) configured with the k-score scoring algorithm (134), against the UniProt human database. The search parameters were therefore as follows: enzyme: trypsin; maximum missed cleavages: 1; static modifications: carboxamidomethylation on cysteine, light dimethyl on N-terminus and lysine; dynamic modifications: oxidation on methionine, difference between light and heavy dimethyl labeled on N-terminus and lysine; parent monoisotopic mass tolerance: 2.5 Da. Peptide identifications were assigned probability by PeptideProphet (135). Relative quantitation of heavy and light peptide abundance was performed with Xpress (136) version 2.1. Proteins present in sample were inferred using ProteinProphet (135). To minimize interassay variation, the two exosome samples were labeled with different stable isotopes, combined and analyzed together simultaneously in a single measurement for quantitative comparison.

3.2.16. Statistical analysis

All statistical analyses were performed using Prism (GraphPad Software, Inc., La Jolla, CA). Results are presented as mean ± standard error of the mean (SEM), unless otherwise noted. All statistical analyses were performed using a one-way general linear ANOVA, followed by Tukey's test for pairwise comparisons. Significance was asserted at $p < 0.05$.

3.3. Results

3.3.1. Nanoparticle tracking analysis (NTA) via NanoSight

Analysis via TEM showed that L3.6pl cells exhibited changes to the membrane morphology upon plectin knockdown via shRNA (**Fig. 2.4**). Cells with plectin knockdown have membranes that, in appearance, resemble those of the more normal HPDE cells, rather than those of cancerous cells. Based on this observation, we investigated whether plectin affects various exosomal characteristics in PDAC cells. In assessing the size of PDAC exosomes, NanoSight analysis showed similar results as DLS (**Fig. 2.6**) (57.67 ± 20.00 nm) (**Fig. 3.1A**). Additionally, PDAC cells produced >10-fold higher amounts of exosomes compared to HPDE (**Fig. 3.1B**). Conditioned medium from keratinocytes, cells that are rich in cytosolic plectin, did not yield enough exosomes to be detected via NanoSight. We also discovered that knockdown of plectin decreased exosome production by ~5-fold in all three PDAC cell lines tested, indicating a possible role of plectin in efficient PDAC exosome production. Interestingly, although HPDE cells produce less exosomes, the exosomes were larger in size than PDAC exosomes. We also analyzed exosomes from the indicated cell lines for protein content. Plectin knockdown resulted in decreased exosmal protein content in all three cell lines tested (**Fig. 3.1C**).

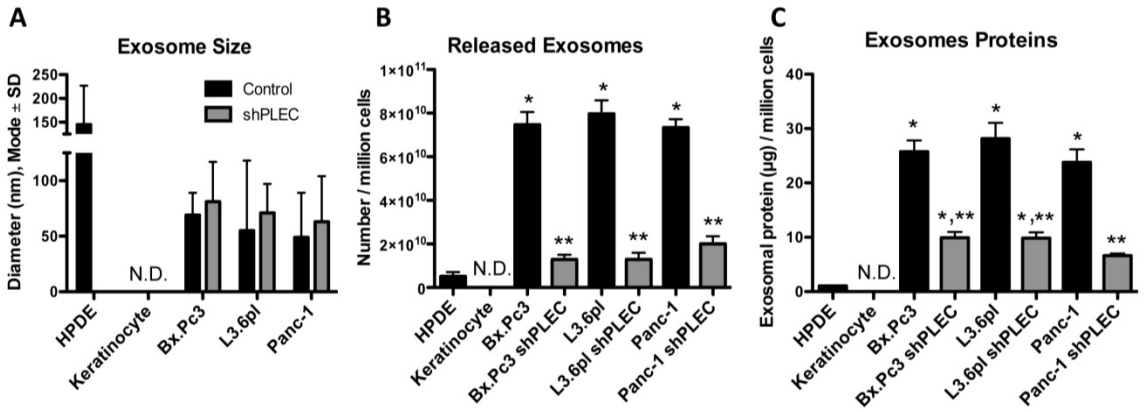

Figure 3.1. Nanoparticle tracking analysis (NTA) via NanoSight. **A)** Exosomes size in diameter (mode ± SD), **B)** Number of exosomes released per million cells, **C)** Amount of proteins present in exosomes. *Significant to HPDE ($p < 0.0001$), **Significant to parental controls ($p < 0.0001$), ND = Not detectable.

3.3.2. Plectin knockdown reduces exosome secretion in PDAC

Ostrowski *et al.* have recently shown that Rab27a and Rab27b are involved in the exosome secretory pathway (104). Specifically, silencing *RAB27A* and *RAB27B* inhibits exosome production without changing exosomal protein composition. Therefore, we created Rab27a and Rab27b knockdown PDAC cell lines as controls to compare exosome formation and the amount of exosomes produced against plectin-knockdown cells. As expected, Rab27a and Rab27b-knockdown PDAC cells both demonstrated a decrease in exosome production (**Fig. 3.2**). Plectin knockdown resulted in a similar decrease in exosome production, again indicating that plectin plays a role in the formation and/or secretion of exosomes in PDAC.

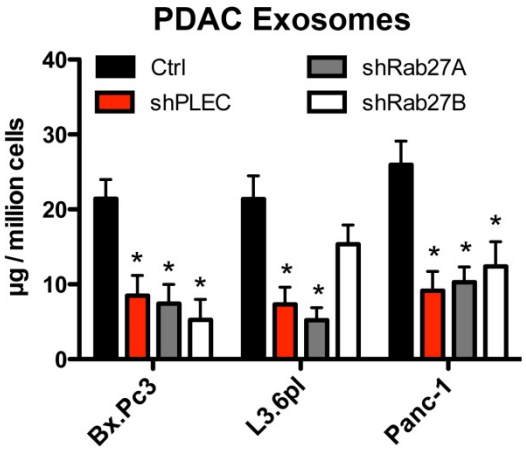

Figure 3.2. Rab27a, Rab27b, and plectin knockdown decreases exosome production. *Significant to control ($p < 0.0001$).

To investigate the potential of plectin cell surface localization through an exosome mediated mechanism, we applied the PTP binding assay to Rab27a knockdown cells. Rab27a knockdown resulted in significantly decreased exosome formation as well as PTP binding (**Fig. 3.3**). Indeed, the levels of PTP binding to Rab27a knockdown cells were similar to that of plectin knockdown cells. However, knockdown of Rab27a and b did not influence plectin expression (**Fig. 3.4**). Similarly, plectin knockdown had no effect on Rab27a or b expression, indicating that lack of plectin cell surface localization due to Rab27a knockdown is not due to decreased plectin expression.

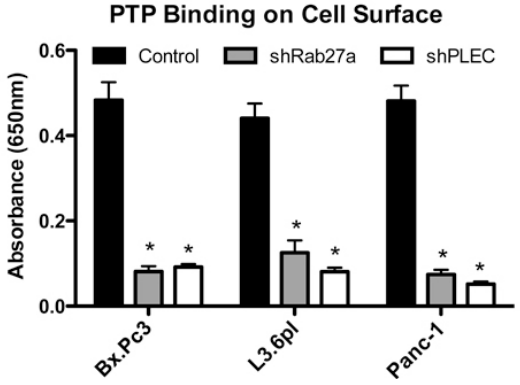

Figure 3.3. Rab27a knockdown decreases cell-surface PTP binding. *Significant to control ($p < 0.0001$).

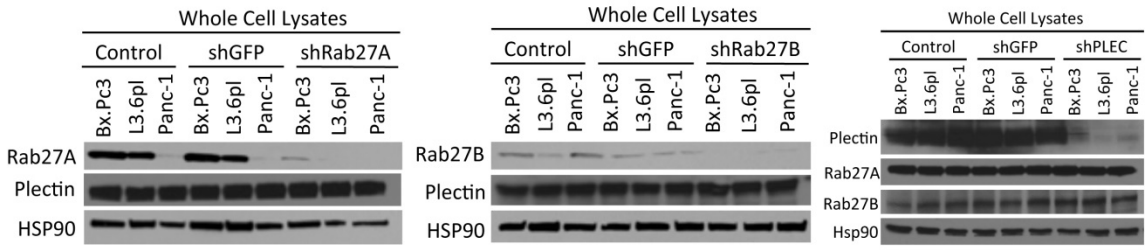

Figure 3.4. Immunoblot analysis showing that Rab27A and Rab27B knockdown does not affect plectin expression levels. Plectin knockdown also does not affect Rab27A/B expression levels.

3.3.3. Overexpression of plectin-1a and 1f increases exosome secretion

Next, we tested whether different plectin isoforms affected exosome secretion in HPDE cells (**Fig. 3.5A**), which produce significantly less exosomes compared to PDAC cells (**Fig. 3.1B**). We also examined whether plectin isoforms affect exosome secretion in PDAC cells that already produce abundant exosomes (**Fig. 3.5B-D**). The cells were transfected with pDS89 (full-length plectin-1), pDS94 (full-length plectin-1c), pGR244 (EGFP-tagged mouse plectin-1a), or pGR258 (EGFP-tagged mouse plectin-1f. We found that although plectin-1a overexpression led to a 1.6-fold increase in exosome production in HPDE, it was not to the level of PDAC cells, which were >10-fold higher than HPDE (**Fig. 3.1B**). Similarly, plectin-1f overexpression resulted in only a 1.2-fold increase. Our results indicate that plectin-1a overexpression can induce HPDE cells to produce more exosomes, but plectin-1a alone is not sufficient to produce exosomes to the level of cancer cells. This is further explained by the absence of exosomes in the case of keratinocytes that express high levels of plectin-1a (**Fig. 3.1**) (64, 65). Interestingly, overexpressing plectin-1a and 1f also increase the ability of PDAC cells to produce exosomes. Therefore, plectin-1a/1f overexpression can further induce cancer cells to produce exosomes, suggesting that these isoforms may be the key players in plectin mislocalization and possibly PDAC progression. Similar to HPDE, plectin-1 and plectin-1c overexpression did not result in significant changes.

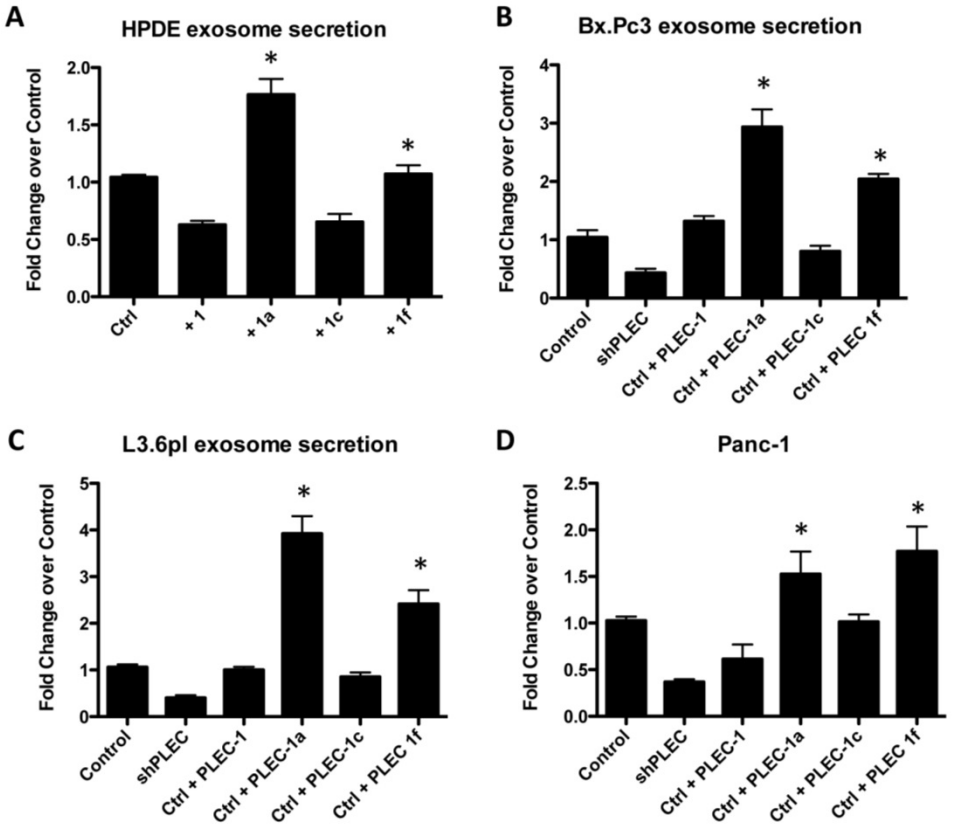

Figure 3.5. Exosome secretion from **A)** HPDE, **B)** Bx.Pc3, **C)** L3.6pl, and **D)** Panc-1 transfected with plectin-1, 1a, 1c, or 1f. *Significant to control ($p<0.0001$).

3.3.4. Plectin-positive exosomes restore the growth of tumors that lack the exosome machinery

Our findings that plectin is an exosomal protein and that exosomes have the ability to transfer cell-surface plectin led us to investigate whether plectin-positive exosome secretion had phenotypic consequences on PDAC cells. We used the exosome impaired cells that we created with shRNA knockdown of Rab27a and Rab27b. Interfering with exosome secretion through Rab27a knockdown resulted in a delay in PDAC cell growth *in vitro* (**Fig. 3.6**) as well as *in vivo* (**Fig. 3.7**). As shown in **Fig. 3.4**, these cells are still plectin-positive, do not display cell surface plectin (**Fig. 3.3**), and produce significantly lower amounts of exosomes (**Fig. 3.2**). Because Rab27a knockdown resulted in a more significant decrease to exosome secretion compared to Rab27b knockdown (**Fig. 3.2**),

only the Rab27a-knockdown cells were used for *in vivo* studies. To determine if Rab27a knockdown alone was inhibiting growth of the tumors we injected plectin-rich exosomes purified from control L3.6pl cells intratumorally into L3.6pl-derived tumors as described in Bobrie *et al.* (5 µg resuspended in 50 µl PBS) (105). Remarkably, not only was tumor growth rescued by plectin-containing exosomes, but the rate of tumor growth was greater than that of the control tumors with endogenous plectin indicating the dramatic impact of plectin-rich exosomes on tumor growth. Growth of Rab27a knockdown tumors injected with plectin-negative exosomes or PBS was indistinguishable from untreated Rab27a knockdown tumors. Thus, exogenous plectin-rich exosomes are sufficient to restore growth in tumors in which exosome secretion is impaired.

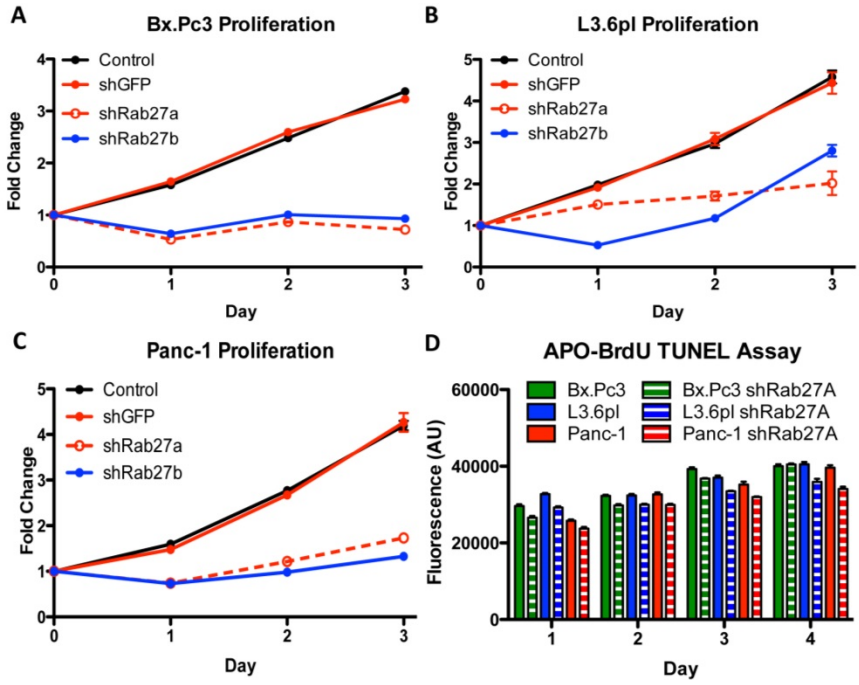

Figure 3.6. shRab27a/b decreases PDAC proliferation. **A)** Bx.Pc3, **B)** L3.6pl, **C)** Panc-1, and **D)** corresponding APO-brdU assay results.

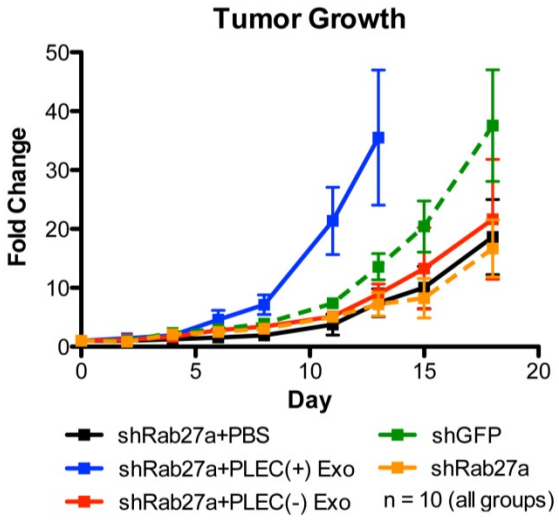

Figure 3.7. Plectin-rich exosomes enhanced the growth of L3.6pl shRab27a tumors while plectin-negative exosomes did not have any effect on tumor growth (n=10).

Rab27a silencing also affected migration and invasion, albeit in the latter case its effect was less pronounced (**Fig. 3.8**). Overall, these results indicate that exosomes as well as plectin localized in these exosomes are important factors in pancreatic cancer growth and progression.

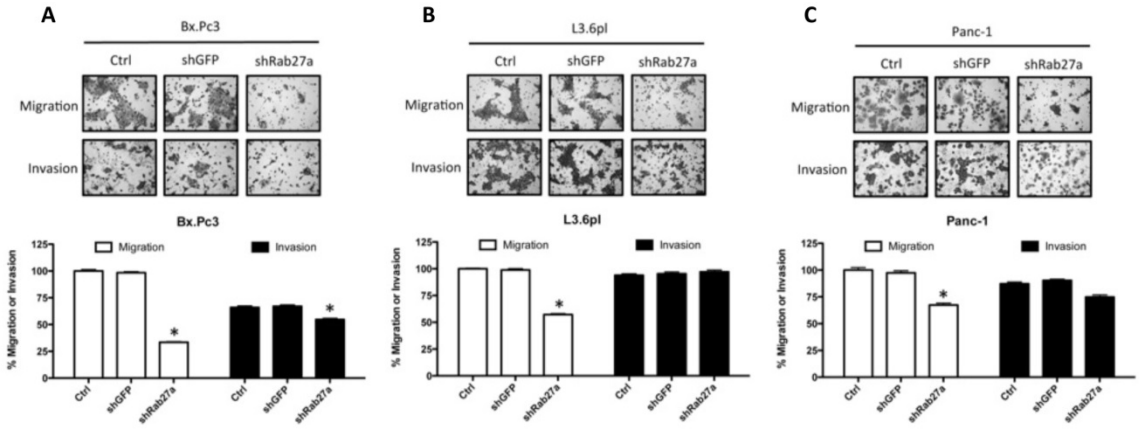

Figure 3.8. Migration and invasion of Rab27a-knockdown cells. **A)** Bx.Pc3, **B)** L3.6pl, and **C)** Panc-1. Inhibiting exosome formation via Rab27a knockdown exhibited significantly lower migration in all three cell lines. *Significant to both control and shGFP ($p < 0.0001$).

3.3.5. Plectin-positive and –negative exosomes derived from PDAC have differential and biologically active molecules

Our results showed that plectin-positive exosomes have a functional role in the growth of pancreatic tumor. It is possible that plectin, as a scaffolding protein, complexes with various molecules and signaling proteins to promote pathogenesis. In an initial approach, we used a phospho-antibody array (Phospho-Kinase Array, Proteome Profiler Array Kit, R&D Systems) to investigate changes in a subset of phosphorylation events after plectin knockdown in both whole cell lysates and purified exosomes (**Fig. 3.9**). Interestingly, there were a number of phospho-kinases that were more active in L3.6pl shPLEC exosomes compared to control exosomes. These include AKT (T308), p53 (S392 and S46), and p70 S6K (T421/S424). Due to the role of exosome-localized plectin in pancreatic tumor growth (**Fig. 3.7**), the knockdown of plectin may be affecting tumor suppressor proteins. In whole cell lysates, AKT (S473) was significantly more active. The only protein expression that was decreased in plectin-knockdown was β-catenin in whole cell lysates. Previous research has shown that the Wnt/β-catenin signaling pathway is aberrantly activated in pancreatic cancer and also involved in pancreatic cancer chemoresistance (137, 138). Further studies should be conducted to investigate the role that plectin has on the proteome of PDAC exosomes.

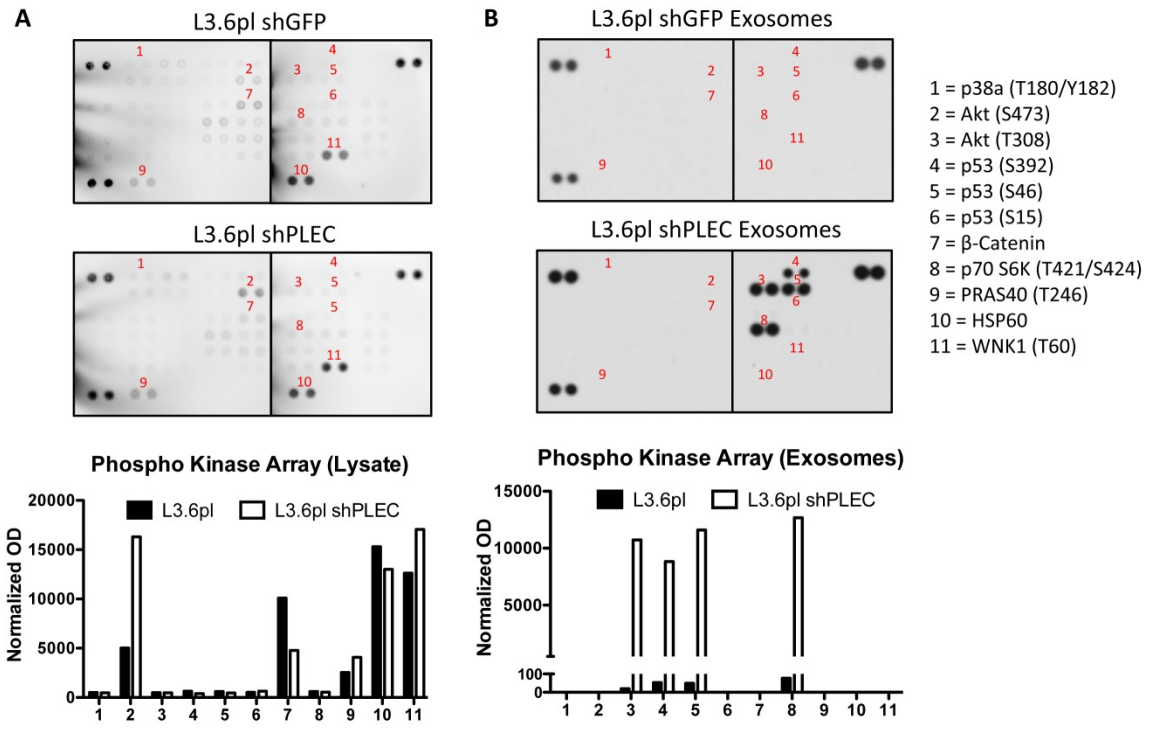

Figure 3.9. Proteome profile of phospho-kinases in L3.6pl vs. L3.6pl shPLEC. **A)** Cell lysates, **B)** exosomes.

Furthermore, we performed a quantitative mass spectrometry analysis to compare the differences in the proteome of plectin-positive and -negative PDAC exosomes. In a comparison of exosomes from L3.6pl with L3.6pl shPLEC, 345 non-redundant proteins were identified (ProteinProphet score ≥0.85, FDR 1.5%). Among them, 34 proteins were overexpressed in L3.6pl exosomes with 2-fold or greater changes when compared to L3.6pl shPLEC exosomes (**Table 3.1**, 2-fold or higher overexpression is denoted in blue). 18 proteins were underexpressed in L3.6pl exosomes with 2-fold or greater changes (**Table 3.2**, 2-fold or higher underexpression is denoted in red). Plectin was significantly depleted in L3.6pl shPLEC exosomes with an 8-fold decrease in abundance compared L3.6pl which serves as an important internal control (**Table 3.1**).

Table 3.1. List of proteins from control and plectin-knockdown L3.6pl exosome mass spectrometry analysis with control/shPLEC ratio greater than 1. 2-fold or higher changes are shown in blue (overexpressed in control).

Gene Name	Protein Description	Ctrl/shPLEC
SACM1L	SAC1 Suppressor Of Actin Mutations 1-Like	20.43
RPL15	60S ribosomal protein L15	13.79
PLEC1	**Plectin**	**8.06**
EEF1A2	Elongation factor 1-alpha 2	7.99
KIF4A	Chromosome-associated kinesin KIF4A	7.42
SERPINE2	SERPINE2 protein, Glia-derived nexin	6.64
VWF	Von Willebrand factor	5.71
RPL8	60S ribosomal protein L8	4.87
C7	Complement component C7 precursor	4.37
DKFZp434N1526	NF-kappa-B inhibitor-interacting Ras-like protein 2	3.83
SERPINF1	Serpin peptidase inhibitor, clade F	3.80
RAN	GTP-binding nuclear protein Ran	3.52
UBE1	Ubiquitin-activating enzyme E1	3.28
HBG2, HBE1	HBE1 protein, PRO2979, Hemoglobin, gamma A	3.08
ADRM1	Proteasomal ubiquitin receptor ADRM1	3.01
EEF1B2	Elongation factor 1-beta	2.97
APP	amyloid beta (A4) precursor protein	2.96
AKR1C2	Aldo-keto reductase family 1, member C2	2.95
HMCN1	Hemicentin-1	2.93
SPOCK1	Testican-1	2.54
CCT3	T-complex protein 1 subunit gamma	2.26
KRT10	Keratin 10	2.24
STC1	Stanniocalcin-1	2.18
RRM1	Ribonucleoside-diphosphate reductase large subunit	2.17
IDH1	Isocitrate dehydrogenase 1 (NADP+), soluble	2.17
RPS20	40S ribosomal protein S20	2.16
EEF1D	Eukaryotic Translation Elongation Factor 1 Delta	2.11
RPS3A	Ribosomal Protein S3A	2.11
SYNCRIP	Synaptotagmin Binding, Cytoplasmic RNA Interacting Protein	2.09
HSPA9B	Heat shock 70kDa protein 9B	2.07
C5	Complement component 5	2.05
PCBP1	Poly(rC)-binding protein 1	2.03
MAT2A	Methionine Adenosyltransferase II, Alpha	2.02
XRCC5	X-Ray Repair Complementing Defective Repair In Chinese Hamster Cells 5	2.00
GPI	Glucose-6-phosphate isomerase	1.99
PPP1CB	Protein Phosphatase 1, Catalytic Subunit, Beta Isozyme	1.97
NOLC1	Nucleolar And Coiled-Body Phosphoprotein 1	1.92

KRT1	Keratin 1	1.91
EEF1A1	Eukaryotic Translation Elongation Factor 1 Alpha 1	1.90
XRCC6	X-Ray Repair Complementing Defective Repair In Chinese Hamster Cells 6	1.87
RPL10A	60S ribosomal protein L10a	1.85
RPS4X	40S ribosomal protein S4, X isoform	1.83
GAPD	Glyceraldehyde 3-phosphate dehydrogenase	1.82
PDIA6	Protein Disulfide Isomerase Family A, Member 6	1.81
FST	Follistatin	1.81
YBX1	Y Box Binding Protein 1	1.81
FLNB	Filamin B, Beta	1.80
MDH2	Malate Dehydrogenase 2, NAD (Mitochondrial)	1.78
KTN1	Kinectin 1 (Kinesin Receptor)	1.77
ATIC	5-Aminoimidazole-4-Carboxamide Ribonucleotide Formyltransferase/IMP Cyclohydrolase	1.75
EPRS	Glutamyl-Prolyl-TRNA Synthetase	1.73
PRDX3	Peroxiredoxin 3	1.72
ETF1	Eukaryotic Translation Termination Factor 1	1.70
RP11-102M16.2	PAI-1 mRNA-binding protein	1.69
HNRPA1	Heterogeneous nuclear ribonucleoprotein A1	1.69
S100A6	Protein S100-A6	1.69
EIF2S1	Eukaryotic translation initiation factor 2 subunit 1	1.68
SNRPD1	Small Nuclear Ribonucleoprotein D1	1.68
RPS2	40S Ribosomal Protein S2	1.67
PFN1	Profilin 1	1.65
HSPA4	Heat shock 70kDa protein 4	1.65
LGALS3BP	Lectin, Galactoside-Binding, Soluble, 3 Binding Protein	1.64
EPPK1	Epiplakin 1	1.62
KRT17	Keratin 17	1.61
RPL3	60S ribosomal protein L3	1.59
EEF1G	Elongation factor 1-gamma	1.58
ENO1	Enolase 1, (Alpha)	1.56
A2M	Alpha-2-Macroglobulin	1.54
CLSTN1	Calsyntenin 1	1.54
RPL7	60S ribosomal protein L7	1.53
ACTR3	ARP3 Actin-Related Protein 3 Homolog	1.51
RPL29	60S ribosomal protein L29	1.51
KPNB1	Importin subunit beta-1	1.51
NME2	Nucleoside diphosphate kinase B	1.50
ECHS1	Enoyl Coenzyme A hydratase, short chain, 1, mitochondrial	1.50
ALB	Albumin	1.49
HMGN1	Non-histone chromosomal protein HMG-14	1.49
SUB1	Activated RNA polymerase II transcriptional coactivator p15	1.48

NCL	Nucleolin	1.48
RAP1B	Ras-related protein Rap-1b	1.48
ARFGEF3	Brefeldin A-inhibited guanine nucleotide-exchange protein 3	1.48
HNRPK	Heterogeneous nuclear ribonucleoprotein K	1.47
PGK1	Phosphoglycerate Kinase 1	1.47
KRT9	Keratin 9	1.46
AHCY	Adenosylhomocysteinase	1.45
QSCN6	quiescin Q6 sulfhydryl oxidase 1	1.45
SMC3	Structural maintenance of chromosomes 3	1.44
RPS8	40S ribosomal protein S8	1.44
PZP	Pregnancy-Zone Protein	1.43
SQSTM1	Sequestosome 1	1.43
ALDOA	Aldolase A, Fructose-Bisphosphate	1.42
KRT5	Keratin 5	1.42
EIF5A	Eukaryotic translation initiation factor 5A-1	1.42
RPLP1	60S acidic ribosomal protein P1	1.41
CAND1	Cullin-associated NEDD8-dissociated protein 1	1.41
TPI1	Triosephosphate isomerase	1.40
PYGL	Phosphorylase, Glycogen, Liver	1.40
MRLC3	Myosin regulatory light chain 12A	1.40
F2	coagulation factor II (thrombin)	1.39
GSTP1	Glutathione S-transferase P	1.39
RPS3	40S ribosomal protein S3	1.38
RPSA	40S ribosomal protein SA	1.38
PRDX5	Peroxiredoxin-5, mitochondrial	1.38
LDHB	Lactate Dehydrogenase B	1.37
PKM2	Pyruvate kinase isozymes M1/M2	1.37
PGAM1	Phosphoglycerate Mutase 1 (Brain)	1.37
EIF3H	Eukaryotic translation initiation factor 3 subunit H	1.37
SLC7A5	Solute carrier family 7 member 5	1.37
TUBB2C	Tubulin beta-4B chain	1.36
HBA2	Hemoglobin, alpha 2	1.36
PSMD2	26S proteasome non-ATPase regulatory subunit 2	1.36
RAB1A	RAB1A, Member RAS Oncogene Family	1.35
COPA	Coatomer subunit alpha	1.34
RPLP2	60S acidic ribosomal protein P2	1.32
YWHAE	14-3-3 protein epsilon	1.32
VDAC2	Voltage-dependent anion-selective channel protein 2	1.32
SUPT6H	Transcription elongation factor SPT6	1.32
PTMA	Prothymosin, alpha	1.31
SLC25A6	ADP/ATP translocase 3	1.31
KRT2	Kertain 2	1.31

ATP5F1	ATP synthase subunit b, mitochondrial	1.31
LTBP4	Latent Transforming Growth Factor Beta Binding Protein 4	1.30
PDIA3	Protein disulfide isomerase family A, member 3	1.30
H2AFX	H2A histone family, member X	1.29
RPL9	60S ribosomal protein L9	1.29
CLEC11A	C-type lectin domain family 11 member A	1.28
TUBA1B	Tubulin alpha-1B chain	1.28
PTPRS	Receptor-type tyrosine-protein phosphatase S	1.28
COL6A1	Collagen, type VI, alpha 1	1.27
HNRNPA2B1	Heterogeneous nuclear ribonucleoprotein A2/B1	1.27
SFN	14-3-3 protein sigma	1.26
RPL6	60S ribosomal protein L6	1.26
NPM1	Nucleophosmin	1.24
C4A	Complement C4-A	1.24
MYH9	Myosin, heavy chain 9, non-muscle	1.24
HNRPU	Heterogeneous nuclear ribonucleoprotein U	1.23
FAT2	FAT tumor suppressor homolog 2	1.23
HSPD1	Heat shock 60kDa protein 1	1.22
YWHAB	14-3-3 protein beta/alpha	1.22
FASN	Fatty acid synthase	1.21
AHSG	Alpha-2-HS-glycoprotein	1.21
HSP90AB1	Heat shock protein 90kDa alpha (cytosolic), class B member 1	1.21
EEF2	Eukaryotic elongation factor 2	1.21
SET	Protein SET	1.21
HYOU1	Hypoxia up-regulated protein 1	1.20
TRIP11	Thyroid receptor-interacting protein 11	1.20
COMP	Cartilage oligomeric matrix protein	1.19
CFL1	Cofilin 1 (non-muscle; n-cofilin)	1.19
PRDX2	Peroxiredoxin-2	1.19
ANXA6	Annexin A6	1.19
ITIH3	Inter-alpha-trypsin inhibitor heavy chain H3	1.18
CALR	Calreticulin	1.18
SLC3A2	4F2 cell-surface antigen heavy chain	1.17
TUBB2A	Tubulin beta-2A chain	1.17
KRT13	Keratin 13	1.17
ATP5B	ATP synthase subunit beta, mitochondrial i	1.16
MYL6	Myosin light polypeptide 6	1.16
FSCN1	Fascin	1.16
RPL18	60S ribosomal protein L18	1.16
LAMB2	Laminin subunit beta-2	1.16
ANXA1	Annexin A1	1.15
LAMA3	Laminin, Alpha 3	1.15

GSN	Gelsolin	1.14
HSPCA	Heat Shock Protein 90kDa Alpha (Cytosolic), Class A Member 1	1.14
TKT	Transketolase	1.14
CSE1L	CSE1 Chromosome Segregation 1-Like	1.14
SMOC1	SPARC Related Modular Calcium Binding 1	1.14
TUBB1	Tubulin beta-1 chain	1.13
HNRNPAB	Heterogeneous nuclear ribonucleoprotein A/B	1.13
HIST1H1B	Histone H1.5	1.13
PSMD5	26S proteasome non-ATPase regulatory subunit 5	1.13
RPS6	Ribosomal protein S6	1.13
THBS1	Thrombospondin 1	1.12
TLN1	Talin-1	1.12
DDX48	Eukaryotic Translation Initiation Factor 4A3	1.12
PSMB3	Proteasome subunit beta type-3	1.12
BASP1	Brain acid soluble protein 1	1.11
P4HB	Protein disulfide-isomerase	1.11
GDI2	Rab GDP dissociation inhibitor beta	1.11
ACTG1	Actin, gamma 1	1.10
CLEC3B	Tetranectin	1.09
PAICS	Phosphoribosylaminoimidazole Carboxylase, Phosphoribosylaminoimidazole Succinocarboxamide Synthetase	1.09
FBLN1	Fibulin-1	1.09
ZFP106	Zinc finger protein 106 homolog	1.09
CALM3	Calmodulin 3	1.08
PDCD6IP	Programmed cell death 6-interacting protein	1.08
NUP133	Nuclear pore complex protein Nup133	1.08
CCT6A	T-complex protein 1 subunit zeta	1.07
AGRIN	Agrin	1.07
COL6A3	Collagen, type VI, alpha 3	1.07
CLU	Clusterin	1.07
RPL4	60S ribosomal protein L4	1.07
LAMA5	Laminin, Alpha 5	1.06
RPL22	60S ribosomal protein L22	1.06
NUMA1	Nuclear Mitotic Apparatus Protein 1	1.06
ADAMTS-13	A disintegrin and metalloproteinase with a thrombospondin type 1 motif, member 13	1.06
FLNA	Filamin A, alpha	1.05
RAB10	Ras-related protein Rab-10	1.05
TUBA4A	Tubulin alpha-4A chain	1.05
VTN	Vitronectin	1.05
MSN	Moesin	1.04
IMPDH2	Inosine-5'-monophosphate dehydrogenase 2	1.04
ATP5A1	ATP Synthase, H+ Transporting, Mitochondrial F1 Complex, Alpha	1.03

	Subunit 1, Cardiac Muscle	
CCT7	T-complex protein 1 subunit eta	1.03
C3	Complement component 3	1.02
APOC3	Apolipoprotein C-III	1.02
COL2A1	Collagen, type II, alpha 1	1.02
KRT8	Keratin 8	1.02
CKB	Brain-type creatine kinase	1.02
F13A1	Coagulation Factor XIII, A1 Polypeptide	1.01
HIST1H3A	Histone H3.1	1.01
PHB	Prohibitin	1.01
ARF5	ADP-ribosylation factor 5	1.01

Table 3.2. List of proteins from control and plectin-knockdown L3.6pl exosome mass spectrometry analysis with control/shPLEC ratio less than 1. 2-fold or higher changes are shown in red (underexpressed in control).

Gene Name	Protein Description	Ctrl/shPLEC
COBL	Cordon-Bleu WH2 Repeat Protein	0.04
YWHAG	14-3-3 protein gamma	0.06
DMBT1	Deleted in malignant brain tumors 1 protein	0.08
COL4A1	Collagen, type IV, alpha 1	0.08
RPS9	40S ribosomal protein S9	0.16
COL4A2	Collagen alpha-2(IV) chain	0.18
COL1A1	Collagen, type I, alpha 1	0.27
SERPINH1	Heat shock protein 47	0.29
APOE	Apolipoprotein E	0.30
RPL10	60S ribosomal protein L10	0.31
NAP1L1	Nucleosome assembly protein 1-like 1	0.33
SERPINC1	Serpin Peptidase Inhibitor, Clade C, Antithrombin	0.34
PRDX1	Peroxiredoxin-1	0.37
TUFM	Elongation factor Tu, mitochondrial	0.40
CD55	CD55 Molecule, Decay Accelerating Factor For Complement	0.41
SLC2A1	Solute Carrier Family 2 (Facilitated Glucose Transporter), Member 1	0.42
RPL28	60S ribosomal protein L28	0.47
PYCARD	Apoptosis-associated speck-like protein containing a CARD or ASC	0.50
TFRC	Transferrin receptor protein 1	0.52
FGFBP1	Fibroblast growth factor-binding protein 1	0.52
ANXA5	Annexin A5	0.53
VCP	Valosin-containing protein	0.54
PSMA8	Proteasome (Prosome, Macropain) Subunit, Alpha Type, 8	0.55
CANX	Calnexin	0.55
GANAB	Neutral alpha-glucosidase AB	0.55
TINAGL1	Tubulointerstitial nephritis antigen-like	0.55
HIST1H4A	Histone H4	0.56
SDC4	Syndecan-4	0.56
IGF2R	Insulin-Like Growth Factor 2 Receptor	0.57
YWHAQ	14-3-3 protein theta	0.58
APOM	Apolipoprotein M	0.58
SDCBP	Syntenin-1	0.59
COLEC11	Collectin Sub-Family Member 11	0.59
MYO18B	Myosin-XVIIIb	0.60
KIF23	Kinesin-like protein KIF23	0.61
HTRA1	Serine protease HTRA1	0.62
APMAP	Adipocyte Plasma Membrane Associated Protein	0.62
CTSD	Cathepsin D	0.63

HIST2H3A	Histone Cluster 2, H3a	0.64
EFEMP1	EGF-containing fibulin-like extracellular matrix protein 1	0.64
POF1B	Premature Ovarian Failure, 1B	0.64
SNX29	Sorting Nexin 29	0.65
HSPE1	Heat Shock 10kDa Protein 1	0.66
RPS7	40S ribosomal protein S7	0.67
TACSTD1	Tumor-associated calcium signal transducer 1	0.67
BANF1	Barrier To Autointegration Factor 1	0.68
CCT4	Chaperonin Containing TCP1, Subunit 4 (Delta)	0.68
TXN	Thioredoxin	0.68
IGF2	Insulin-like growth factor 2	0.69
GNB4	Guanine Nucleotide Binding Protein (G Protein), Beta Polypeptide 4	0.71
KIF5B	Kinesin-1 heavy chain	0.72
KIAA1199	Protein KIAA1199	0.73
HSPA1B	Heat shock 70kDa protein 1B	0.74
VIM	Vimentin	0.74
C9	Complement component 9	0.74
PSAP	Prosaposin	0.75
APOB	Apolipoprotein B	0.75
ARFGAP3	ADP-ribosylation factor GTPase-activating protein 3	0.75
HSPA5	Heat Shock 70kDa Protein 5 (Glucose-Regulated Protein, 78kDa)	0.76
APLP2	Amyloid beta (A4) precursor-like protein 2	0.76
ACLY	ATP Citrate Lyase	0.76
COL5A1	Collagen, type V, alpha 1	0.76
MT2A	Metallothionein 2A	0.77
HNRNPH1	Heterogeneous Nuclear Ribonucleoprotein H1 (H)	0.77
ALDH3A1	Aldehyde Dehydrogenase 3 Family, Member A1	0.78
PPIB	Peptidyl-prolyl cis-trans isomerase B	0.79
CCT2	T-complex protein 1 subunit beta	0.79
HIST1H2BK	Histone H2B type 1-K	0.79
RPS13	40S ribosomal protein S13	0.79
ITIH4	Inter-Alpha-Trypsin Inhibitor Heavy Chain Family, Member 4	0.79
PGD	Phosphogluconate Dehydrogenase	0.79
CCDC144A	Coiled-Coil Domain Containing 144A	0.80
APOA1	Apolipoprotein A-I	0.81
GRN	Granulin	0.82
CLTC	Clathrin heavy chain 1	0.82
ATP1A1	ATPase, Na+/K+ Transporting, Alpha 1 Polypeptide	0.83
C4BPA	Complement Component 4 Binding Protein, Alpha	0.84
VIL2	Villin-2, ezrin	0.85
YWHAZ	14-3-3 protein zeta/delta	0.85
NOTCH3	Neurogenic locus notch homolog protein 3	0.85

C8B	Complement Component 8, Beta Polypeptide	0.86
FN1	Fibronectin 1	0.86
ANXA2	Annexin A2	0.87
C6	Complement Component 6	0.88
RACGAP1	Rac GTPase-activating protein 1	0.88
TCP1	T-complex protein 1 subunit alpha	0.89
LAMA2	Laminin, Alpha 2	0.89
PSMC2	26S protease regulatory subunit 7	0.89
THBS4	Thrombospondin-4	0.90
C8G	Complement Component 8, Gamma Polypeptide	0.90
CFH	Complement factor H	0.91
CTNNA1	Catenin (Cadherin-Associated Protein), Alpha 1	0.91
LAMC1	Laminin subunit gamma-1	0.92
MARCKS	Myristoylated alanine-rich C-kinase substrate	0.92
THBS3	Thrombospondin-3	0.92
RAB8A	Ras-related protein Rab-8A	0.92
MASP2	Mannan-binding lectin serine protease 2	0.92
USH2A	Usherin	0.92
FGG	Fibrinogen gamma chain	0.93
C1QTNF3	Complement C1q tumor necrosis factor-related protein 3	0.93
APOH	Apolipoprotein H	0.93
SPATA2L	Spermatogenesis Associated 2-Like	0.93
F5	Coagulation Factor V (Proaccelerin, Labile Factor)	0.94
KRT18	Keratin 18	0.94
FGB	Fibrinogen Beta Chain	0.94
PHB2	Prohibitin 2	0.94
THRAP3	Thyroid hormone receptor-associated protein 3	0.94
SLC25A5	Solute Carrier Family 25 (Mitochondrial Carrier; Adenine Nucleotide Translocator), Member 5	0.95
RPLP0	60S acidic ribosomal protein P0	0.95
LAMB1	Laminin subunit beta-1	0.95
MASP1	Mannan-binding lectin serine protease 1 also known asmannose-associated serine protease 1	0.95
UBB	Ubiquitin B	0.95
H2AFV	Histone H2A.V	0.96
PPP2R1A	Serine/threonine-protein phosphatase 2A 65 kDa regulatory subunit A alpha isoform	0.96
AFP	Alpha-Fetoprotein	0.97
GC	Group-Specific Component (Vitamin D Binding Protein)	0.97
HSP90B1	Heat shock protein 90kDa beta member 1	0.97
GPC1	Glypican 1	0.97
CCT8	Chaperonin Containing TCP1, Subunit 8 (Theta)	0.97
SNF1LK2	Serine/threonine-protein kinase SIK2	0.97

TAGLN2	Transgelin 2	0.98
HIST1H1C	Histone H1.2	0.98
EIF4A2	Eukaryotic Translation Initiation Factor 4A2	0.98
DDX3X	ATP-dependent RNA helicase DDX3X	0.98
LRP1	Low density lipoprotein receptor-related protein 1	0.99
KRT7	Keratin 7	0.99
KRT19	Keratin 19	0.99
DNAJB11	DnaJ homolog subfamily B member 11	0.99
SLC16A3	Solute Carrier Family 16, Member 3 (Monocarboxylic AcidTransporter 4)	0.99

Table 3.3. List of proteins from control and plectin-knockdown L3.6pl exosome mass spectrometry analysis with control/shPLEC ratio equal to 1.

Gene Name	Protein Description	Ctrl/shPLEC
HSPG2	Perlecan, heparan sulfate proteoglycan 2	1.00
SERPINA10	Serpin peptidase inhibitor, clade A	1.00
ITIH2	Inter-alpha-trypsin inhibitor heavy chain H2	1.00

We have confirmed the differential expression of three proteins via western blot (**Fig. 3.10**). Our data indicate that plectin is not only necessary for exosome formation; it has important functions for protein content of the exosomes.

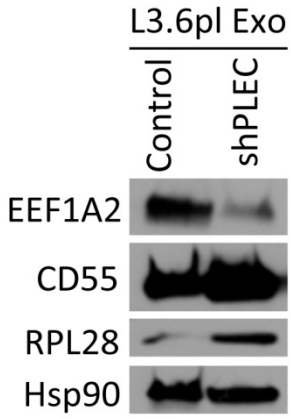

Figure 3.10. Immunoblot verification of proteins underexpressed (EEF1A2) and overexpressed (CD55 and RPL28) in plectin-knockdown L3.6pl exosomes from mass spectrometry analysis.

3.4. Summary and discussion

In this chapter, we saw that plectin knockdown reduced exosome secretion as well as exosomal protein content, suggesting that plectin may be involved in the exosome secretory pathways in PDAC. On the other hand, overexpression of plectin isoforms 1a and 1f significantly increased exosome production in HPDE, although not to the level of PDAC cells. Therefore, plectin functions in the exosome secretion process, but plectin alone is not sufficient to induce non-transformed HPDE to behave like cancer cells.

When the exosome formation was inhibited by shRNA-mediated knockdown of Rab27a, we found that the tumor growth was dramatically reduced. However, plectin-positive exosomes were able to rescue the tumor growth in Rab27a-knockdown L3.6pl tumors. Surprisingly, Rab27a-knockdown tumors injected with plectin-rich exosomes surpassed the growth of the control tumor. These effects suggest that the mislocalization of plectin to the exosomes may be important for pancreatic cancer progression and metastasis. It is also possible that plectin-positive exosomes may harbor various oncogenic proteins because plectin has been shown to for complex with signaling proteins (59, 121, 139) as well as contain phosphorylation sites for kinases (50).

Furthermore, previous studies have also shown an involvement of exosomes in other cancer types such as prostate cancer and breast cancer (87, 140). Plectin demonstrated profound effects on PDAC tumor growth through exosome transfer. Our results show that plectin localization in exosomes and transfer of plectin-positive exosomes between cells could play a role in the progression PDAC by enhancing tumor growth. Plectin-positive exosomes produced by pancreatic cancer may enhance aggressive phenotypes

by amplifying autocrine and/or paracrine signaling of the tumor cells. Alternatively, because plectin is a scaffolding protein, absence of plectin may result in a decrease in total protein content. Direct binding partners of plectin may no longer have a scaffold and thus deactivate and/or degrade over time.

Why is the presence of plectin in the exosomes necessary to enhance PDAC growth? As a scaffolding protein, plectin is likely to carry a complex of numerous signaling molecules in the exosomes and thereby promotes tumor growth. Indeed, proteomic analysis of plectin-positive and plectin-negative exosomes indicate that plectin is not only necessary for efficient exosome production but also modulates exosome content. The analysis revealed the largest change in plectin-negative exosomes being a 20-fold loss of SACM1L, a phosphatidylinositide phosphatase, a protein important in vesicle trafficking and membrane dynamics. Interestingly, the second most decreased protein is a 60S ribosomal protein important to protein biosynthesis. Several of the top 25 losses to the exosomes are involved in protein synthesis. Consistent with NTA analysis, a protein that is a known marker of exosomes (Hsp70) was also decreased upon plectin-knockdown. Further studies should be conducted to investigate whether hindering plectin localization on the cell surface by inhibition of exosome formation in early stage PanIN would halt progression into PDAC.

Overall, results in this chapter demonstrate a novel role of plectin in promoting exosome secretion as well as a potential capacity to transport various proteins and signaling molecules. This new finding suggests the importance of plectin in propagating signal transduction involved in pancreatic cancer growth and progression through scaffolding and exosome transfer.

CHAPTER 4

EFFECTS OF PLECTIN DEREGULATION ON PDAC PROLIFERATION, MIGRATION, AND INVASION

Works from chapters 2-4 are published in Unexpected gain of function for the scaffolding protein plectin due to mislocalization in pancreatic cancer. Shin SJ, Smith JA, Rezniczek GA, Pan S, Chen R, Brentnall TA, Wiche G, and Kelly KA. *Proc Natl Acad Sci U S A.* 2013 Nov;110(48): 19414–19419.(122)

4.1. Introduction

Plectin is overexpressed in pancreatic ductal adenocarcinoma (PDAC) and high-grade precursor lesion pancreatic intraepithelial neoplasia (PanIN)-III, but not in normal pancreas, chronic pancreatitis, or low-grade precursor lesions PanIN-I and PanIN-II (32). Therefore, plectin may be involved in the aggressive nature of pancreatic cancer. Determining the expression profile and function of plectin in PDAC may provide important insights leading to better detection and improved management of PDAC.

The role of plectin in organizing the cytoskeletal network in other tissue types has been studied extensively. It has been shown that plectin deficiency leads to epidermolysis bullosa and muscular dystrophy (46, 48, 71). However, the functional role that plectin may have in PDAC progression has not yet been studied. In addition, plectin has 11 alternative exons that directly splice into plectin exon 2 that all originate from the amino terminus. Of these 11 exons, 8 are coding, resulting in 8 different isoforms of plectin. Although most of the isoforms have been studied in normal physiology or other diseases, the isoforms that are present in pancreatic cancer and their functional role has yet to be elucidated. Understanding the role of specific plectin isoforms in PDAC will provide important insights into current therapeutic approaches.

Based on the distinct roles played by different plectin isoforms, the cytoplasmic expression of plectin in normal keratinocytes and muscle cells (45, 55, 64, 66, 126), and our previous findings of plectin overexpression in PDAC (31, 32), we sought to investigate whether plectin is important in PDAC progression, tumorigenesis, invasion and metastasis, and the profile and function of plectin isoforms in PDAC. We

hypothesized that PDAC has an aberrant plectin isoform expression and that plectin has a role in PDAC growth and migration.

Lastly, due to abrogation of cell surface plectin upon interfering plectin-integrin β4 interaction (**Chapter 2**) as well as integrin β4 involvement in functions associated with the genesis and progression in many cancer types (141, 142), we further investigated the contribution of plectin-integrin β4 interactions on PDAC cell migration and invasion using PLEC-Trunc. We hypothesized that plectin interaction with integrin β4 has a significant effect on PDAC growth and migration.

4.2. Materials and methods

4.2.1. Cell culture

Bx.Pc3, C6, HUVEC, NIH-3T3, and Panc-1 cell lines were obtained from ATCC. Bx.Pc3 was grown in RPMI medium; C6 was grown in F-12K medium; HUVEC was grown in EBM; and NIH-3T3 and Panc-1 were grown in DMEM. L3.6pl and HPDE were obtained from Dr. Craig Logsdon (University of Texas, MD Anderson Cancer Center). L3.6pl was grown in DMEM; HPDE was grown in keratinocyte medium. All media were supplemented with 10% (vol/vol) FBS, 1% pen-strep, and 1% L-glutamine except EBM (supplemented with bovine brain extract with heparin, hEGF, hydrocortisone, GA-1000, and 5% FBS), keratinocyte medium (supplemented with human recombinant epidermal growth factor 1-53 and bovine pituitary extract), and F-12K medium (supplemented with 2.5% FBS, 15% horse serum, 1% pen-strep, and 1% L-glutamine).

4.2.2. shRNA lentiviral transduction

Lentivirus vector encoding shRNA against human plectin was obtained from Dr. Nabeel Bardeesy (Massachusetts General Hospital and Harvard Medical School). shRNA against plectin isoforms 1a, 1c, and 1f were cloned into pLKO.1 puro by selecting regions of exon 1, which were obtained from The RNAi Consortium (TRC). The target sequences are: 5'-AGGGCCTCTGAGGGCAAGAAA-3' for plectin-1a, 5'-TCTCTGAAGATGTCTCCAATG-3' for plectin-1c, and 5'-AGGTGCGCGAGAAGTACAAAG-3' for plectin-1f. Lentivirus vector encoding shRNA against human integrin β4 was obtained from Santa Cruz Biotechnology. Cells were infected with integrin β4 shRNA lentiviral particles according to manufacturer's protocol. Briefly, cells were seeded on 12-well plates and grown to 50% confluence. Old media

were replaced by media containing polybrene (4 µg/ml). Lentiviral particles were thawed at room temperature and gently mixed before adding to the cells. Three different ratios of virions to cells were used (1:1, 2:1, and 3:2). The infected cells were incubated overnight and media were replaced (without polybrene). Stably transfected cells were selected by puromycin treatment (2 µg/ml for Bx.Pc3, 3 µg/ml for L3.6pl, 4 µg/ml for Panc-1, and 6.5 µg/ml for Han14.3). To further select stable clones, a single colony was isolated using the trypsin method (125). Downregulation of each protein was verified via immunoblot.

4.2.3. Antibodies for immunoblotting

Primary antibodies were purchased from Abcam (plectin [E398P]); R&D Systems (integrin β4 [422325]); Cell Signaling Technology (Hsp90 [C45G5]); and obtained from Dr. Gerhard Wiche (Plectin-1a, Plectin-1c, and Plectin-1f). Horseradish peroxidase-conjugated secondary antibodies were purchased from R&D Systems. Primary antibodies were diluted 1:1000 in 1% milk-TBST and secondary antibodies were diluted 1:5000 in 1% milk-TBST for immunoblotting.

4.2.4. SDS-PAGE and Immunoblotting

Cells were grown in 10-cm petri dishes (BD Falcon) to approximately 70% confluence. Cells and exosomes samples were lysed in 300 - 500 µl of lysis buffer (1% Triton X-100, 1mM EDTA, and 1mM protease inhibitor cocktail in PBS). Protein concentrations were determined using a bicinchoninic acid (BCA) protein assay kit (Thermo Scientific). Equal amounts (20 µg) of proteins in SDS sample buffer (containing β-mercaptoethanol) were resolved on 5% or 4-15% polyacrylamide gels (BioRad) and transferred onto PVDF membranes. The membranes were blocked with 1% milk-TBST, incubated with primary antibody solution for 3 h at room temperature, washed 3x5 min with TBST, incubated with secondary antibody solution for 30 min at room temperature, and washed 4x5 min

with TBST. The membranes were then subjected to chemiluminescence and autoradiography.

4.2.5. RNA extraction and reverse transcriptase polymerase chain reaction

Total cell RNA was extracted and cDNA was synthesized using the FastLane Cell cDNA kit (Qiagen) according to the manufacturer's protocol. Human RNA samples were obtained from Dr. Todd Bauer (University of Virginia). Reactions were repeated in triplicate in three independent experiments. PCR amplification of plectin using different plectin isoform primers was done by subjecting the reaction to 95°C for 15 min, 30 cycles of denaturation at 95°C for 30 s, annealing at 55°C for 30 s, and elongation at 72°C for 1 min. Upon completion of 30 cycles, the reaction was subjected to a final extension at 72°C for 5 min and stored at 4°C. Amplified cDNA fragments were resolved on agarose gel containing ethidium bromide and visualized under UV light (2% agarose gel was used for all plectin isoforms and 1% agarose gel was used for GAPDH). The primer sequences are provided in supplemental **Tables 4.1-3**.

Table 4.1. Primer sequences for analyzing expression of human plectin isoforms.

Isoform	Forward Sequence	Reverse Sequence
PLEC-1	5'-GTGGTACCCTGCCTGCTG-3'	5'-GAGGTGCTTGTTGACCCACT-3'
PLEC-1a	5'-GCCGAAAGAGAACCAGCTC-3'	5'-GAGGTGCTTGTTGACCCACT-3'
PLEC-1b	5'-GTTGTGGGTCACGTTGTCAC-3'	5'-TGATGAGGTGCTTGTTGACC-3'
PLEC-1c	5'-TGTCTCCAATGGAAGCAGTG-3'	5'-TGATGAGGTGCTTGTTGACC-3'
PLEC-1d	5'-CCTGTGACCTCCCACACC-3'	5'-GAGGTGCTTGTTGACCCACT-3'
PLEC-1e	5'-TGGACTCTGCCTGGTGGT-3'	5'-GAGGTGCTTGTTGACCCACT-3'
PLEC-1f	5'-ACGAGCAGGACTTCATCCAG-3'	5'-GAGGTGCTTGTTGACCCACT-3'
PLEC-1g	5'-GAGGGAGGTCTTGCTGGAG-3'	5'-GAGGTGCTTGTTGACCCACT-3'

Table 4.2. Primer sequences for analyzing expression of rat plectin isoforms.

Isoform	Forward Sequence	Reverse Sequence
PLEC-1	5'-GATCGTACCTGCCTCTCTGC-3'	5'-AGACACCACAGGGGTTTCAG-3'
PLEC-1a	5'-GAGTTACTGTCCAGAGCGGC-3'	5'-GAGGTTGTCCTCTGAGCTGG-3'
PLEC-1b	5'-CTGTACATTGTCCCCTGGCT-3'	5'-TGACAACATGACCCACGACT-3'
PLEC-1c	5'-AGTGGCAGTGGCTGAAGGTA-3'	5'-CACAGAACCACCTCCACTCC-3'
PLEC-1d	5'-ACAGGCTTGCTGCCTTAGAG-3'	5'-ACGATCTTCATTGGGGACAG-3'
PLEC-1e	5'-ATTGATCAGCAGAAGCTCCG-3'	5'-ACTTAGGGGCTGAGAACGGT-3'
PLEC-1f	5'-CATGGCCCATCTGCTGAC-3'	5'-ACGGTCTCGTTCATCTTTGT-3'
PLEC-1g	5'-TCTTCACTTCGCAGAGGGAG-3'	5'-TACACAACACAGTTGCCCGT-3'

Table 4.3. Primer sequences for analyzing expression of mouse plectin isoforms.

Isoform	Forward Sequence	Reverse Sequence
PLEC-1	5'-CTTGTGCTTAGAACCGGAGC-3'	5'-ACCTGTAGATTGGTGACGCC-3'
PLEC-1a	5'-AGCACCTGAGAACTGAGGGA-3'	5'-GAGGTTGTCCTCTGAGCTGG-3'
PLEC-1b	5'-TCGTGGGTCATGTTGTCACT-3'	5'-ACTGATGTGCCTCTGAGCCT-3'
PLEC-1c	5'-AAGTGGAGGTGGTTCTGTGG-3'	5'-ACTGATGTGCCTCTGAGCCT-3'
PLEC-1d	5'-CAGGCTTGCTGCCTCAGA-3'	5'-ACGATCTTCATTGGGGACAG-3'
PLEC-1e	5'-TGTGCAGTCCTGGACACAGT-3'	5'-TTTGAGGGAGCTGATCTCGT-3'
PLEC-1f	5'-GTTCTTCTCCCGCCAGCAT-3'	5'-TTGTACTTCTCCCGCACCTC-3'
PLEC-1g	5'-TCAGCCTTCAACACAAGCAC-3'	5'-CTGCGAAGTGAAGACTCCCT-3'

4.2.6. PTP binding on the cell surface

$1x10^4$ cells were seeded into wells of a 96-well plate and incubated at 37°C and 5% CO_2 for 24 h. The cells were washed once with PBS and fixed with 4% PFA for 10 min. The cells were blocked with 1% BSA in PBS for 1 h and incubated with 1 µM PTP n PBS-1% BSA for 2 h. Then the cells were incubated with HRP-conjugated anti-fluorescein antibodies (Invitrogen) for 30 min. After washing, the cells were incubated with TMB (Sigma) for 10 min and absorbance was measured at 650 nm.

4.2.7. Cell proliferation assay

The number of viable cells was determined by quantifying ATP presence using the CellTiter-Glo Cell Viability Luminescent Assay according to the manufacturer's protocol (Promega). Briefly, 10,000 cells were seeded into wells of an opaque-walled 96-well plate and incubated at 37°C and 5% CO_2 for 24 h. The CellTiter-Glo® Buffer and CellTiter-Glo® Substrate were thawed, equilibrated to room temperature, and mixed 1 min prior to the experiment. 100 µl of the substrate mixture was then added to each well and gently mixed and incubated for 10 min at room temperature in dark. The luminescence was recorded using FLUOstar OPTIMA microplate reader.

4.2.8. APO-BrdU TUNEL Assay

The TUNEL assay was performed according to the manufacturer's protocol (A23210, Invitrogen). Briefly, cells were washed with PBS, then fixed with 1% PFA for 15 minutes on ice, then incubated with ice-cold 70% ethanol overnight at -20°C. The cells were washed with wash buffer twice, incubated with DNA-labeling solution containing reaction buffer, TdT enzyme, and BrdUTP for 1 hour at 36°C, washed with rinse buffer twice, then incubated with antibody solution containing AlexaFluor® 488 dye–labeled anti-BrdU antibody. The cells were washed three times with rinse buffer and fluorescence was recorded using FLUOStar Omega microplate reader.

4.2.9. Migration and invasion assay

A transwell migration assay (BD Biosciences) was used to determine cell migration and invasion. Briefly, the chambers were rehydrated with serum free media at 37°C and 5% CO_2 for two hours. After rehydration, $5x10^4$ cells were plated in each chamber with serum free media. The chambers were placed into the wells containing media with 10% FBS and incubated overnight at 37°C and 5% CO_2. 8.0 µm polyethylene terephthalate

(PET) membrane chambers were used for migration and matrigel-coated 8.0 µm PET membrane chambers were used for invasion. After overnight incubation, non-migrating and non-invading cells were removed from the upper membrane surface with a cotton swab. The membranes were washed with PBS, fixed with 4% PFA, and stained with 1% crystal violet in 20% ethanol. To quantify migrating and invading cells, the membranes were imaged at 40X magnification and the cell numbers were counted in 5 different fields of view in triplicate (15 measurements total for each group). Percent invasion was determined as number of invading cells / number of migrating cells x 100.

4.2.10. Plasmids and transfections.

pGR244 and pGR258, encoding C-terminal fusions of EGFP to full-length plectin-1a and plectin-1f inserts, respectively, were derived from pEGFP-N2 (Clontech) and have previously been described (126). pDS89 and pDS94 (derived from pBS with full-length plectin-1 and plectin-1c inserts (exons 1 to 32) flanked by in-frame EcoRI sites, respectively) were provided by Dr. Gerhard Wiche. PLEC-Trunc, corresponding to exons 1a-9 (containing the actin-binding domain of plectin which also serves as the N-terminal integrin β4 binding region of plectin), was generated by PCR using pGR244 as a template (forward primer: 5'-GCGAATTCACCATGTCTCAGCACCGGCTCCGTGTG-3', reverse primer: 5'-GCGGATCCGGAACTTGCGCTCCTCAAAAGCAGCGG-3'). The PCR product was inserted into pEGFP-N2 using EcoRI and BamHI restriction sites. Plasmids were transfected into cells with Lipofectamine LTX (Invitrogen) according to the manufacturer's protocol. Transfection of the EGFP-tagged plasmids (pGR244 and pGR258) was verified via fluorescence microscopy.

4.2.11. Subcutaneous tumor growth

500,000 of the control cells were s.c. injected into the left dorsal flank of male immune-deficient nude mice. 500,000 of the plectin-knockdown cells were s.c. injected into the right dorsal flanks. Tumor sizes were measured with a caliper and the volumes were calculated as $V = ab^2/2$ (a = longest diameter, b = shortest diameter). One animal from day 0 and day 5 were euthanized for immunoblot analysis. The tumors were excised, homogenized in RIPA buffer (50 mmol/L Trizma Base, 1% Triton X-100, 0.25% sodium desoxycholate, 100 mmol/L EDTA, 150 mmol/L NaCl) with a protease inhibitor cocktail (0.001 mg/mL aprotinin, bestatin, pepstatin, leupeptin, and 0.005 mg/mL 20 mmol/L PMSF; Sigma-Aldrich). The lysate was cleared by centrifugation. BCA assay, SDS-PAGE, and immunoblot were performed the same way as in section *4.2.4*. All *in vivo* experiments were performed according to a protocol approved by the University of Virginia Animal Care and Use Committee.

4.2.12. Orthotopic tumor growth

750,000 of the control and plectin-knockdown L3.6pl cells were injected into the tail of the pancreas of 50 male immune-deficient mice (5 mice per group per time point). 750,000 of the control and plectin-knockdown Han14.3 cells were injected into the head of the pancreas of 40 male FVB mice (5 mice per group per time point). Pancreas and other organs with metastases were excised, and tumor size, volume, and weight were measured at each time point. Tumor sizes were measured with a caliper and the volumes were calculated as $V = ab^2/2$ (a = longest diameter, b = shortest diameter). Day 0 pancreas weight data were collected from wildtype pancreas without tumor injection. All *in vivo* experiments were performed according to a protocol approved by the University of Virginia Animal Care and Use Committee.

4.2.13. Statistical analysis

All statistical analyses were performed using Prism (GraphPad Software, Inc., La Jolla, CA). Results are presented as mean ± standard error of the mean (SEM), unless otherwise noted. All statistical analyses were performed using a one-way general linear ANOVA, followed by Tukey's test for pairwise comparisons. Significance was asserted at $p < 0.05$.

4.3. Results

4.3.1. PDAC exhibits distinct pattern of plectin isoform expression

The plectin locus has a complex organization, with eleven alternative first exons, eight of which are coding, giving rise to at least eight different plectin isoforms (55). Based on the distinct roles played by different plectin isoforms in normal cells, the cytoplasmic expression of plectin in normal keratinocytes and muscle cells (45, 55, 66), and our previous findings of plectin overexpression (32) and cell surface localization in PDAC (**Chapter 2**), we sought to investigate the profile of plectin isoforms in PDAC cell lines. Three PDAC cell lines (Bx.Pc3, L3.6pl, and Panc-1) were chosen due to their mutation profiles. Bx.Pc3 has wildtype *K-Ras*, whereas both L3.6pl and Panc-1 have mutant *K-Ras*. However, L3.6pl represents highly metatstatic PDAC and Panc-1 represents a dedifferentiated phenotype. HPDE cells were used for comparison. Using immunoblot and RT-PCR analyses, we found that HPDE cells and PDAC cell lines express comparable levels of total plectin (**Fig. 4.1A**), but they exhibit distinct expression patterns of the individual plectin isoforms (**Fig. 4.1B** and **Fig. 4.2** for C6). Notably, plectin isoforms 1a and 1f isoforms were undetectable in HPDE cells but prominently expressed in the PDAC cell lines tested, whereas isoform 1 was restricted to HPDE cells. Plectin 1g was expressed in all cell lines regardless of their cancer status. As expected based on our previous results (32), human specimens of normal pancreata had nearly undetectable amounts of plectin whereas PDAC had high levels of 1a and 1f with specimen 2 having high levels of 1d, as well. Thus, despite the similar total levels of plectin in HPDE cells, PDAC exhibit a deregulated expression of a specific set of plectin isoforms.

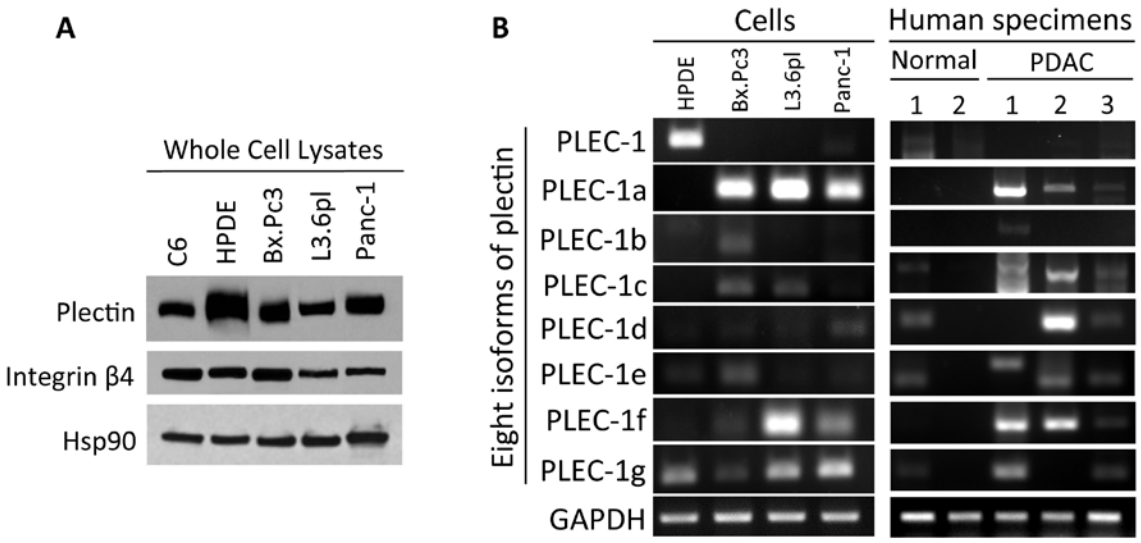

Figure 4.1. A) Immunoblot analysis showing total plectin expression in C6, HPDE, and PDAC cell lines. **B)** PCR analysis showing mRNAs of specific plectin isoforms.

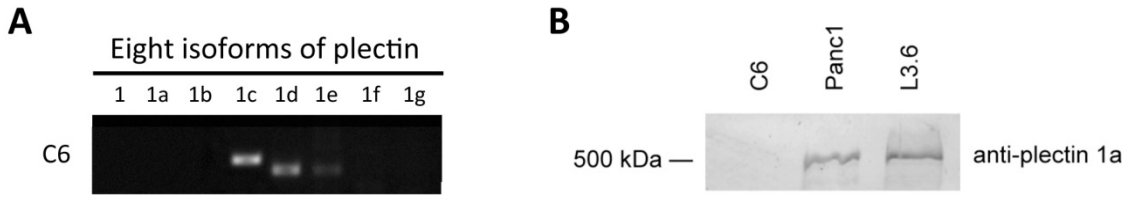

Figure 4.2. A) PCR analysis of plectin isoform expression in C6 cells. C6 cells do not express plectin isoform 1a. **B)** Immunoblot analysis using antibodies specific for plectin isoform 1a shows that C6 does not express plectin-1a whereas Panc-1 and L3.6pl do.

4.3.2. Plectin deregulation increases proliferation, migration, and invasion of PDAC cells

We sought to determine whether the altered plectin expression generated a measurable impact on PDAC cells by creating pan-plectin- and plectin isoform 1a-, 1c-, and 1f-knockdown cells (**Fig. 4.3**). Using the PTP-binding assay, we found that knockdown of pan-plectin, plectin-1a, and 1f significantly decreased cell surface plectin (**Fig. 4.4**), suggesting that plectin-1a and 1f are important isoforms in PDAC. Knockdown of plectin 1c, which is the major isoform found in C6 cells, did not alter PTP binding, indicating that plectin-1c may not be on the surface of PDAC cells. Although C6 cells express plectin

and produce exosomes, the presence of 1c and the exclusion of 1a and 1f isoforms may indicate that the expression of plectin-1a and 1f, but not 1c, is necessary for incorporation into exosomes. An alternative explanation is that there were no changes on PTP binding upon plectin-1c knockdown due to low endogenous levels of plectin-1c compared to isoforms 1a or 1f in control PDAC cell lines (**Fig. 4.3** middle panel).

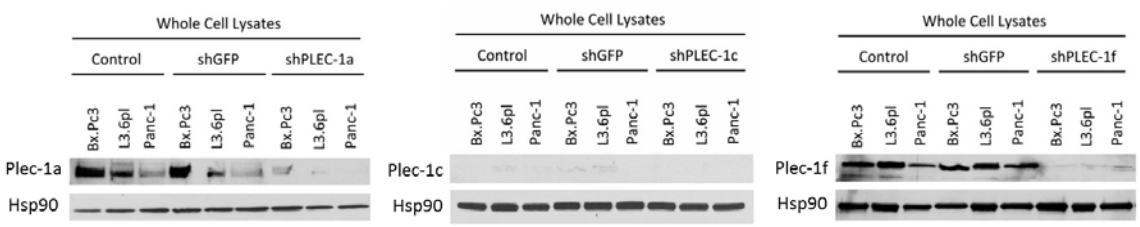

Figure 4.3. Knockdown verification of plectin-1a, 1c, and 1f via immunoblotting.

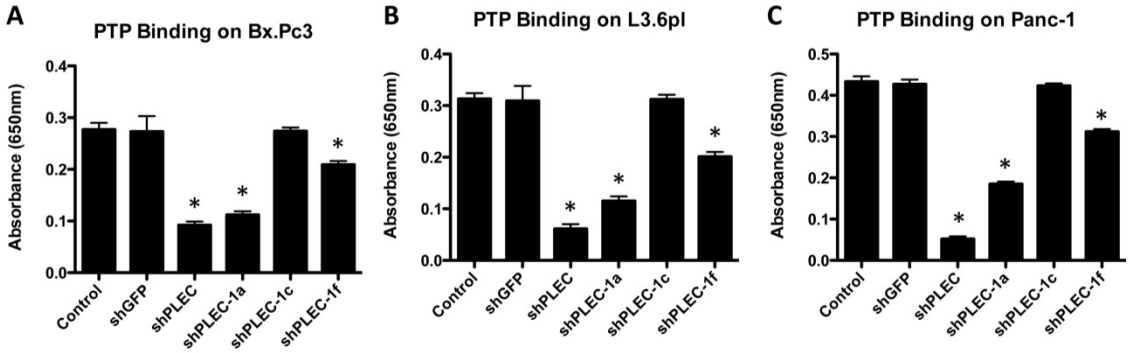

Figure 4.4. shRNA knockdown of pan-plectin and plectin isoforms 1a and 1f resulted in a significant decrease in cell-surface PTP binding. *Significant to both control and shGFP ($p<0.0001$).

To study the impact of plectin expression on PDAC cell proliferation, we used cell viability (**Fig. 4.5A-C** and **Fig. 4.6A-C**) and APO-BrdU TUNEL (**Fig. 4.5D-F** and **Fig. 4.6D-F**) assays. We found that knockdown of pan-plectin expression all but eliminated proliferation of the rapidly growing PDAC cells. For lentiviral experiments, pLKO.1 (backbone vector) containing shGFP was used as a control. The effect on proliferation appears to be due to reduction in plectin 1a and 1f because selective knockdown of

either isoform reduced proliferation (**Fig. 4.5**) and selective expression rescued proliferation in the pan-plectin knockdown cells (**Fig. 4.6**).

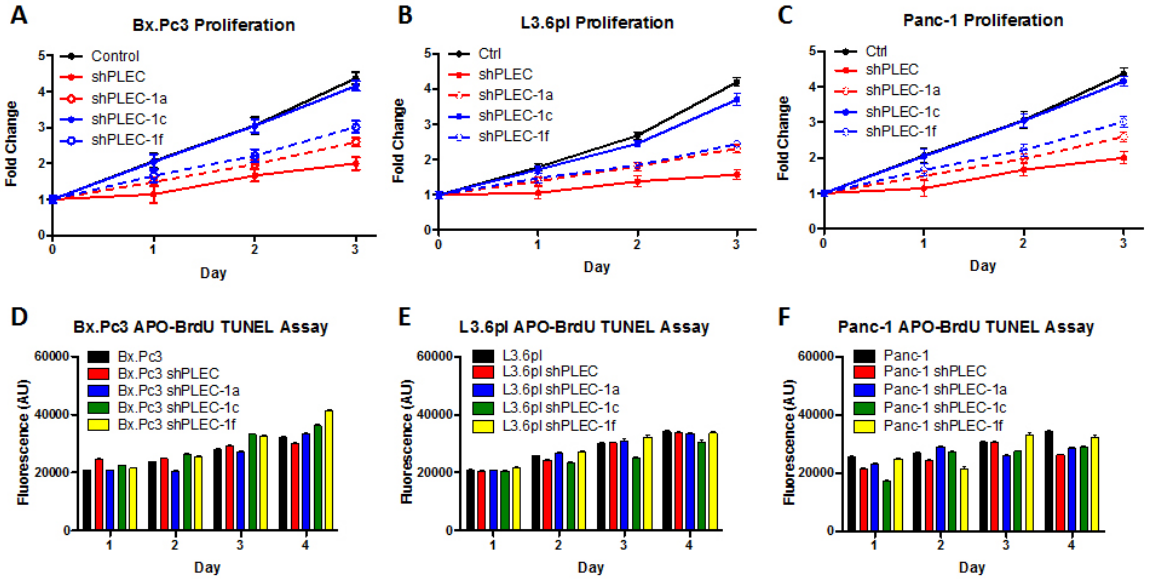

Figure 4.5. A-C) Cell viability assays showing increased ATP in control PDAC cells compared to pan plectin knockdown and isoform knockdowns. **A)** Bx.Pc3, **B)** L3.6pl, and **C)** Panc-1. **D-F)** Corresponding APO-BrdU assay results. **D)** Bx.Pc3, **E)** L3.6pl, and **F)** Panc-1.

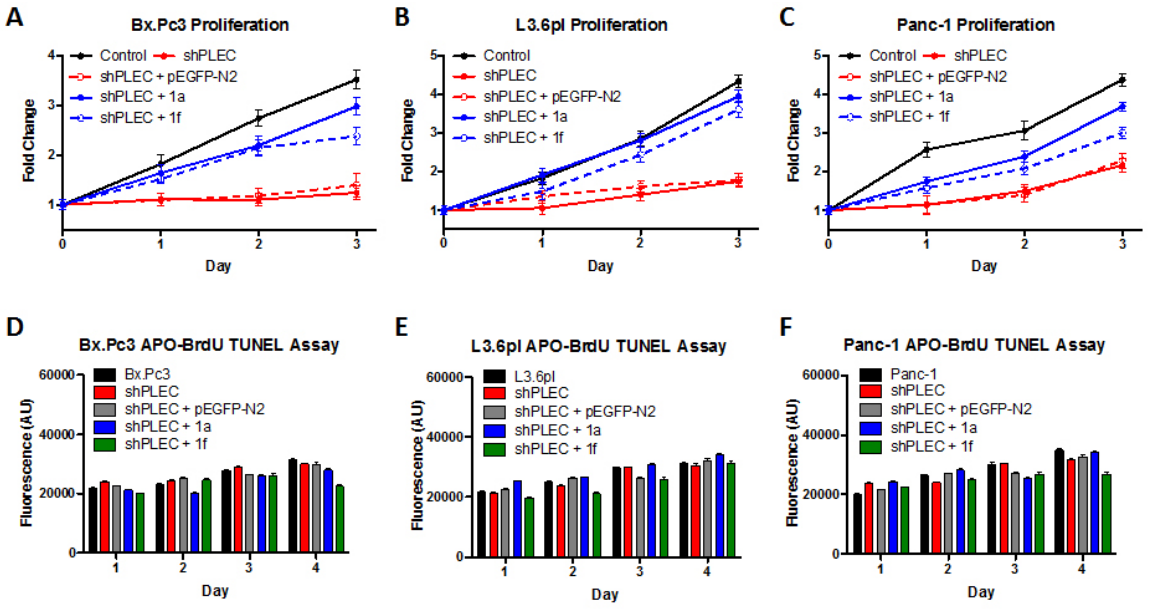

Figure 4.6. A-C) Cell viability assays showing proliferation of plectin-knockdown cells overexpressing plectin-1a and 1f. **A)** Bx.Pc3, **B)** L3.6pl, and **C)** Panc-1. **D-F)** Corresponding APO-BrdU assay results. **D)** Bx.Pc3, **E)** L3.6pl, and **F)** Panc-1.

The decrease in proliferation was not the result of modulation of apoptosis as the apoptotic rates were identical between plectin-positive and plectin-knockdown cells. Interestingly, plectin 1c reduction did not result in a significant decrease in proliferation. Again, this may be due to low endogenous levels of plectin-1c in PDAC cells compared to the other isoforms or that this isoform is not incorporated into the exosomes and the cell surface. Therefore, the expression of plectin isoforms 1a and 1f in PDAC cells, which are not present in non-transformed pancreatic cells, enhances the proliferation of PDAC cells.

Likewise, in transwell migration assays, we found that knockdown of pan-plectin, plectin-1a, and plectin-1f resulted in significant decreases in migration and invasion in three different PDAC cell lines (**Fig. 4.7**). Again, the reduction was partially rescued by selective expression of plectin-1a or -1f (**Fig. 4.8**). These results suggest that the plectin-1a and -1f isoforms have important and overlapping roles in the malignant growth of PDAC cells. Unlike proliferation, plectin-1c knockdown resulted in a significant decrease in migration and invasion (21%) but to a lesser extent than the plectin 1a (47.6%) and 1f (39.1%) knockdowns. This could be due to the lower endogenous plectin-1c levels in PDAC, isoform 1c may not be on the cell surface, and it may signal through an alternate pathway.

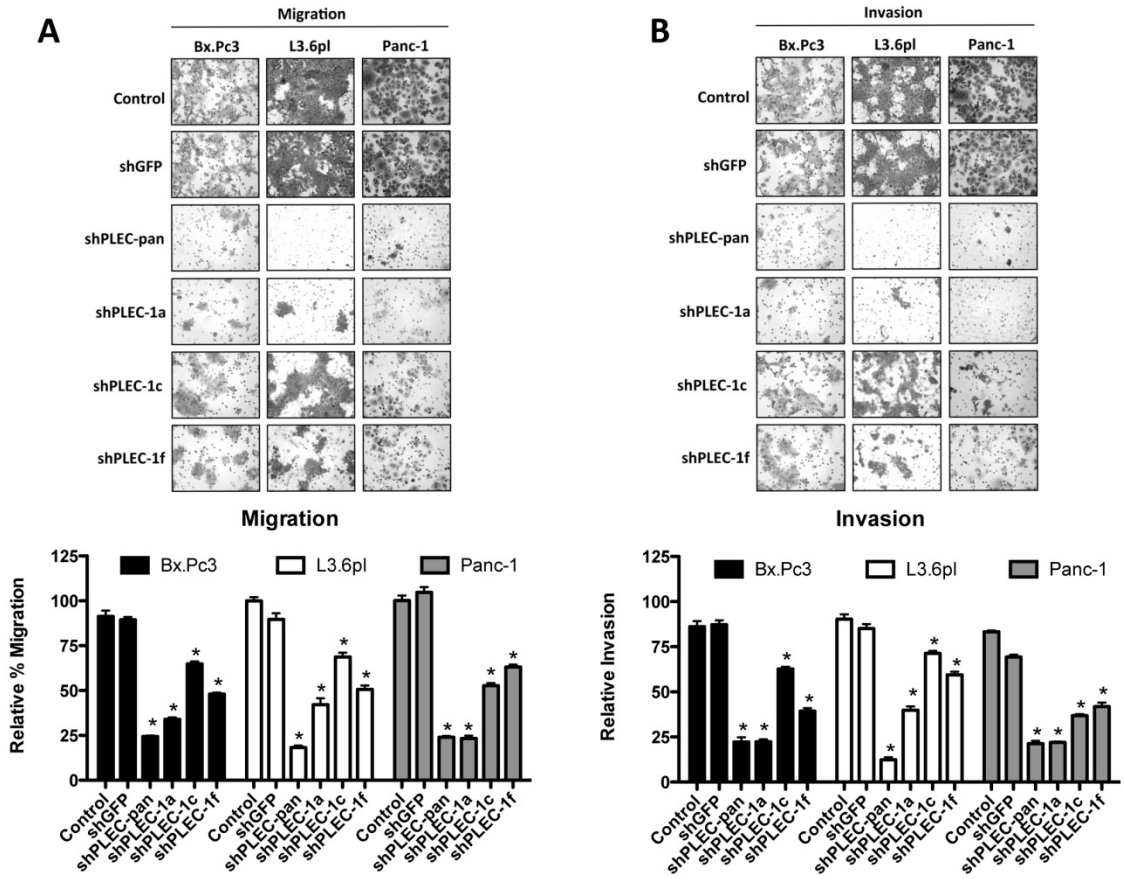

Figure 4.7. Isoform-specific knockdown of plectin-1a and 1f resulted in significant reduction in **A)** migration and **B)** invasion of PDAC cell lines. *Significant to control ($p<0.0001$).

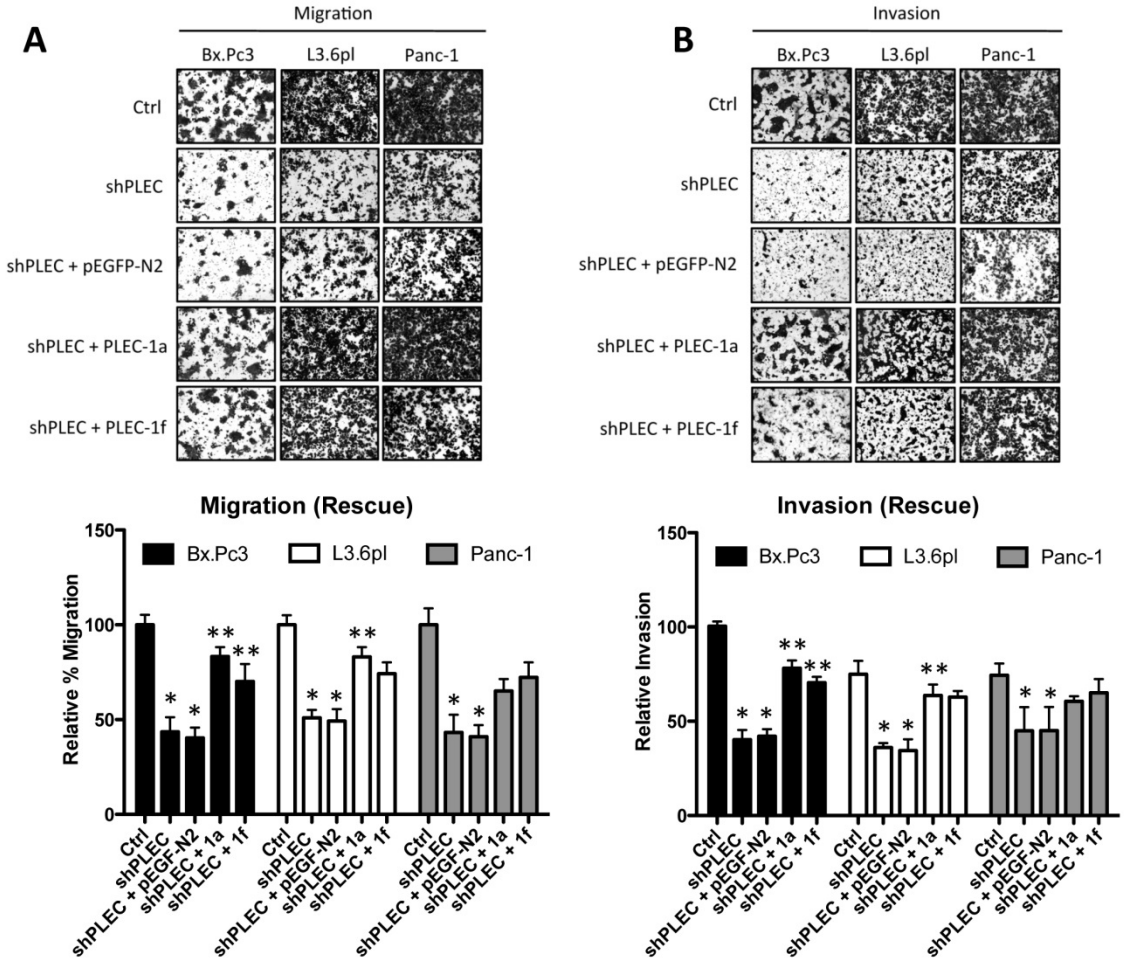

Figure 4.8. Overexpression of plectin-1a and 1f increased **A)** migration and **B)** invasion in L3.6pl plectin-knockdown cells. *Significant to control ($p<0.0001$), **significant to both shPLEC and shPLEC + pEGFP-N2 ($p<0.0001$).

4.3.3. Plectin-integrin β4 interaction has an important role in PDAC migration

Based on our finding that integrin β4 is critical for the exosome localization of plectin, we sought to investigate the contribution of plectin-integrin β4 interactions on PDAC cell migration and invasion. To achieve this, PDAC cells were transfected with PLEC-Trunc, which is the truncated plectin mutant that resulted in decreased PTP binding on PDAC cell surface (**Chapter 2**). PLEC-Trunc transfected cells demonstrated strong reductions in migration and invasion, comparable to those seen upon plectin knockdown (**Fig. 4.9**). The effects of PLEC-Trunc on migration and invasion indicate that the interaction of plectin with integrin and/or mislocalization of plectin play an important role in the mobility of pancreatic cancer cells.

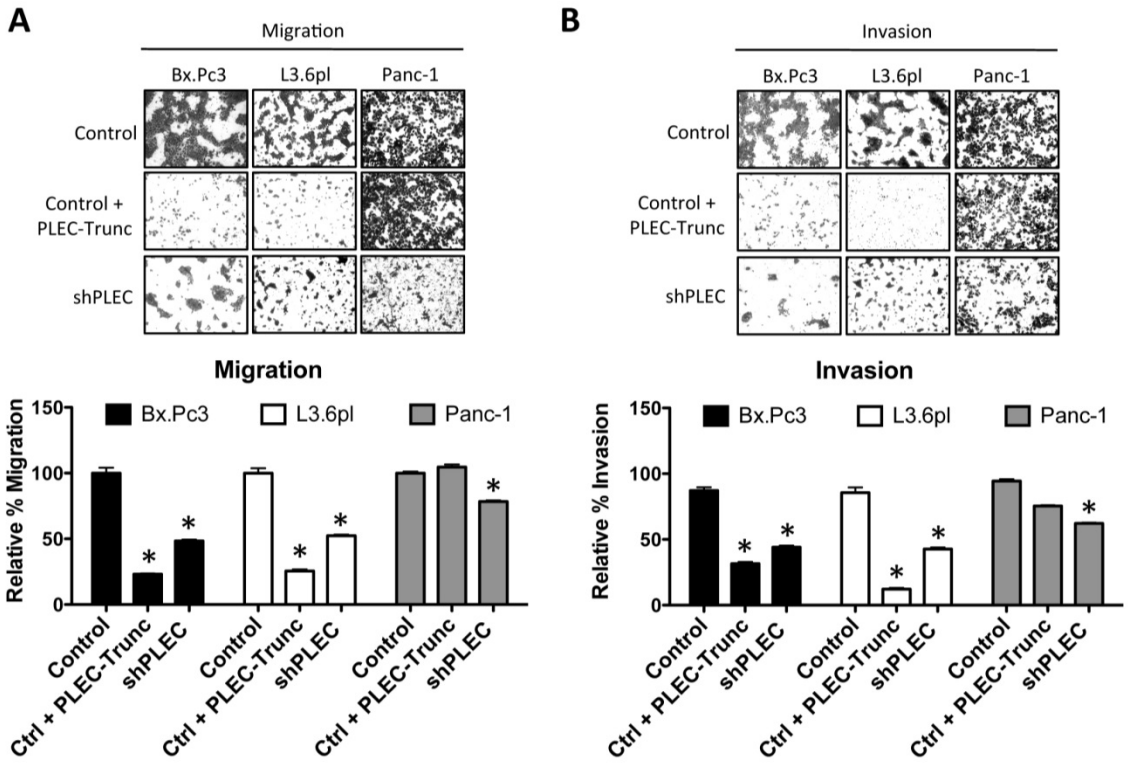

Figure 4.9. PLEC-Trunc transfection decreased **A)** migration as well as **B)** invasion of PDAC cells. * Significant to control ($p < 0.0001$).

Studies in gliomas have suggested that trafficking of the oncogenic receptor EGFRvIII via membrane vesicles can promote neoplastic transformation of non-transformed neighboring cells (87). Thus, we assessed whether transfer of plectin-containing exosomes may likewise have functional significance via transfer of plectin-rich exosomes to cells of other types. We found that plectin-containing PDAC exosomes strongly enhanced the migration and invasion of not only the transformed C6 glioma cells but also non-transformed NIH-3T3 fibroblasts (**Fig. 4.10**). Importantly, these effects were largely plectin-dependent as exosomes from plectin-knockdown PDAC cells did not cause an increase in migration and invasion in C6 or NIH-3T3 cells. Additionally, the effects of plectin-containing exosomes were abrogated by transfection of these cells with PLEC-Trunc. Thus plectin and its localization in the exosomes, and plectin interaction with integrin β4 play a role in migration and invasion of cells other than PDAC, and plectin transfer via exosomes may also contribute to heterotypic signaling to the tumor microenvironment.

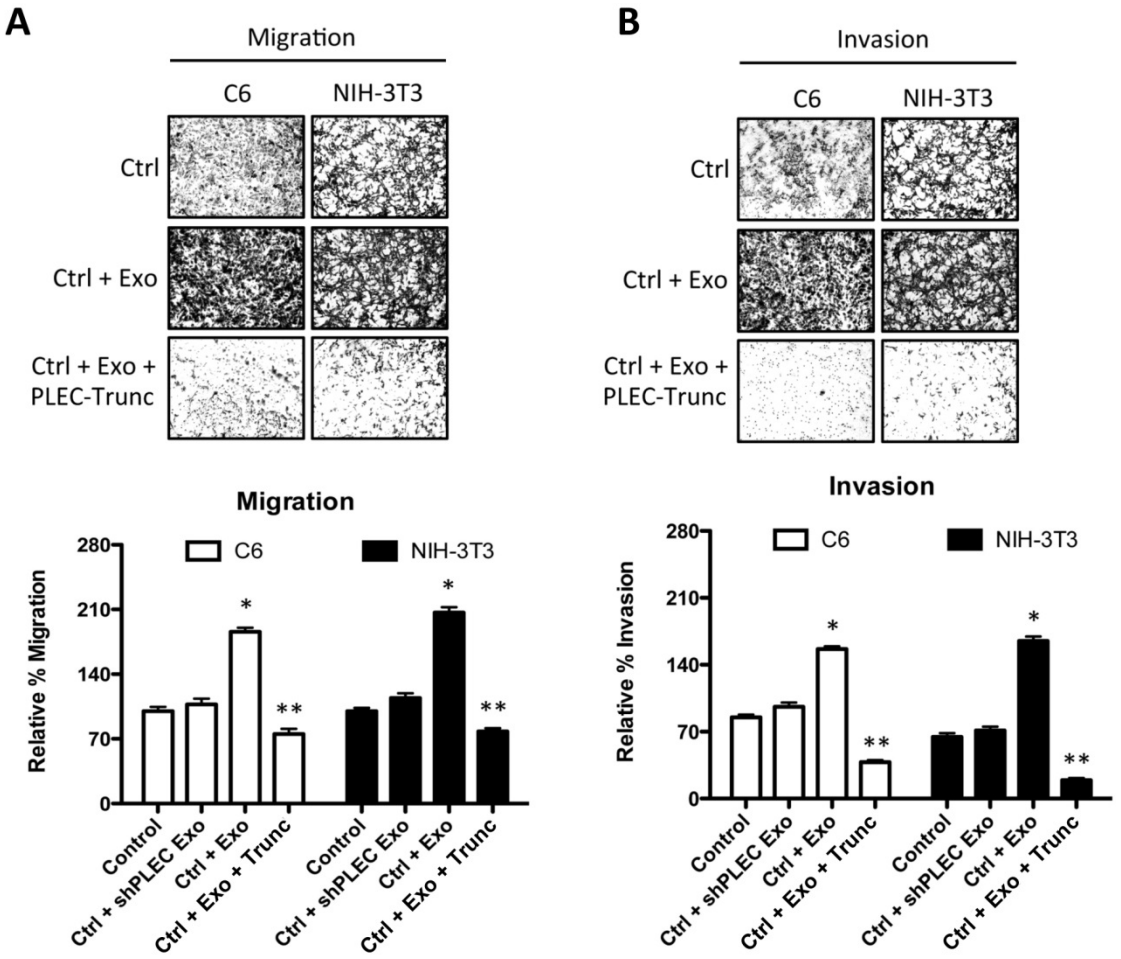

Figure 4.10. Plectin-rich PDAC exosomes increase migration and invasion of cells that lack plectin on the surface. **A)** Migration and **B)** invasion were increased in C6 and NIH-3T3 cells treated with exosomes from L3.6pl, but the effect was abrogated upon PLEC-TRUNC transfection. *Significant to control and +shPLEC exo ($p < 0.0001$), **significant to control + Exo ($p < 0.0001$).

4.3.4. Plectin is required for PDAC tumor growth in vivo

Next, we investigated the effect of plectin knockdown in PDAC *in vivo* tumor growth. Knockdown of plectin significantly delayed tumor growth of PDAC cell line xenografts (**Fig. 4.11**). Interestingly, the growth rates of control and plectin-knockdown tumors were equal by day 9 after injection. When *ex vivo* tumors were evaluated via immnoblot, the tumors that formed from the pan-plectin-knockdown cells had significantly higher plectin expression at day 5 as compared to the levels of day 0 input cells, further indicating the importance of plectin in pancreatic tumor growth.

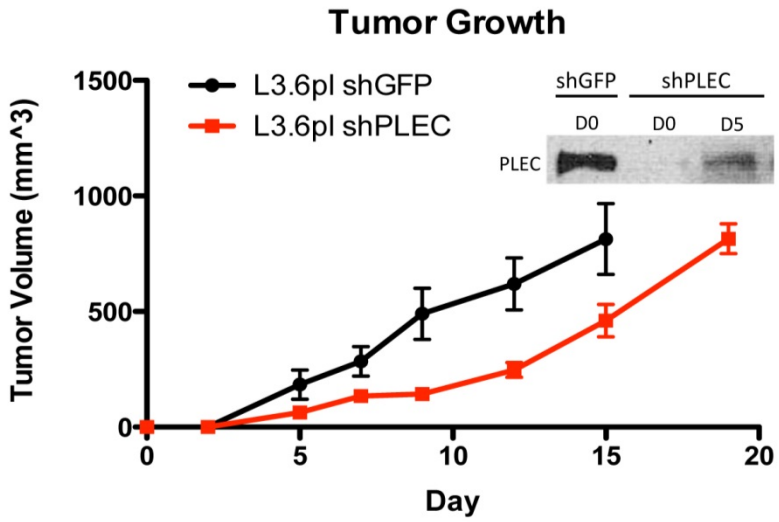

Figure 4.11. Subcutaneous growth of plectin-positive versus plectin-negative tumors. Plectin-positive tumors grew twice as fast as plectin-negative tumors until day 9, but the tumor growth rates were equal after 9 days. Tumors were excised from mice at the indicated time points, homogenized in RIPA buffer with protease inhibitor cocktail, and subjected to immunoblotting (inset). Plectin expression was restored in tumors at day 5, suggesting that plectin may be responsible for equal growth rates of plectin-positive and plectin-negative tumors after day 9.

We also evaluated the role of plectin on the growth and metastases of orthotopically implanted PDAC in immunocompromised mice (**Fig. 4.12**). Pancreata were injected with either plectin-positive or plectin-knockdown L3.6pl cells. Animals at each time point (n =

5 per time point, n = 25 total per group) were sacrificed, tumor volumes determined, pancreas weight measured, and the presence of metastases noted (fraction in graph represents the number of animals from the time point that had metastases). For the immunocompromised animals, the volume for plectin positive and negative tumors began to diverge at day 8 post injection. By day 16, the plectin-positive tumor-bearing animals had to be sacrificed due to moribund conditions. At day 12, two out of five and at day 16, five out of five animals had metastatic deposits. In contrast, plectin knockdown tumor-bearing animals had minimal tumor burden with no detectable metastases.

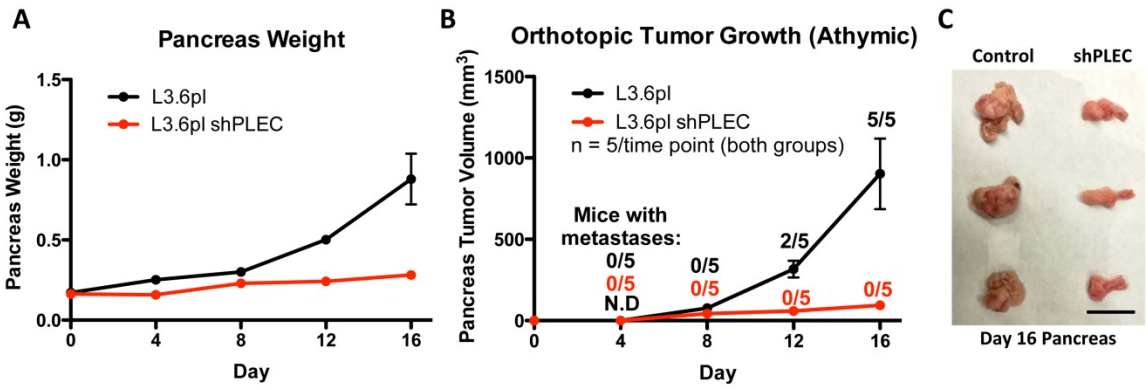

Figure 4.12. A) Weight of pancreas + tumor and **B)** orthotopic growth of plectin-positive and plectin-negative L3.6pl tumors in athymic nude mice. **C)** White light images of control and plectin-knockdown tumors excised on day 16. N.D. = not detectable/measurable via caliper. #/5 indicates the number of mice with metastases. Scale bar = 20mm.

Further, the immune system has been shown to play a key role in tumor development and progression. Therefore, we assessed the role of plectin in PDAC in an immunocompetent, syngeneic mouse model using Han14.3 cells (**Fig. 4.13**), which were derived from spontaneous PDAC arising in *Pft1-Cre; LSL-K-Ras^{G12D}; p53 +/−* mice in the background of an inbred FVB/NJ strain (32). As in the immunocompromised animals, in immunocompetent animals, the growth of plectin-positive tumors was faster than that of plectin-knockdown tumors. The tumor growth rate began to diverge at day 6. One of the

Han14.3 shPLEC tumors was not detectable at day 6. By day 10, Han14.3 tumor volume was 5-fold larger compared to those of Han14.3 shPLEC tumors. Due to the aggressive nature of this tumor and according to the rules of Animal Care and Use Committee, we had to sacrifice FVB mice bearing Han14.3 and Han14.3 shPLEC 10 days post tumor injection. Similar to L3.6pl tumors in immunodeficient mice, all five Han14.3 tumors resulted in metastases whereas only one mouse bearing Han14.3 shPLEC tumor had metastasis. This further strengthens our hypothesis that plectin is important in PDAC growth.

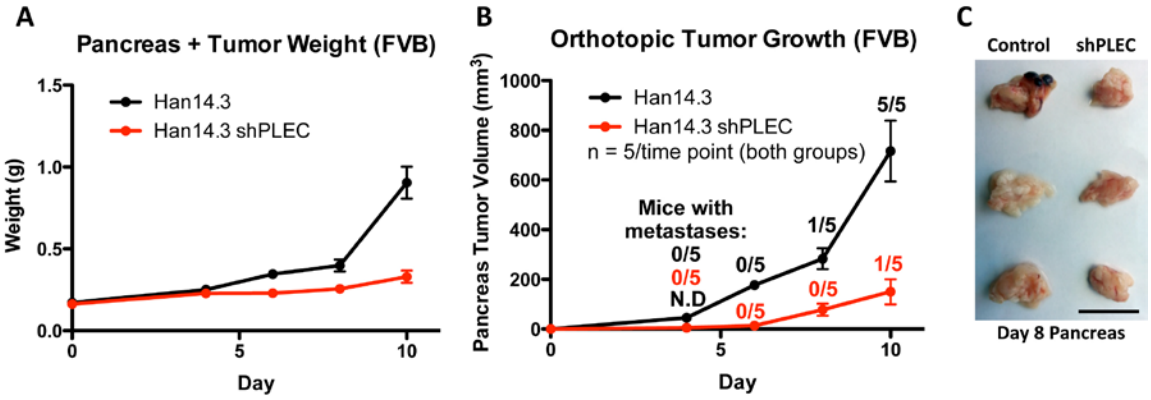

Figure 4.13. A) Weight of pancreas + tumor and **B)** orthotopic growth of plectin-positive and plectin-negative Han14.3 tumors in syngeneic FVB mice. **C)** White light images of control and plectin-knockdown tumors excised on day 8. N.D. = not detectable/measurable via caliper. #/5 indicates the number of mice with metastases. Scale bar = 10mm.

4.4. Summary and discussion

Previously, we discovered that plectin is overexpressed in PDAC and high-grade precursor lesion PanIN-III, but not in normal pancreata or low-grade precursor lesions PanIN-I and PanIN-II (32). Additionally, our findings on the role of plectin in PDAC exosome secretion led us to hypothesize that plectin may be involved in the aggressive nature of pancreatic cancer. Furthermore, the plectin locus has a complex organization, with eleven alternative first exons, eight of which are coding, giving rise to at least eight different plectin isoforms (55). Based on the distinct roles played by different plectin isoforms, the cytoplasmic expression of plectin in normal keratinocytes and muscle cells (55, 66) and our previous findings of plectin overexpression in PDAC (31), we sought to investigate whether plectin is important in PDAC progression, tumorigenesis, invasion and metastasis, and the profile and function of plectin isoforms in PDAC.

First, we investigated plectin isoform expression in PDAC compared to HPDE or normal pancreata and demonstrated that PDAC exhibits deregulated expression of plectin isoforms, with isoforms 1a and 1f predominantly expressed. Knockdown of these isoforms resulted in decreased binding of PTP on PDAC cell surface, suggesting that these isoforms may be the isoforms mainly responsible for plectin cell surface localization, as knockdown of isoform 1c did not significantly reduce PTP binding. Because plectin-rich exosomes were able to stimulate the growth of PDAC tumors, these isoforms may be the main isoforms responsible for PDAC growth and aggression.

Next, we investigated the functional role of plectin in PDAC through lentiviral-based knockdown with concurrent rescue. We examined whether plectin has a role in PDAC

proliferation, migration, invasion, and tumorigenesis. Using isoform-specific knockdown, we found that plectin-1a and 1f, the isoforms mainly present in PDAC in PCR analysis, decrease PDAC proliferation, migration, and invasion significantly. To further study the effects of these isoforms, we used pan-plectin knockdown PDAC cells, overexpressed plectin-1a and 1f, and evaluated the ability of these isoforms to rescue PDAC growth and migration. These rescue experiments confirmed that plectin-1a and 1f indeed were able to restore the growth and migration of PDAC cells.

To further understand the role of plectin and its relationship with integrin β4, we examined the effect of plectin-integrin interaction β4 on PDAC migration and invasion. To evaluate this, we used PLEC-Trunc, a truncated form of plectin only containing the ABD region. PLEC-Trunc has a higher affinity to integrin β4 than full-length plectin and was shown to decrease cell surface plectin in PDAC cells (**Chapter 2**). We found that overexpressing PLEC-Trunc resulted in a significant decrease in migration and invasion, most likely due to disruption of interaction between endogenous plectin and integrin β4. Moreover, incubating cell lines that are devoid of cell surface plectin, NIH-3T3 fibroblasts and C6 glioma, with plectin-rich exosomes increased invasion and migration. This was expected due to the correlation between exosomal plectin and enhanced migration in PDAC and the ability of plectin-rich exosomes to transfer plectin on to the surfaces of NIH-3T3 and HUVEC as observed in **Chapter 2**. This effect, however, was eliminated with PLEC-Trunc transfection. Taken together, our data indicate that the plectin-integrin β4 interaction is important for PDAC progression. Additional studies need to be conducted to delineate if the plectin-integrin β4 complex propagates the growth and migratory signals through the integrin β4 pathway or other alternative pathways. It is also possible that plectin transports many signaling proteins and other effector oncogenes that amplify the signal transduction pathway.

Finally, we studied the growth of orthotopic tumors generated with plectin-knockdown PDAC cells. Compared to control tumors, plectin-knockdown tumors were 10-fold and 5-fold smaller in immunocompetent and immunocompromised mice, respectively. Importantly, the mice bearing plectin-knockdown tumors showed almost no metastases whereas 100% of the control tumors generated metastases. As plectin knockdown inhibits exosome production, it is difficult to determine whether the effect is from intracellular or exosomal plectin. However, results from **Chapter 3** showed that plectin-rich exosomes were able to enhance PDAC tumor growth, suggesting that reduction in orthotopic tumor growth may be due to exosomal and cell surface plectin.

It is interesting to note that plectin-1a and 1f are the major isoforms involved in PDAC growth, migration, and invasion. Plectin-1a is crucial for maintaining the homeostasis of the cytoskeletal structures (64, 65) and plectin-1f is important for muscle structure and integrity (68). Interestingly, Fuchs *et al.* showed that plectin-1a and 1f are abundant in small intestine whereas plectin-1 expression is less pronounced (55). Pancreas secretes enzymes into a part of small intestine that connects to stomach. A recent study by Gubergrits *et al.* showed that there is an increased enzymatic activity in the small intestines of patients with chronic pancreatitis (143). They hypothesized that the rise in enzyme activity may be due to compensatory tension in intestinal digestion in patients suffering from exocrine insufficiency of pancreas. Due to pancreatitis patients' high risk for developing PDAC, there may be a link between overactive pancreatic enzymes and plectin-1a and 1f expression in development of PDAC. An alternative hypothesis is that the lack of plectin-1 in PDAC cell lines contributes to enhanced growth and migration. Because plectin-1 was shown to be involved in leukocyte infiltration (61), plectin-1 may play an anti-tumor immune response, as it was isoform exclusive to normal HPDE.

In this chapter, we showed that plectin enhances the growth and metastasis of pancreatic cancer as well as fibroblasts and endothelial cells, which are important components of tumor microenvironment. Further studies should be conducted to determine the potential for plectin and the identified isoforms to promote transition from PanIN-III to PDAC by expressing the identified plectin isoforms in pancreatic ductal epithelial cells. Identifying the functional role of plectin at early stages of PDAC may provide important insights leading to better treatment of PDAC.

CHAPTER 5

CONCLUSIONS AND FUTURE DIRECTIONS

5.1. Conclusions

Previously, we determined plectin to be a highly specific biomarker for the transition of non-invasive to invasive pancreatic cancer (31). We demonstrated the feasibility of targeting plectin with imaging agents as a method for the early detection that is critically needed for this terminal disease (32). Surprisingly, the normally cytoplasmic plectin was found on the surface of PDAC cells and has since been shown to be upregulated in several cancers, including esophageal cancer and head and neck squamous cell carcinoma (144, 145). Tissue microarray analysis revealed that other cancer types including cholangiocarcinoma, colorectal adenocarcinoma, lung adenocarcinoma, and ovarian serous carcinoma also express plectin (146), suggesting that upregulation of plectin may play an important role in other cancer types as well.

Many types of normal and cancerous cells are known to secrete extracellular vesicles of endocytic origin known as exosomes. We demonstrate that plectin-rich exosomes can be isolated from tissue culture medium as well as serum of tumor-bearing mice. In addition, incubation of cells with plectin-rich exosomes could confer cell surface plectin on cells that were previously devoid of such expression. These data suggest that surface localization of plectin requires exosomes. Furthermore, transient expression of plectin isoforms 1a and 1f in C6 and HPDE cells reveals that translocation of these isoforms to the cell surface when abnormally upregulated is not unique to PDAC.

Integrin β4, a known binding partner of plectin, was also found in the PDAC exosomes. Therefore, we examined whether the interaction between plectin and integrin β4 was necessary for plectin inclusion in the exosomes. Integrin β4 presence in exosomes is not

plectin dependent as knockdown of plectin did not alter levels of integrin β4 in exosomes. However plectin was absent from exosomes in integrin β4-knockdown cells indicating the reliance of plectin on integrin β4 for exosome localization. Thus, our data indicate that plectin is translocalized to the cell surface by anchoring to integrin β4 in the exosomes.

Further, we have shown that plectin is necessary for efficient exosome secretion, equivalent to Rab27a and Rab27b. Inhibition of exosome secretion by knockdown of Rab27a eliminates surface localization of plectin but has no effect on the levels of plectin expression. Quantitative comparison of the protein content of exosomes from control and plectin-knockdown PDAC cells through mass spectrometry revealed that several proteins are differentially expressed. For example, Cobl (Cordon-Bleu WH2 Repeat Protein) was 25-fold higher in plectin-knockdown exosomes. Cobl was identified as an actin nucleation factor mostly expressed in brain. It was found to be involved in morphogenesis of the central nervous system and some of its properties were shown to resemble those of formin (147). Among the downregulated proteins, SACM1L, a phosphatidylinositide phosphatase that regulates golgi membrane morphology and mitotic spindle organization (148), was reduced 20-fold upon plectin knockdown. The second most downregulated protein after plectin knockdown was ribosomal protein RPL15 with a 15-fold decrease compared to the control exosomes. Interestingly, RPL15, which is present in the cytoplasm, was shown to be overexpressed in esophageal tumors (149) and gastric cancer (150). In addition, there was a 2-fold decrease in HSPA9B (Hsp70), which is a putative exosome marker. This further reinforces our data that plectin knockdown reduces exosome secretion.

Plectin upregulation coupled with mislocalization has profound effects on PDAC. When plectin expression is silenced in PDAC cells, proliferation, invasion and migration are negatively impacted. We demonstrated that the major isoforms involved in PDAC growth and progression are plectin-1a and 1f. Overexpression of these isoforms in pan-plectin knockdown cells resulted in the rescue of growth and migratory phenotypes. Moreover, orthotopic animal models showed that plectin-knockdown tumors were significantly smaller in volume compared to control tumors in both immunodeficient and syngeneic FVB mice with 100% of the control tumors metastasizing. To determine whether the effect is from intracellular or exosomal plectin, we examined whether isolated, PDAC-derived exosomes from either plectin-positive or plectin-knockdown cells had physiological effects on the tumor cells. Similar to the reports of Peinado *et al.* (117), when the exosome formation was inhibited by shRNA-mediated knockdown of Rab27a, we found that the tumor growth was decreased correspondingly. However, although cytoplasmic levels of plectin remained unchanged in the Rab27a knockdown tumors, intratumoral injection of plectin-rich exosomes, but not exosomes from plectin-knockdown cells, overcame the growth inhibition due to Rab27a knockdown. Plectin-rich exosomes not only rescued tumor growth but also promoted a growth rate that was faster than that of control tumors. These effects suggest that the translocalization of plectin to the exosomes may play an important role in pancreatic cancer growth and progression, possibly through scaffolding and transferring of various signaling molecules that interact with plectin to the tumor microenvironment.

Exosomes have already been shown to enhance tumor growth and metastasis via horizontal propagation of oncogenes in other cancer types (87, 111, 117, 151). However, the mechanisms for exosome production, secretion and regulation are still poorly understood. In this study, we confirmed the cell surface localization of plectin using flow

cytometry, plectin targeting peptide (PTP)-binding assays and transmission electron microscopy (TEM). As we investigated how the protein was translocated to the cell surface, we observed functional roles for the mislocalized plectin in pancreatic cancer cell lines and potentially, the tumor microenvironment. We illuminated a new mechanism for plectin deregulation in cancer, involving isoform-specific upregulation, mislocalization and extracellular trafficking via integrin β4-binding and exosome secretion. Loss of plectin has dramatic effects on PDAC biology, part of which is mediated through exosomes.

In conclusion, studies in this dissertation reveal a novel mechanism behind plectin mislocalization as well as an important role of plectin in pancreatic cancer aggression. Plectin also exhibited potential for promoting paracrine growth of stromal cells via exosome transfer. Thus our study provides important information about the regulation of a clinically relevant biomarker. This novel role of plectin may have important consequences in PDAC pathogenesis as well as other tumors where plectin is shown to be expressed. Therefore, the important role of plectin warrants further investigations.

5.2. Future directions

5.2.1. Studies in pancreatic intraepithelial neoplasia (PanIN) using PDECs

Investigating the functional effect of plectin in cells that mimic the beginning stages of PDAC would provide important insights into how this protein facilitates PDAC progression. Mutational activation of *K-Ras* is the first and most frequently detected genetic lesion in PDAC (152). Bar-Sagi's group developed pancreatic ductal epithelial cells (PDECs) with and without *K-Ras* mutation that resemble early stage PDAC to show that oncogenic *K-Ras* is involved in PDAC initiation by preventing cells from entering a state of permanent growth arrest (152). Therefore, investigating the growth properties of PDEC and the potential role of plectin in this process will be critical for understanding the initiation of PDAC. Proposed study will utilize PDECs transfected with plectin constructs to assess plectin's ability to induce cellular growth, migration, and invasion *in vitro* and pancreatic tumorigenesis *in vivo*. If plectin is capable of inducing PDECs to form a tumor, mutations that occur in PanIN-II and PanIN-III (inactivation of *p53* tumor suppressor and loss of *BRCA2/LKB1*) may be present. Based on our data, we hypothesize that the transfection of plectin into PDECs will cause an increased cellular growth *in vitro* and enable PDECs to form a tumor *in vivo.* We further expect that PDECs with plectin expression may show a ductal morphology as seen in PDAC and behave similarly to PDAC cell lines with an increased migration and invasion.

5.2.2. Conditional knockout of plectin-1a/1f and K-Ras/p53 mutant animal models

It has been shown that pan-plectin knockout mice die only 2-3 days after birth due to severe skin blistering and muscle disorders (45). Due to their short life span, pan-plectin knockout mice have a limited potential as animal models for studying PDAC. Therefore,

future studies can be conducted using the conditional Cre/loxP knockout system, where a mouse line that is deficient in specific plectin isoforms can be generated. Another approach can be used to generate plectin deficiency in certain tissues of mice without affecting their development. This can be achieved by conditional plectin gene knockout by crossing mouse lines carrying a floxed plectin gene with Cre-expressing transgenic mice. Ackerl *et al.* already have generated a mouse line bearing floxed plectin alleles that is plectin-1c-deficient in stratified epithelia without affecting isoform expression in other tissues (153). Conditional plectin-1a or 1f knockout mice can be then crossed with invasive PDAC mouse models that have endogenous *K-Ras*^{G12D} and *p53*^{R172H} expression (154). Comparison between the *K-Ras*^{G12D} *p53*^{R172H} mice and *K-Ras*^{G12D} *p53*^{R172H} crossed with plectin knockout mice will provide important insight into the role that plectin plays in pancreatic tumorigenesis.

5.2.3. Cell surface plectin and plectin-positive exosomes in other cancer types

We examined whether normal cells that produce abundant exosomes (JAWSII immature dendritic cells and renal cells) (155, 156) or cells that are rich in cytosolic plectin (keratinocyte and C6 glioma) (64, 157) also have plectin on their cell surface. We found that these cell types did not exhibit PTP surface binding except for renal cells (**Fig. 5.1**). This indicated that not all cell types rich in plectin or exosomes induce cell surface localization of plectin. In addition, studies from Peinado *et al.* showed that melanoma cells produce exosomes that can educate bone marrow progenitor cells towards metastatic phenotype (117). This motivated us to examine melanoma cell lines for the presence of cell surface plectin (**Fig. 5.2**). Surprisingly, melanoma cell lines exhibited 4-fold increase in cell surface binding compared to C6 negative control, similar to the level of PDAC cell lines. Future studies can be conducted on other cancer cell types that

express plectin or produce exosomes to examine the role that plectin may have on tumor aggressiveness.

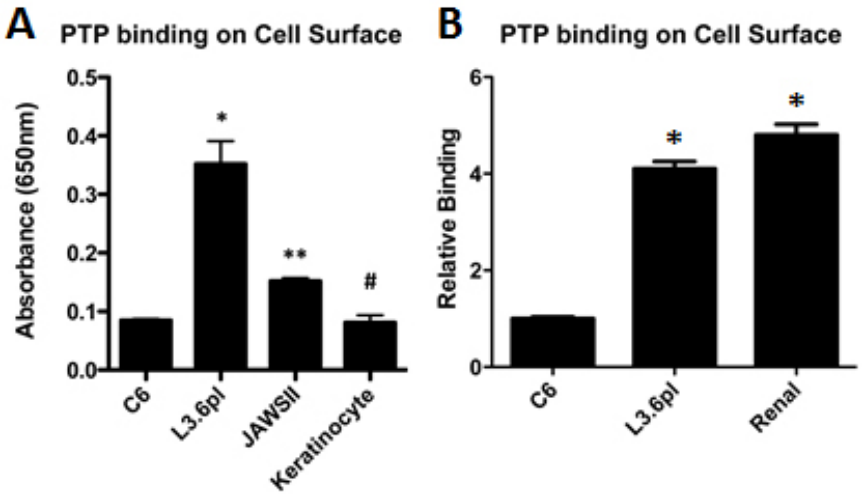

Figure 5.1. PTP binding on the surface of **A)** C6, L3.6pl, JAWSII immature dendritic cells, and normal human adult keratinocytes, and **B)** renal cells. *Significant to C6 ($P < 0.0001$); **significant to both C6 and L3.6pl ($P < 0.0001$); #significant to L3.6pl ($P < 0.0001$).

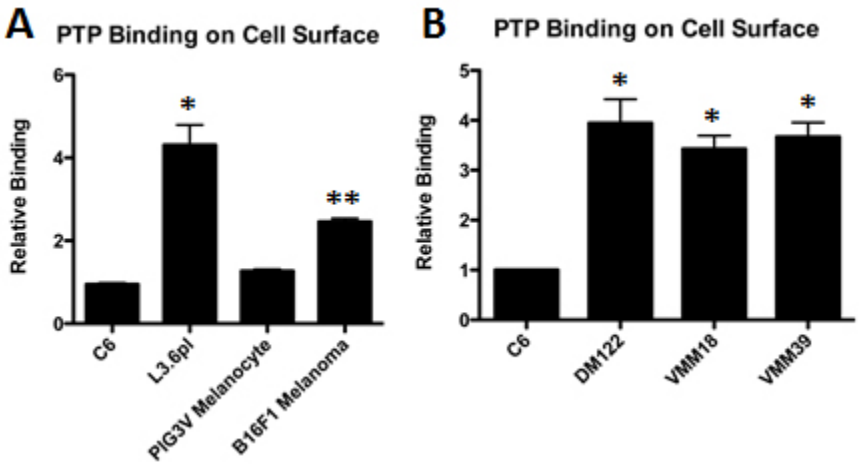

Figure 5.2. PTP binding on the surface of **A)** PIG3V melanocytes and B16F1 melanoma, and **B)** three different melanoma cell lines compared to C6. *Significant to C6 ($P < 0.0001$); **significant to both C6 and L3.6pl ($P < 0.0001$).

5.2.4. Signal transduction pathways

Plectin knockdown induced significant changes in migration and invasion of PDAC and cells of microenvironment. However, we have yet to show the signaling pathways that are affected by plectin downregulation or pathways that induce changes in plectin expression. A potential method is to utilize pharmacological inhibition. Low *et al.* showed that PI3K isoform p110δ is involved in regulation of membrane fission for cytokine secretion (158). PI3K pathway has also been implicated in invasion of many tumor types (159-161). Thus, this pathway may be important in modulating the secretion of plectin-rich exosomes to induce increased migration. To test this, PDAC cells can be treated with p110δ-specific inhibitor (IC87114) and compared with pan-p110 inhibitor (SF1126) to examine whether the production levels of exosomes decrease in PDAC. Various concentrations and treatment time points will be necessary to optimize the drug inhibition and observe the degree of inhibition over time. Changes in plectin and other signaling molecules in the inhibited cells can be monitored via western blot.

We have performed preliminary studies using pan-PI3K and MEK1/2 inhibitors (**Fig. 5.3**). We hypothesized that the expression of plectin will be decreased after PI3K inhibition due to its involvement in membrane fission for cytokine secretion. In addition to PI3K, MEK1/2 inhibition may also affect plectin expression because PI3K and MAPK pathways are two major signaling cascades involved in PDAC. To our surprise, we found that MEK1/2 inhibition did not affect plectin expression. Additionally, PI3K inhibition for 1 h resulted in an increase in plectin expression in PDAC cell lines. 24 h drug treatment did not result in any changes. This may be due to the degradation of the inhibitor and thus inefficient inhibition as pAKT was partially expressed. A possible explanation for an increase in plectin expression is that after PI3K inhibition, exosome secretion is hindered

due to inefficient membrane fission, and plectin is no longer secreted via exosomes into the extracellular milieu, thereby increasing total intracellular plectin. Due to the importance of plectin in PDAC tumor growth, there is a possibility that the plectin expression may be increased to compensate for PI3K inhibition to sustain cancer cell survival.

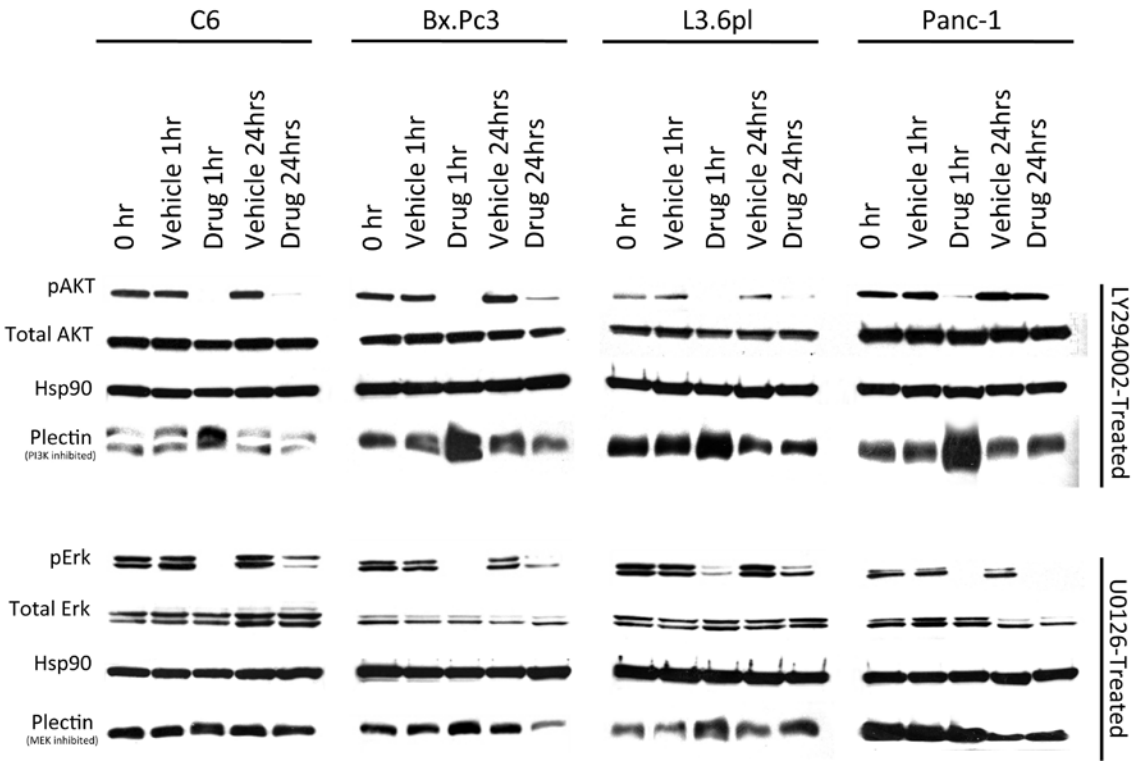

Figure 5.3. Pharmacological inhibition of PI3K or MEK1/2. Plectin expression increased after 1 h treatment with LY294002, a pan-PI3K inhibitor.

Previous studies have demonstrated that the interaction of plectin and IFs is differentially regulated by phosphorylation of various protein kinases (58, 162). For example, plectin-lamin B interaction was shown to be decreased upon phosphorylation by cAMP-dependent protein kinase (PKA) or calcium-dependent protein kinase C (PKC). On the other hand, plectin's interaction with vimentin was increased upon PKA phosphorylation, but decreased after PKC phosphorylation (58). Recently, plectin was found to modulate

signals to PKC through binding and sequestration of RACK1, the receptor for activated C kinase 1 (139). It was shown that upon PKC activation, RACK1 was released from the cytoskeleton and transferred to the detergent-soluble cell compartment, where it formed an inducible triple complex with one of the PKC isozymes, PKCδ, and with plectin. PI3K pathway also activates PKB, which then activates PKC (163). Based on this study, we performed preliminary experiments to determine whether the PKC expression levels change upon plectin knockdown. We found that PKCα/β was downregulated in plectin-knockdown cells (**Fig. 5.4**). Further studies should be performed to determine if PI3K or PKC is involved in the secretion of plectin-containing exosomes.

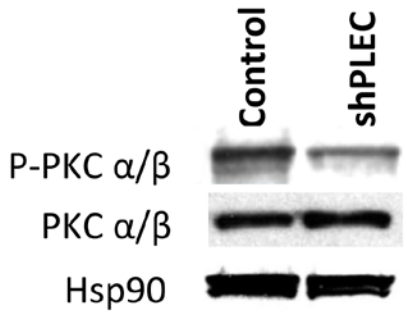

Figure 5.4. PKC α/β phosphorylation decreases with plectin knockdown.

References

1. Hezel AF, Kimmelman AC, Stanger BZ, Bardeesy N, & Depinho RA (2006) Genetics and biology of pancreatic ductal adenocarcinoma. *Genes & development* 20(10):1218-1249.

2. Yeo TP *et al.* (2002) Pancreatic cancer. *Current problems in cancer* 26(4):176-275.

3. Society AC (2012) Cancer Facts & Figures 2012. in *American Cancer Society* (Atlanta).

4. Jemal A *et al.* (2009) Cancer statistics, 2009. *CA: a cancer journal for clinicians* 59(4):225-249.

5. Goggins M (2007) Identifying molecular markers for the early detection of pancreatic neoplasia. *Seminars in oncology* 34(4):303-310.

6. Levine JS & Ahnen DJ (2006) Clinical practice. Adenomatous polyps of the colon. *The New England journal of medicine* 355(24):2551-2557.

7. Kerlikowske K (1997) Efficacy of screening mammography among women aged 40 to 49 years and 50 to 69 years: comparison of relative and absolute benefit. *Journal of the National Cancer Institute. Monographs* (22):79-86.

8. Berger AC *et al.* (2008) Postresection CA 19-9 predicts overall survival in patients with pancreatic cancer treated with adjuvant chemoradiation: a prospective validation by RTOG 9704. *Journal of clinical oncology : official journal of the American Society of Clinical Oncology* 26(36):5918-5922.

9. Hess V *et al.* (2008) CA 19-9 tumour-marker response to chemotherapy in patients with advanced pancreatic cancer enrolled in a randomised controlled trial. *The lancet oncology* 9(2):132-138.

10. Ferrone CR *et al.* (2006) Perioperative CA19-9 levels can predict stage and survival in patients with resectable pancreatic adenocarcinoma. *Journal of clinical oncology : official journal of the American Society of Clinical Oncology* 24(18):2897-2902.

11. Karmazanovsky G, Fedorov V, Kubyshkin V, & Kotchatkov A (2005) Pancreatic head cancer: accuracy of CT in determination of resectability. *Abdominal imaging* 30(4):488-500.

12. Chari ST (2007) Detecting early pancreatic cancer: problems and prospects. *Seminars in oncology* 34(4):284-294.

13. Pelaez-Luna M, Takahashi N, Fletcher JG, & Chari ST (2007) Resectability of presymptomatic pancreatic cancer and its relationship to onset of diabetes: a retrospective review of CT scans and fasting glucose values prior to diagnosis. *The American journal of gastroenterology* 102(10):2157-2163.

14. Ito Y *et al.* (2012) Endoscopic management of pancreatic duct injury by endoscopic stent placement: a case report and literature review. *World journal of emergency surgery : WJES* 7(1):21.

15. Bloomston M *et al.* (2006) Fibrinogen gamma overexpression in pancreatic cancer identified by large-scale proteomic analysis of serum samples. *Cancer research* 66(5):2592-2599.

16. Misek DE, Kuick R, Hanash SM, & Logsdon CD (2005) Oligonucleotide-directed microarray gene profiling of pancreatic adenocarcinoma. *Methods in molecular medicine* 103:175-187.

17. Network NCC (2010) Pancreatic Adenocarcinoma. . in *Clinical Practice Guidelines in Oncology 2009*.

18. Li D, Xie K, Wolff R, & Abbruzzese JL (2004) Pancreatic cancer. *Lancet* 363(9414):1049-1057.

19. Greenhill C (2011) Pancreatic cancer: Gemcitabine confirmed as the first-line therapy for pancreatic cancer. *Nature Reviews Gastroenterology and Hepatology* 8:3.

20. Burris HA, 3rd *et al.* (1997) Improvements in survival and clinical benefit with gemcitabine as first-line therapy for patients with advanced pancreas cancer: a randomized trial. *Journal of clinical oncology : official journal of the American Society of Clinical Oncology* 15(6):2403-2413.

21. Dahan L *et al.* (2010) Combination 5-fluorouracil, folinic acid and cisplatin (LV5FU2-CDDP) followed by gemcitabine or the reverse sequence in metastatic pancreatic cancer: final results of a randomised strategic phase III trial (FFCD 0301). *Gut* 59(11):1527-1534.

22. Bramhall SR *et al.* (2002) A double-blind placebo-controlled, randomised study comparing gemcitabine and marimastat with gemcitabine and placebo as first line therapy in patients with advanced pancreatic cancer. *British journal of cancer* 87(2):161-167.

23. Philip PA *et al.* (2010) Phase III study comparing gemcitabine plus cetuximab versus gemcitabine in patients with advanced pancreatic adenocarcinoma: Southwest Oncology Group-directed intergroup trial S0205. *Journal of clinical oncology : official journal of the American Society of Clinical Oncology* 28(22):3605-3610.

24. Kindler HL *et al.* (2010) Gemcitabine plus bevacizumab compared with gemcitabine plus placebo in patients with advanced pancreatic cancer: phase III trial of the Cancer and Leukemia Group B (CALGB 80303). *Journal of clinical oncology : official journal of the American Society of Clinical Oncology* 28(22):3617-3622.

25. Moore MJ *et al.* (2007) Erlotinib plus gemcitabine compared with gemcitabine alone in patients with advanced pancreatic cancer: a phase III trial of the National Cancer Institute of Canada Clinical Trials Group. *Journal of clinical oncology : official journal of the American Society of Clinical Oncology* 25(15):1960-1966.

26. Miyabayashi K *et al.* (2013) Erlotinib prolongs survival in pancreatic cancer by blocking gemcitabine-induced MAPK signals. *Cancer research* 73(7):2221-2234.

27. Lowy AMaP, P. (2008) Pancreatic Intraepithelial Neoplasia. Pancreatic Cancer. *MD Anderson Solid Tumor Oncology Series* 18:41-51.

28. Kimura W (2003) How many millimeters do atypical epithelia of the pancreas spread intraductally before beginning to infiltrate? *Hepato-gastroenterology* 50(54):2218-2224.

29. Luttges J *et al.* (2000) Ductal lesions in patients with chronic pancreatitis show K-ras mutations in a frequency similar to that in the normal pancreas and lack nuclear immunoreactivity for p53. *Cancer* 88(11):2495-2504.

30. Luttges J *et al.* (2003) Lack of apoptosis in PanIN-1 and PanIN-2 lesions associated with pancreatic ductal adenocarcinoma is not dependent on K-ras status. *Pancreas* 27(3):e57-62.

31. Kelly KA *et al.* (2008) Targeted nanoparticles for imaging incipient pancreatic ductal adenocarcinoma. *PLoS medicine* 5(4):e85.

32. Bausch D *et al.* (2011) Plectin-1 as a novel biomarker for pancreatic cancer. *Clinical cancer research : an official journal of the American Association for Cancer Research* 17(2):302-309.

33. Wiche G (1998) Role of plectin in cytoskeleton organization and dynamics. *Journal of cell science* 111 (Pt 17):2477-2486.

34. Wiche G (1989) Plectin: general overview and appraisal of its potential role as a subunit protein of the cytomatrix. *Critical reviews in biochemistry and molecular biology* 24(1):41-67.

35. Errante LD, Wiche G, & Shaw G (1994) Distribution of plectin, an intermediate filament-associated protein, in the adult rat central nervous system. *Journal of neuroscience research* 37(4):515-528.

36. Yaoita E, Wiche G, Yamamoto T, Kawasaki K, & Kihara I (1996) Perinuclear distribution of plectin characterizes visceral epithelial cells of rat glomeruli. *The American journal of pathology* 149(1):319-327.

37. Wiche G, Krepler R, Artlieb U, Pytela R, & Denk H (1983) Occurrence and immunolocalization of plectin in tissues. *The Journal of cell biology* 97(3):887-901.

38. Wiche G & Furtner R (1980) Microtubule associated proteins stabilize the colchicine binding activity of tubulin. *FEBS letters* 116(2):247-250.

39. Pytela R & Wiche G (1980) High molecular weight polypeptides (270,000-340,000) from cultured cells are related to hog brain microtubule-associated proteins but copurify with intermediate filaments. *Proceedings of the National Academy of Sciences of the United States of America* 77(8):4808-4812.

40. Rezniczek GA, de Pereda JM, Reipert S, & Wiche G (1998) Linking integrin alpha6beta4-based cell adhesion to the intermediate filament cytoskeleton: direct interaction between the beta4 subunit and plectin at multiple molecular sites. *The Journal of cell biology* 141(1):209-225.

41. Litjens SH *et al.* (2003) Specificity of binding of the plectin actin-binding domain to beta4 integrin. *Molecular biology of the cell* 14(10):4039-4050.

42. Koster J, van Wilpe S, Kuikman I, Litjens SH, & Sonnenberg A (2004) Role of binding of plectin to the integrin beta4 subunit in the assembly of hemidesmosomes. *Molecular biology of the cell* 15(3):1211-1223.

43. Eger A, Stockinger A, Wiche G, & Foisner R (1997) Polarisation-dependent association of plectin with desmoplakin and the lateral submembrane skeleton in MDCK cells. *Journal of cell science* 110 (Pt 11):1307-1316.

44. Seifert GJ, Lawson D, & Wiche G (1992) Immunolocalization of the intermediate filament-associated protein plectin at focal contacts and actin stress fibers. *European journal of cell biology* 59(1):138-147.

45. Andra K *et al.* (1997) Targeted inactivation of plectin reveals essential function in maintaining the integrity of skin, muscle, and heart cytoarchitecture. *Genes & development* 11(23):3143-3156.

46. Gache Y *et al.* (1996) Defective expression of plectin/HD1 in epidermolysis bullosa simplex with muscular dystrophy. *The Journal of clinical investigation* 97(10):2289-2298.

47. Chavanas S *et al.* (1996) A homozygous nonsense mutation in the PLEC1 gene in patients with epidermolysis bullosa simplex with muscular dystrophy. *The Journal of clinical investigation* 98(10):2196-2200.

48. McLean WH *et al.* (1996) Loss of plectin causes epidermolysis bullosa with muscular dystrophy: cDNA cloning and genomic organization. *Genes & development* 10(14):1724-1735.

49. Smith FJ *et al.* (1996) Plectin deficiency results in muscular dystrophy with epidermolysis bullosa. *Nature genetics* 13(4):450-457.

50. Malecz N, Foisner R, Stadler C, & Wiche G (1996) Identification of plectin as a substrate of p34cdc2 kinase and mapping of a single phosphorylation site. *The Journal of biological chemistry* 271(14):8203-8208.

51. Rezniczek GA, Janda L, & Wiche G (2004) Plectin. *Methods in cell biology* 78:721-755.

52. Nikolic B, Mac Nulty E, Mir B, & Wiche G (1996) Basic amino acid residue cluster within nuclear targeting sequence motif is essential for cytoplasmic plectin-vimentin network junctions. *The Journal of cell biology* 134(6):1455-1467.

53. Elliott CE *et al.* (1997) Plectin transcript diversity: identification and tissue distribution of variants with distinct first coding exons and rodless isoforms. *Genomics* 42(1):115-125.

54. Andra K, Nikolic B, Stocher M, Drenckhahn D, & Wiche G (1998) Not just scaffolding: plectin regulates actin dynamics in cultured cells. *Genes & development* 12(21):3442-3451.

55. Fuchs P *et al.* (1999) Unusual 5' transcript complexity of plectin isoforms: novel tissue-specific exons modulate actin binding activity. *Human molecular genetics* 8(13):2461-2472.

56. Wiche G, Herrmann H, Leichtfried F, & Pytela R (1982) Plectin: a high-molecular-weight cytoskeletal polypeptide component that copurifies with intermediate filaments of the vimentin type. *Cold Spring Harbor symposia on quantitative biology* 46 Pt 1:475-482.

57. Foisner R *et al.* (1988) Cytoskeleton-associated plectin: in situ localization, in vitro reconstitution, and binding to immobilized intermediate filament proteins. *The Journal of cell biology* 106(3):723-733.

58. Foisner R, Traub P, & Wiche G (1991) Protein kinase A- and protein kinase C-regulated interaction of plectin with lamin B and vimentin. *Proceedings of the National Academy of Sciences of the United States of America* 88(9):3812-3816.

59. Lunter PC & Wiche G (2002) Direct binding of plectin to Fer kinase and negative regulation of its catalytic activity. *Biochemical and biophysical research communications* 296(4):904-910.

60. Zhang T, Haws P, & Wu Q (2004) Multiple variable first exons: a mechanism for cell- and tissue-specific gene regulation. *Genome research* 14(1):79-89.

61. Abrahamsberg C *et al.* (2005) Targeted ablation of plectin isoform 1 uncovers role of cytolinker proteins in leukocyte recruitment. *Proceedings of the National Academy of Sciences of the United States of America* 102(51):18449-18454.

62. Osmanagic-Myers S *et al.* (2006) Plectin-controlled keratin cytoarchitecture affects MAP kinases involved in cellular stress response and migration. *The Journal of cell biology* 174(4):557-568.

63. Winter L, Abrahamsberg C, & Wiche G (2008) Plectin isoform 1b mediates mitochondrion-intermediate filament network linkage and controls organelle shape. *The Journal of cell biology* 181(6):903-911.

64. Andra K *et al.* (2003) Plectin-isoform-specific rescue of hemidesmosomal defects in plectin (-/-) keratinocytes. *The Journal of investigative dermatology* 120(2):189-197.

65. Walko G *et al.* (2011) Targeted proteolysis of plectin isoform 1a accounts for hemidesmosome dysfunction in mice mimicking the dominant skin blistering disease EBS-Ogna. *PLoS genetics* 7(12):e1002396.

66. Kostan J, Gregor M, Walko G, & Wiche G (2009) Plectin isoform-dependent regulation of keratin-integrin alpha6beta4 anchorage via Ca2+/calmodulin. *The Journal of biological chemistry* 284(27):18525-18536.

67. Valencia RG *et al.* (2013) Intermediate filament-associated cytolinker plectin 1c destabilizes microtubules in keratinocytes. *Molecular biology of the cell* 24(6):768-784.

68. Konieczny P *et al.* (2008) Myofiber integrity depends on desmin network targeting to Z-disks and costameres via distinct plectin isoforms. *The Journal of cell biology* 181(4):667-681.

69. Burgstaller G, Gregor M, Winter L, & Wiche G (2010) Keeping the vimentin network under control: cell-matrix adhesion-associated plectin 1f affects cell shape and polarity of fibroblasts. *Molecular biology of the cell* 21(19):3362-3375.

70. Wiche G & Winter L (2011) Plectin isoforms as organizers of intermediate filament cytoarchitecture. *Bioarchitecture* 1(1):14-20.

71. Rezniczek GA, Walko G, & Wiche G (2010) Plectin gene defects lead to various forms of epidermolysis bullosa simplex. *Dermatologic clinics* 28(1):33-41.

72. Hung MC & Link W (2011) Protein localization in disease and therapy. *Journal of cell science* 124(Pt 20):3381-3392.

73. Payne AS, Kelly EJ, & Gitlin JD (1998) Functional expression of the Wilson disease protein reveals mislocalization and impaired copper-dependent trafficking of the common H1069Q mutation. *Proceedings of the National Academy of Sciences of the United States of America* 95(18):10854-10859.

74. Tanaka AR *et al.* (2003) Effects of mutations of ABCA1 in the first extracellular domain on subcellular trafficking and ATP binding/hydrolysis. *The Journal of biological chemistry* 278(10):8815-8819.

75. Hoover BR *et al.* (2010) Tau mislocalization to dendritic spines mediates synaptic dysfunction independently of neurodegeneration. *Neuron* 68(6):1067-1081.

76. Frescas D, Valenti L, & Accili D (2005) Nuclear trapping of the forkhead transcription factor FoxO1 via Sirt-dependent deacetylation promotes expression of glucogenetic genes. *The Journal of biological chemistry* 280(21):20589-20595.

77. Robben JH, Knoers NV, & Deen PM (2006) Cell biological aspects of the vasopressin type-2 receptor and aquaporin 2 water channel in nephrogenic diabetes insipidus. *American journal of physiology. Renal physiology* 291(2):F257-270.

78. Fabbro M & Henderson BR (2003) Regulation of tumor suppressors by nuclear-cytoplasmic shuttling. *Experimental cell research* 282(2):59-69.

79. Dansen TB & Burgering BM (2008) Unravelling the tumor-suppressive functions of FOXO proteins. *Trends in cell biology* 18(9):421-429.

80. Hu MC *et al.* (2004) IkappaB kinase promotes tumorigenesis through inhibition of forkhead FOXO3a. *Cell* 117(2):225-237.

81. Koster R *et al.* (2010) Cytoplasmic p21 expression levels determine cisplatin resistance in human testicular cancer. *The Journal of clinical investigation* 120(10):3594-3605.

82. Asada M *et al.* (1999) Apoptosis inhibitory activity of cytoplasmic p21(Cip1/WAF1) in monocytic differentiation. *The EMBO journal* 18(5):1223-1234.

83. Huang S *et al.* (2003) Sustained activation of the JNK cascade and rapamycin-induced apoptosis are suppressed by p53/p21(Cip1). *Molecular cell* 11(6):1491-1501.

84. Liang J *et al.* (2002) PKB/Akt phosphorylates p27, impairs nuclear import of p27 and opposes p27-mediated G1 arrest. *Nature medicine* 8(10):1153-1160.

85. Kim J *et al.* (2009) Cytoplasmic sequestration of p27 via AKT phosphorylation in renal cell carcinoma. *Clinical cancer research : an official journal of the American Association for Cancer Research* 15(1):81-90.

86. Thery C (2011) Exosomes: secreted vesicles and intercellular communications. *F1000 biology reports* 3:15.

87. Al-Nedawi K, Meehan B, Kerbel RS, Allison AC, & Rak J (2009) Endothelial expression of autocrine VEGF upon the uptake of tumor-derived microvesicles

containing oncogenic EGFR. *Proceedings of the National Academy of Sciences of the United States of America* 106(10):3794-3799.

88. Chaput N *et al.* (2004) Exosome-based immunotherapy. *Cancer immunology, immunotherapy : CII* 53(3):234-239.

89. Azmi AS, Bao B, & Sarkar FH (2013) Exosomes in cancer development, metastasis, and drug resistance: a comprehensive review. *Cancer metastasis reviews*.

90. van Niel G, Porto-Carreiro I, Simoes S, & Raposo G (2006) Exosomes: a common pathway for a specialized function. *Journal of biochemistry* 140(1):13-21.

91. Johnstone RM, Adam M, Hammond JR, Orr L, & Turbide C (1987) Vesicle formation during reticulocyte maturation. Association of plasma membrane activities with released vesicles (exosomes). *The Journal of biological chemistry* 262(19):9412-9420.

92. Vidal MJ & Stahl PD (1993) The small GTP-binding proteins Rab4 and ARF are associated with released exosomes during reticulocyte maturation. *European journal of cell biology* 60(2):261-267.

93. Rieu S, Geminard C, Rabesandratana H, Sainte-Marie J, & Vidal M (2000) Exosomes released during reticulocyte maturation bind to fibronectin via integrin alpha4beta1. *European journal of biochemistry / FEBS* 267(2):583-590.

94. Zitvogel L *et al.* (1998) Eradication of established murine tumors using a novel cell-free vaccine: dendritic cell-derived exosomes. *Nature medicine* 4(5):594-600.

95. Kleijmeer MJ *et al.* (1995) MHC class II compartments and the kinetics of antigen presentation in activated mouse spleen dendritic cells. *J Immunol* 154(11):5715-5724.

96. Escola JM *et al.* (1998) Selective enrichment of tetraspan proteins on the internal vesicles of multivesicular endosomes and on exosomes secreted by human B-lymphocytes. *The Journal of biological chemistry* 273(32):20121-20127.

97. Raposo G *et al.* (1996) B lymphocytes secrete antigen-presenting vesicles. *The Journal of experimental medicine* 183(3):1161-1172.

98. Peters PJ *et al.* (1989) Molecules relevant for T cell-target cell interaction are present in cytolytic granules of human T lymphocytes. *European journal of immunology* 19(8):1469-1475.

99. Raposo G *et al.* (1997) Accumulation of major histocompatibility complex class II molecules in mast cell secretory granules and their release upon degranulation. *Molecular biology of the cell* 8(12):2631-2645.

100. Heijnen HF, Schiel AE, Fijnheer R, Geuze HJ, & Sixma JJ (1999) Activated platelets release two types of membrane vesicles: microvesicles by surface shedding and exosomes derived from exocytosis of multivesicular bodies and alpha-granules. *Blood* 94(11):3791-3799.

101. Ristorcelli E *et al.* (2008) Human tumor nanoparticles induce apoptosis of pancreatic cancer cells. *FASEB journal : official publication of the Federation of American Societies for Experimental Biology* 22(9):3358-3369.

102. Tadokoro H, Umezu T, Ohyashiki K, Hirano T, & Ohyashiki JH (2013) Exosomes derived from hypoxic leukemia cells enhance tube formation in endothelial cells. *The Journal of biological chemistry*.

103. Marimpietri D *et al.* (2013) Proteome profiling of neuroblastoma-derived exosomes reveal the expression of proteins potentially involved in tumor progression. *PloS one* 8(9):e75054.

104. Ostrowski M *et al.* (2010) Rab27a and Rab27b control different steps of the exosome secretion pathway. *Nature cell biology* 12(1):19-30; sup pp 11-13.

105. Bobrie A *et al.* (2012) Rab27a supports exosome-dependent and -independent mechanisms that modify the tumor microenvironment and can promote tumor progression. *Cancer research* 72(19):4920-4930.

106. Savina A, Fader CM, Damiani MT, & Colombo MI (2005) Rab11 promotes docking and fusion of multivesicular bodies in a calcium-dependent manner. *Traffic* 6(2):131-143.

107. Mittelbrunn M & Sanchez-Madrid F (2012) Intercellular communication: diverse structures for exchange of genetic information. *Nature reviews. Molecular cell biology* 13(5):328-335.

108. Zoller M (2009) Tetraspanins: push and pull in suppressing and promoting metastasis. *Nature reviews. Cancer* 9(1):40-55.

109. Mathivanan S, Ji H, & Simpson RJ (2010) Exosomes: extracellular organelles important in intercellular communication. *Journal of proteomics* 73(10):1907-1920.

110. Subra C, Laulagnier K, Perret B, & Record M (2007) Exosome lipidomics unravels lipid sorting at the level of multivesicular bodies. *Biochimie* 89(2):205-212.

111. Valadi H *et al.* (2007) Exosome-mediated transfer of mRNAs and microRNAs is a novel mechanism of genetic exchange between cells. *Nature cell biology* 9(6):654-659.

112. Lotvall J & Valadi H (2007) Cell to cell signalling via exosomes through esRNA. *Cell adhesion & migration* 1(3):156-158.

113. Schorey JS & Bhatnagar S (2008) Exosome function: from tumor immunology to pathogen biology. *Traffic* 9(6):871-881.

114. Peche H, Heslan M, Usal C, Amigorena S, & Cuturi MC (2003) Presentation of donor major histocompatibility complex antigens by bone marrow dendritic cell-derived exosomes modulates allograft rejection. *Transplantation* 76(10):1503-1510.

115. Lai RC *et al.* (2010) Exosome secreted by MSC reduces myocardial ischemia/reperfusion injury. *Stem cell research* 4(3):214-222.

116. Luga V *et al.* (2012) Exosomes mediate stromal mobilization of autocrine Wnt-PCP signaling in breast cancer cell migration. *Cell* 151(7):1542-1556.

117. Peinado H *et al.* (2012) Melanoma exosomes educate bone marrow progenitor cells toward a pro-metastatic phenotype through MET. *Nature medicine* 18(6):883-891.

118. Li W *et al.* (2013) Exosomes derived from Rab27aoverexpressing tumor cells elicit efficient induction of antitumor immunity. *Molecular medicine reports* 8(6):1876-1882.

119. Georgescu MM (2010) PTEN Tumor Suppressor Network in PI3K-Akt Pathway Control. *Genes & cancer* 1(12):1170-1177.

120. Geerts D *et al.* (1999) Binding of integrin alpha6beta4 to plectin prevents plectin association with F-actin but does not interfere with intermediate filament binding. *The Journal of cell biology* 147(2):417-434.

121. Yu PT *et al.* (2012) The RON-receptor regulates pancreatic cancer cell migration through phosphorylation-dependent breakdown of the hemidesmosome. *International journal of cancer. Journal international du cancer* 131(8):1744-1754.

122. Shin SJ *et al.* (2013) Unexpected gain of function for the scaffolding protein plectin due to mislocalization in pancreatic cancer. *Proceedings of the National Academy of Sciences of the United States of America*.

123. de Pereda JM, Lillo MP, & Sonnenberg A (2009) Structural basis of the interaction between integrin alpha6beta4 and plectin at the hemidesmosomes. *The EMBO journal* 28(8):1180-1190.

124. Fontao L *et al.* (2001) The interaction of plectin with actin: evidence for cross-linking of actin filaments by dimerization of the actin-binding domain of plectin. *Journal of cell science* 114(Pt 11):2065-2076.

125. Goldman R (2005) *Live Cell Imaging: A Laboratory Manual* (Cold Spring Harbor Library Press, New York).

126. Rezniczek GA, Abrahamsberg C, Fuchs P, Spazierer D, & Wiche G (2003) Plectin 5'-transcript diversity: short alternative sequences determine stability of gene products, initiation of translation and subcellular localization of isoforms. *Human molecular genetics* 12(23):3181-3194.

127. Park JE *et al.* (2010) Hypoxic tumor cell modulates its microenvironment to enhance angiogenic and metastatic potential by secretion of proteins and exosomes. *Molecular & cellular proteomics : MCP* 9(6):1085-1099.

128. Zomer A *et al.* (2010) Exosomes: Fit to deliver small RNA. *Communicative & integrative biology* 3(5):447-450.

129. Rana S, Yue S, Stadel D, & Zoller M (2012) Toward tailored exosomes: the exosomal tetraspanin web contributes to target cell selection. *The international journal of biochemistry & cell biology* 44(9):1574-1584.

130. Herrmann H & Wiche G (1987) Plectin and IFAP-300K are homologous proteins binding to microtubule-associated proteins 1 and 2 and to the 240-kilodalton subunit of spectrin. *The Journal of biological chemistry* 262(3):1320-1325.

131. Yang M *et al.* (2009) Stimulation of glioma cell motility by expression, proteolysis, and release of the L1 neural cell recognition molecule. *Cancer cell international* 9:27.

132. Raposo G & Stoorvogel W (2013) Extracellular vesicles: exosomes, microvesicles, and friends. *The Journal of cell biology* 200(4):373-383.

133. Craig R & Beavis RC (2004) TANDEM: matching proteins with tandem mass spectra. *Bioinformatics* 20(9):1466-1467.

134. Keller A, Eng J, Zhang N, Li XJ, & Aebersold R (2005) A uniform proteomics MS/MS analysis platform utilizing open XML file formats. *Molecular systems biology* 1:2005 0017.

135. Nesvizhskii AI, Vitek O, & Aebersold R (2007) Analysis and validation of proteomic data generated by tandem mass spectrometry. *Nature methods* 4(10):787-797.

136. Han DK, Eng J, Zhou H, & Aebersold R (2001) Quantitative profiling of differentiation-induced microsomal proteins using isotope-coded affinity tags and mass spectrometry. *Nature biotechnology* 19(10):946-951.

137. Zeng G *et al.* (2006) Aberrant Wnt/beta-catenin signaling in pancreatic adenocarcinoma. *Neoplasia* 8(4):279-289.

138. Cui J, Jiang W, Wang S, Wang L, & Xie K (2012) Role of Wnt/beta-catenin signaling in drug resistance of pancreatic cancer. *Current pharmaceutical design* 18(17):2464-2471.

139. Osmanagic-Myers S & Wiche G (2004) Plectin-RACK1 (receptor for activated C kinase 1) scaffolding: a novel mechanism to regulate protein kinase C activity. *The Journal of biological chemistry* 279(18):18701-18710.

140. Di Vizio D *et al.* (2009) Oncosome formation in prostate cancer: association with a region of frequent chromosomal deletion in metastatic disease. *Cancer research* 69(13):5601-5609.

141. Lu S, Simin K, Khan A, & Mercurio AM (2008) Analysis of integrin beta4 expression in human breast cancer: association with basal-like tumors and prognostic significance. *Clinical cancer research : an official journal of the American Association for Cancer Research* 14(4):1050-1058.

142. Guo W *et al.* (2006) Beta 4 integrin amplifies ErbB2 signaling to promote mammary tumorigenesis. *Cell* 126(3):489-502.

143. Gubergrits NB *et al.* (2012) Morphological and functional alterations of small intestine in chronic pancreatitis. *JOP : Journal of the pancreas* 13(5):519-528.

144. Pawar H *et al.* (2011) Quantitative tissue proteomics of esophageal squamous cell carcinoma for novel biomarker discovery. *Cancer biology & therapy* 12(6):510-522.

145. Katada K *et al.* (2012) Plectin promotes migration and invasion of cancer cells and is a novel prognostic marker for head and neck squamous cell carcinoma. *Journal of proteomics* 75(6):1803-1815.

146. Reynolds F *et al.* (2011) A functional proteomic method for biomarker discovery. *PloS one* 6(7):e22471.

147. Ahuja R *et al.* (2007) Cordon-bleu is an actin nucleation factor and controls neuronal morphology. *Cell* 131(2):337-350.

148. Liu Y *et al.* (2008) The Sac1 phosphoinositide phosphatase regulates Golgi membrane morphology and mitotic spindle organization in mammals. *Molecular biology of the cell* 19(7):3080-3096.

149. Wang Q *et al.* (2001) Cloning and characterization of full-length human ribosomal protein L15 cDNA which was overexpressed in esophageal cancer. *Gene* 263(1-2):205-209.

150. Hsu YA *et al.* (2011) A novel interaction between interferon-inducible protein p56 and ribosomal protein L15 in gastric cancer cells. *DNA and cell biology* 30(9):671-679.

151. Hao S *et al.* (2006) Epigenetic transfer of metastatic activity by uptake of highly metastatic B16 melanoma cell-released exosomes. *Experimental oncology* 28(2):126-131.

152. Lee KE & Bar-Sagi D (2010) Oncogenic KRas suppresses inflammation-associated senescence of pancreatic ductal cells. *Cancer cell* 18(5):448-458.

153. Ackerl R *et al.* (2007) Conditional targeting of plectin in prenatal and adult mouse stratified epithelia causes keratinocyte fragility and lesional epidermal barrier defects. *Journal of cell science* 120(Pt 14):2435-2443.

154. Hingorani SR *et al.* (2005) Trp53R172H and KrasG12D cooperate to promote chromosomal instability and widely metastatic pancreatic ductal adenocarcinoma in mice. *Cancer cell* 7(5):469-483.

155. Yin W, Ouyang S, Li Y, Xiao B, & Yang H (2013) Immature dendritic cell-derived exosomes: a promise subcellular vaccine for autoimmunity. *Inflammation* 36(1):232-240.

156. Knepper MA & Pisitkun T (2007) Exosomes in urine: who would have thought...? *Kidney international* 72(9):1043-1045.

157. Foisner R, Bohn W, Mannweiler K, & Wiche G (1995) Distribution and ultrastructure of plectin arrays in subclones of rat glioma C6 cells differing in intermediate filament protein (vimentin) expression. *Journal of structural biology* 115(3):304-317.

158. Low PC *et al.* (2010) Phosphoinositide 3-kinase delta regulates membrane fission of Golgi carriers for selective cytokine secretion. *The Journal of cell biology* 190(6):1053-1065.

159. Tokunaga E *et al.* (2006) Activation of PI3K/Akt signaling and hormone resistance in breast cancer. *Breast Cancer* 13(2):137-144.

160. Hennessy BT, Smith DL, Ram PT, Lu Y, & Mills GB (2005) Exploiting the PI3K/AKT pathway for cancer drug discovery. *Nature reviews. Drug discovery* 4(12):988-1004.

161. Edling CE *et al.* (2010) Key role of phosphoinositide 3-kinase class IB in pancreatic cancer. *Clinical cancer research : an official journal of the American Association for Cancer Research* 16(20):4928-4937.

162. Foisner R, Malecz N, Dressel N, Stadler C, & Wiche G (1996) M-phase-specific phosphorylation and structural rearrangement of the cytoplasmic cross-linking protein plectin involve p34cdc2 kinase. *Molecular biology of the cell* 7(2):273-288.

163. Koyama N, Kashimata M, Sakashita H, Sakagami H, & Gresik EW (2003) EGF-stimulated signaling by means of PI3K, PLCgamma1, and PKC isozymes regulates branching morphogenesis of the fetal mouse submandibular gland. *Developmental dynamics : an official publication of the American Association of Anatomists* 227(2):216-226.

APPENDIX

LIST OF PUBLICATIONS

Publications

1. **Shin SJ**, Smith JA, Rezniczek G, Wiche G, Kelly KA. “Unexpected gain of function for the scaffolding protein plectin due to mislocalization in pancreatic cancer.” *Proc Natl Acad Sci U S A.* 2013 Nov;110(48):19414–9.

2. Beech JR*, **Shin SJ***, Smith JA, and Kelly KA. “Mechanisms for a targeted delivery of nanoparticles in cancer.” *Curr Pharm Des.*2013;19(37):6560-74.

3. **Shin SJ***, Beech JR*, and Kelly KA. “Targeted nanoparticles in imaging: paving the way for personalized medicine in the battle against cancer.” *Integr Biol (Camb).* 2013 Jan;5(1):29-42.

4. Sefcik LS, Petrie Aronin CE, Awojoodu AO, **Shin SJ**, Mac Gabhann F, Macdonald TL, Wamhoff BR, Lynch KR, Peirce SM, and Botchwey EA. “Selective Activation of Sphingosine 1-Phosphate Receptors 1 and 3 Promotes Local Microvascular Network Growth.” *Tissue Engineering Part A.* 2011 Mar;17(5-6):617-29.

5. Petrie Aronin CE, **Shin SJ**, Naden KB, Rios PD, Sefcik LS, Bagayoko ND, Zawodny SR, Lynch KR, Cui Q, Khan Y, Botchwey EA. “The enhancement of bone allograft incorporation by the local delivery of the sphingosine 1-phosphate receptor targeted drug FTY720.” *Biomaterials.* 2010;31(25):6417-24.

* Equal contribution